Aus dem Institut für Medizinische Immunologie
und dem BIH Centrum für Regenerative Therapien (BCRT)
der Medizinischen Fakultät Charité – Universitätsmedizin Berlin

DISSERTATION

Defining the Role of Cardiac-Derived Cells as Modulators of Major Immune Responses in Inflammatory Environments

Die Rolle Kardial-Abgeleiteter Zellen als Potente Modulatoren von Immunreaktionen unter Inflammation

zur Erlangung des akademischen Grades
Medical Doctor - Doctor of Philosophy (MD/PhD)

vorgelegt der Medizinischen Fakultät
Charité – Universitätsmedizin Berlin

von

Falk Diedrichs

aus Göttingen

Datum der Promotion: 17.09.2021

“We are what we think, and all that we are rises with our thoughts.
With our thoughts we make the world.“

Buddha

The present thesis was composed at the Institute of Medical Immunology and BIH Center for Regenerative Therapies (BCRT) of the Charité – Berlin University of Medicine under the supervision of Prof. Dr. Martina Seifert. The work of this thesis was carried out within the framework of the DFG Graduate School 203, “Berlin-Brandenburg School of Regenerative Therapies” (BSRT).

Table of Contents

Abbreviations

1-MT	=	1-Methyl-L-Tryptophan
7-AAD	=	7-Aminoactinomycin D
ANOVA	=	Analysis of Variance
APC	=	Antigen Presenting Cell
CardAP	=	Cardiac-Derived Adherent Proliferating [Cell]
CD	=	Cluster of Differentiation
CDC	=	Cardiosphere-Derived Cardiac Cell
CFSE	=	Carboxyfluorescein Succinimidyl Ester
cIDH	=	Complete hAAC medium consisting of IMDM / DMEM / Ham’s F12
CPC	=	Cardiac Progenitor Cell
DAPI	=	4’,6-Diamidino-2-Phenylindole
DMEM	=	Dulbecco’s Modified Eagle’s Medium
DMSO	=	Dimethyl Sulfoxide
EDTA	=	Ethylenediaminetetraacetic Acid
FACS	=	Fluorescence-Activated Cell Scanning
FCS	=	Fetal Calve Serum
hAAC	=	Human Atrial Appendage-Derived Cell
HBSS	=	Hank’s Balanced Salt Solution
hiPSC	=	Human Induced Pluripotent Stem Cell
HLA	=	Human Leukocyte Antigen
HUVEC	=	Human Umbilical Vein Endothelial Cell
IDO	=	Indolamin-2,3-Dioxygenase

IFNγ	=	Interferon-gamma
IL	=	Interleukin
IMDM	=	Iscove's Modified Dulbecco's Medium
ISCT	=	International Society of Gene & Cell Therapy
IVT	=	In Vitro Transcription
MFI	=	Mean Fluorescence Intensity
MSC	=	Mesenchymal Stromal Cell
PBMC	=	Peripheral Blood Mononuclear Cell
PBS	=	Phosphate Buffered Saline
PD-1	=	Programmed Death 1
PDGFRα	=	Platelet-Derived Growth Factor Receptor A
PD-L1	=	Programmed Death 1 Ligand 1
PD-L2	=	Programmed Death 1 Ligand 2
PFA	=	Paraformaldehyde
SCA-1	=	Stem Cells Antigen-1
SEM	=	Standard Error of Mean
SLR	=	Signal Log Ratio
TCR	=	T Cell Receptor
TNFα	=	Tumor Necrosis Factor alpha
TNFβ	=	Tumor Necrosis Factor beta
VLE-RPMI	=	Very Low Endotoxin – Roswell Park Memorial Institute [Medium]
WGA	=	Wheat Germ Agglutinin
αMEM	=	Alpha-Modified Minimum Essential Medium

Abstract

The following section was adopted and modified from the original abstract of the preceding publication [1].

Rising numbers of patients with cardiovascular diseases and limited availability of donor hearts require novel and improved therapy strategies. Here, human atrial appendage-derived cells (hAACs) emerged as promising candidates for an allogeneic cell-based treatment. In this thesis, hAACs were analyzed for (I) their cellular characteristics after long-term cryopreservation, (II) their interaction with cells from the adaptive immune system *in vitro*, and (III) their underlying mode of action exerted in the crosstalk with immune cells. (I) Characterization of hAACs, according to standardized classification criteria of the International Society of Cell & Gene Therapy (ISCT), revealed a surface marker profile similar to conventional mesenchymal stromal cells (MSCs). However, hAACs were in contrast unable to differentiate into osteoblasts, chondroblasts or adipocytes *in vitro* and expressed the surface marker CD90 only on a low level. (II) The hAAC product demonstrated a low immunogenic phenotype after IFNγ pre-stimulation by moderate *de novo* expression of HLA-DR, lacking expression of co-stimulatory molecules, and upregulation of the inhibitory ligands PD-L1 and PD-L2. Most importantly, they did not induce allogeneic immune responses in co-cultures with human leukocyte antigen (HLA)-mismatched peripheral blood mononuclear cells (PBMCs). Furthermore, hAACs efficiently suppressed ongoing immune responses, especially in inflammatory environments, as seen in the reduction of T cell proliferation and decline of pro-inflammatory cytokine release (IFNγ, TNFα, TNFβ, IL-17A) in co-cultures with αCD3/αCD28-activated PBMCs. Transwell experiments confirmed that mostly soluble factors were responsible for the observed immunomodulatory effect of hAACs after IFNγ pre-treatment. (III) Lastly, indolamine-2,3-dioxygenase (IDO) could be identified as the key molecule of action involved in the suppression of T cell proliferation and induction of their apoptosis through a genome-wide gene expression analysis of three donors.

Thus, hAACs represent a unique and distinct MSC-like cell subset with atypical but clinically interesting features. Moreover, the presented data not only suggests the safety of the hAAC product for an allogeneic application, but also indicates its compelling potential to limit adverse remodeling after cardiac injury by effectively modulating the misdirected immune system.

Zusammenfassung

Der nachfolgende Text wurde teilweise übernommen und modifiziert aus der Zusammenfassung der vorausgegangenen Publikation [1].

Die steigende Fallzahl von Patienten mit kardiovaskulären Erkrankungen und die eingeschränkte Verfügbarkeit von Spenderherzen erfordert die Entwicklung neuer und verbesserter Therapieoptionen. Vor diesem Hintergrund sind humane Herzohr-abgeleitete Zellen ([engl.] human atrial appendage-derived cells; hAACs) vielversprechende Kandidaten für ein allogenes Behandlungsverfahren. In dieser Dissertation wurden hAACs analysiert bezüglich ihrer (I) zellulären Charakteristika nach langfristiger Kryokonservierung, (II) Interaktionen mit Zellen des adaptiven Immunsystems *in vitro*, und (III) zugrundeliegenden Wirkmechanismen eben jener Interaktionen. (I) Die Charakterisierung von hAACs anhand einheitlicher Kriterien der International Society of Cell & Gene Therapy (ISCT) ergab ein Oberflächenmarkerprofil, das ähnlich zu dem von konventionellen mesenchymal stromalen Zellen (MSCs) war. Im Gegensatz zu diesen waren hAACs *in vitro* allerdings nicht in der Lage, in Osteoblasten, Chondroblasten oder Adipozyten zu differenzieren und exprimierten den Oberflächenmarker CD90 nur zu einem geringen Grad. (II) Das hAAC Zellprodukt besitzt einen niedrig immunogenen Phänotyp nach Stimulation mit IFNγ, der sich durch moderate Expression von HLA-DR, Abwesenheit ko-stimulatorischer Marker, sowie Hochregulation von PD-L1 und PD-L2 Liganden auszeichnet. Bedeutsam ist, dass hAACs keine allogenen Immunreaktionen in Ko-Kulturen mit humanen Leukozyten-Antigen (HLA)-inkompatiblen mononukleären Zellen des peripheren Blutes (PBMCs) induzierten. Weiterhin unterdrückten hAACs besonders wirksam bereits initiierte Immunreaktion, vor allem in inflammatorischen Umgebungen. Dies zeigte sich in einer supprimierten T-Zell Proliferation und reduzierten Freisetzung pro-inflammatorischer Zytokine (IFNγ, TNFα, TNFβ, IL-17A) in Ko-Kulturen mit αCD3/αCD28-aktivierten PBMCs. Transwell Experimente bestätigten, dass hauptsächlich lösliche Faktoren verantwortlich für die beobachteten immunmodulatorischen Eigenschaften von IFNγ vorbehandelten hAACs waren. (III) Durch eine Genom-weite Analyse der Gen Expression von drei Spendern konnte letztlich Indolamin-2,3-Dioxygenase (IDO) als zentrales Schlüsselmolekül der Suppression von T-Zell Proliferation und Induktion derer Apoptose identifiziert werden.

Demzufolge präsentieren sich hAACs als einzigartiger und definierter MSC-artiger Subtyp mit atypischen, aber klinisch interessanten Eigenschaften. Die gezeigten Ergebnisse legen die Sicherheit des hAAC Produktes für eine allogene Anwendung nahe. Zudem deuten sie auch auf die Möglichkeit hin ungünstiges kardiales Remodeling, durch die effektive Modulation des fehlgeleiteten Immunsystems, zu limitieren.

1. Introduction

1.1. Current Clinical Challenges in Regenerative Cardiology

The field of medical and surgical cardiology is currently faced with an ever-growing number of patients with cardiovascular diseases, which remains the leading cause of morbidity and mortality worldwide. Indeed, ischemic heart disease alone causes almost 1.8 million deaths per year in Europe (20 % of all deaths; European Heart Network[1]) and greatly contributes, despite successful treatment, to the development of chronic heart failure in patients. In contrast to other areas of medicine, the surprisingly high prevalence of cardiovascular patients is mainly due to the limited regenerative capacity of the heart [2]. Historically, the human adult myocardium has been considered a terminally differentiated tissue, incapable of self-renewal. Contrary to this paradigm, a little over 10 years ago, research groups independently found a possible mechanism in the heart of adult mammals that contributes to 0.45 to 1.0 % of cell turnover per year [3]. However, this endogenous regeneration is not suitable to restore functional myocardium after major ischemic insults or chronic damage in adults. Instead, the injured tissue releases a plethora of danger signals that trigger an intense inflammatory response [4]. The subsequent infiltration of immune cells orchestrates the clearing of dead cells and mediates, together with activated myofibroblasts, the formation of a permanent scar rather than the replacement with contractile myocardium [4]. The advancement of many pharmacological and surgical strategies led to striking improvements in life quality and extension of lifespan in cardiovascular patients over the last years [5]. Unfortunately, these therapy options still only circumvent the heart's limitation of self-repairing capabilities and thereby prolong, but do not reverse, the progression of cardiomyocyte death and accumulation of scar tissue. Eventually, the spared myocardium adjusts over time and compensates to preserve pump function. When unsuccessful, this supportive mechanism ultimately compromises contractility of the remaining cardiomyocytes, which leads to unavoidable heart failure [2]. As a result, patients with end-stage heart failure are left with no other causal therapy than heart transplantation for this otherwise incurable

[1] "European Cardiovascular Disease Statistics 2017 edition" *CVD Statistics 2017*, February 2017. Online available: http://www.ehnheart.org/cvd-statistics/cvd-statistics-2017.html. (Accessed: 15.05.2020)

disease. However, acknowledging the risk of surgery, the permanent possibility of organ rejection, the ever-limited availability of donor hearts and the immense costs involved, this surgery is mostly unavailable for patients around the world [6].

Despite the recent advances in cardiology, restoring the function of injured myocardial tissue still remains an unmet challenge today. For this reason, the continuous development of new and innovative therapeutic strategies, that attempt to replace non-functional myocardium or to limit progression of scaring in the heart, is urgently needed.

1.2. Cell-Based Therapies as Promising Treatment Options for Cardiac Injury

Researchers suggested in 2001 that bone marrow-derived stem cells could transdifferentiate into cardiomyocytes in a model of acute myocardial infarction after injection into necrotic areas [7]. Ever since, there has been increasing interest in the application of cell-based therapies to achieve the goal of cardiac regeneration. While this study raised immense concerns regarding the reproducibility of findings over the following years [8], a tremendous number of clinical trials using various sources of stem or progenitor cells were initiated. The scientific effort was mainly focused on transplantation of (I) stem cell-derived cardiomyocytes, (II) cardiac progenitor cells (CPCs) and (III) mesenchymal stromal cells (MSCs) from different tissues, as summarized in **Figure 1**.

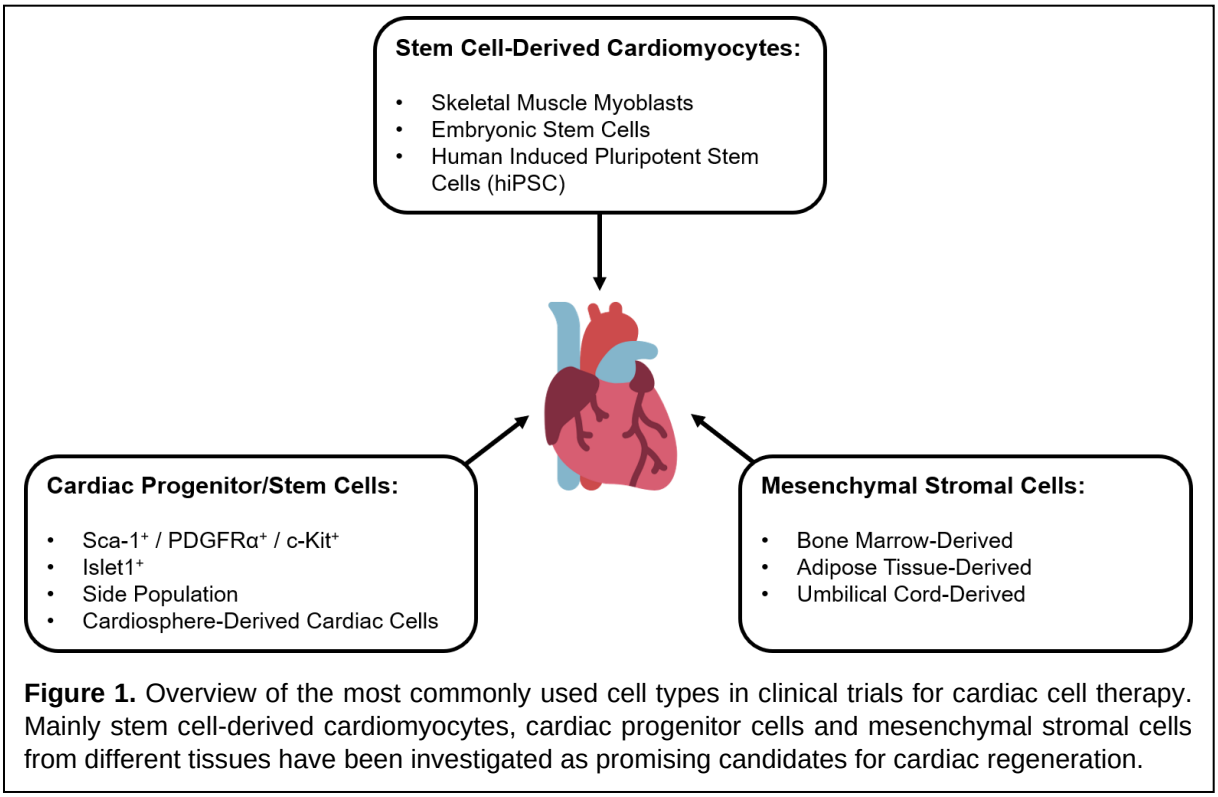

Figure 1. Overview of the most commonly used cell types in clinical trials for cardiac cell therapy. Mainly stem cell-derived cardiomyocytes, cardiac progenitor cells and mesenchymal stromal cells from different tissues have been investigated as promising candidates for cardiac regeneration.

(I) The field of regenerative cardiology was first launched with the idea of simply replacing damaged myocardium by the insertion of contractile tissue [9]. Early attempts with skeletal muscle myoblasts, which matured into a pronounced muscle but lacked expression of specific ion channels found in cardiomyocytes, showed the principal inability for electromechanically coupling with the spared myocardium [9]. Nowadays, human induced pluripotent stem cells (hiPSCs) - originally generated from adult fibroblasts through ectopic co-expression of the four nuclear transcription factors Oct4, Klf4, Sox2 and c-myc - are considered to be the most suitable candidate for the large-scale *in vitro* generation of a sufficient and relatively pure number of cardiomyocytes [10]. Even though hiPSC-derived cardiomyocyte transplantation revealed promising first results in pre-clinical studies by improved cardiac function, several challenges need to be resolved before clinical translation [9]. Specifically, safety concerns based on epigenetic memory, (epi-)genetic aberrations, teratoma formation, arrhythmias due to insufficient electromechanical coupling and particularly immunogenicity of long-term cultured or allogeneic cells are the major issues today [10].

(II) Another interesting therapeutic approach is to directly induce cardiomyogenesis, the formation of new cardiomyocytes, at the site of myocardial damage. The groundbreaking discovery of an endogenous mechanism for regeneration of myocardium led to the identification of several different cell populations within the human heart that exhibit features normally found in stem cells, for instance the ability of self-renewal [11]. These so-called CPCs have been characterized according to the expression of surface markers (including the receptor tyrosine kinase c-kit, stem cells antigen-1 (Sca-1) or the platelet-derived growth factor receptor A (PDGFRα)), transcription factors (Islet-1), the ability to efflux Hoechst dye (side population), as well as the capability to form cardiospheres in 3D culture systems (cardiosphere-derived cardiac cells, CDCs) [9,11]. Interestingly, c-kit$^+$ cells, the most researched among the identified resident CPCs, are reported to differentiate *in vitro* into the main three lineages of cardiac tissues, including smooth muscle cells, endothelial cells, and cardiomyocytes [12]. However, due to varying reports on the cardiogenic potential of injected cells, it remains highly questionable to what extent transplanted c-kit$^+$ CPCs are actually undergoing differentiation to cardiomyocytes in injured hearts of human adults *in vivo* [12,13]. Previously conducted clinical trials highlighted some important limitations. Retention, survival, and long-term engraftment of transplanted CPCs as

well as any cardiomyogenesis are highly limited in the setting of a mammalian myocardial infarction [11]. Therefore, reported modest improvements in cardiac function are mainly linked to a paracrine release that mediate anti-inflammatory, cardioprotective and pro-angiogenic effects [12,13]. Conclusively, the scientific consensus to date suggests that CPCs are rare and mostly heterogeneous cell populations within the human heart. They appear to exert their regenerative effects mainly through secretion of anti-inflammatory, pro-angiogenic and pro-survival factors that facilitate the proliferation and dedifferentiation of progenitor cells *in situ*, while the cardiomyogenic potential is functionally insignificant [9]. To further characterize the secretome of regenerative cell types, the scientific focus currently shifted towards the investigation of extracellular vesicles as important players of paracrine activity. Since they can be selectively isolated and infused as an “off-the-shelf” product into the patient, they represent an attractive alternative to cell-based therapies [14,15]. However, extracellular vesicles are less effective than cells themselves so far, clearly highlighting the need for further research that identifies optimal cell sources and isolation strategies [16].

(III) Mesenchymal stromal cells (MSCs) have emerged as potentially important therapeutics for repair or regeneration of various tissues in numerous medical fields. They are easily isolated, can be expanded to large numbers *ex vivo* in a time-efficient way and demonstrate superior safety by low immunogenicity as well as immunomodulatory capabilities [16]. The International Society for Cell & Gene Therapy (ISCT) defined the following three criteria as a minimum for the characterization of MSCs [17]: First, the ability to adhere to plastic in standard cell culture conditions. Second, the expression of the cell surface markers CD105, CD73, CD90 and the absence of CD45, CD34, CD14 or CD11b, CD79α or CD19 and HLA-DR. Third, a tri-lineage differentiation potential into osteoblasts, chondroblasts, and adipocytes *in vitro*. Interestingly, MSCs can be isolated from virtually all perivascular tissues of any organ, most commonly from the bone marrow, adipose tissue, or the umbilical cord [16]. Contrary to stem cells, MSCs mediate their regenerative properties usually not through differentiation into the target tissue. Instead, they secrete paracrine factors and extracellular vesicles or act through contact-dependent cell interactions, which limits inflammatory damage and establishes a microenvironment beneficial for tissue repair [14]. These immunomodulatory features might thereby play a vital role to prevent adverse remodeling in form of fibrosis, particularly in the context of cardiac

inflammation following myocardial damage. While the inflammatory cascade after myocardial injury is essential for debris removal and initiation of healing, a prolonged and exaggerated pro-inflammatory immune response leads to the induction of apoptosis in viable myocardiocytes and drives the adverse remodeling [4]. In other words, inflammation represents one of the major risk factors for the development of cardiac diseases that has been disregarded previously. Therefore, immunomodulatory therapies attempt to direct the response of the immune system towards an anti-inflammatory and reparative direction that limits secondary ischemic damage, mediates cardioprotective effects and thereby prevents the subsequent development of heart failure. First clinical trials with MSCs from various tissues showed modest but significantly improved cardiac function in patients after application in the setting of acute myocardial infarction and ischemic heart failure [18]. However, the recent scientific consensus demands the identification and thorough characterization - regarding the phenotype and underlying mechanism of action - of additional MSC subtypes for an effective and secure clinical translation [16]. In this context, Le Blanc and colleagues suggest to consider every stromal cell source as an independent entity [16]. This demands the critical assessment of the phenotype and safety for every novel cell type with a focus on the immunological implications. Furthermore, a rating of the potential efficacy could be achieved by comparing promising candidates to well-described MSC populations [16].

To date, no developed cell product was able to convincingly prove superior treatment success regarding improved cardiac regeneration in human patients. Therefore, additional cell sources and subtypes of cell populations should be considered, and their underlying mechanism of action must be uncovered to develop approaches for enhancing the regenerative tendencies of promising cell products and their secretome, including the use of extracellular vesicles.

1.3. Human Cardiac-Derived Mesenchymal-Like Cells Represent a Compelling Allogeneic Treatment Option

It has been proposed that cells isolated from close origin to the target tissue seem to be superior in their functional properties compared to cells from more remote regions [19]. For that reason, our research group previously focused on the isolation of cardiac-derived cells for the treatment of chronic heart failure, which are already primed for the heart's microenvironment and might therefore excel in their cardio-protective effects. These efforts led to the isolation of a so-far unknown cell type from endomyocardial biopsies, called cardiac-derived adherent proliferating (CardAP) cells [20]. A thorough characterization of these CardAP cells revealed typical characteristics normally found in MSCs, but also highlighted the unique identity that clearly differs from other cell types used in therapeutic applications so far [20]: CardAP cells adhere to plastic in cell culture conditions. They do express most of the known mesenchymal stem- and progenitor markers like CD44, CD73, CD105 and CD166, while also lacking the expression of the hematopoietic markers CD14, CD34 and CD45. However, in contrast to the classical surface marker profile of MSCs and fibroblasts, CardAP cells only express the Thy-1 protein CD90 on a low level. Furthermore, CardAP cells could neither be differentiated into adipocytes, osteoblasts, or chondrocytes, nor into myoblasts, collectively defining them as a mesenchymal-like cell subset. These cardiac-derived cells already demonstrated enhanced cardio-protective effects by increasing angiogenesis and cardiomyogenesis, reducing cardiac hypertrophy and fibrosis [21]. However, the number of cells that can be expanded from the 0.1 cm^3 sized endomyocardial biopsies is highly limited, thereby only enabling autologous treatment of diseased patients with CardAP cells. Moreover, previous clinical phase-I studies highlighted some of the fundamental limitations of autologous cell sources [22]. For example, the procurement, expansion, and processing of autologous tissues is time consuming which prevents immediate availability and also represents a high financial and organizational burden [22]. In addition, harvest from elderly and diseased patients with possible co-morbidities raised further concerns regarding the functional integrity and therapeutic efficacy of obtained cells [22]. For that reason, it is essential to provide large batches of healthy and instantly available cells. On the one hand, utilization of allogeneic cell sources could thereby enable a broad and inexpensive realization of an immediately available cell product, that can even be manipulated in advance to fit the patient's individual

needs. On the other hand, transplantation of allogeneic cells and tissues always poses the risk of recognition by the immune system and induction of unwanted immune responses in the recipient.

Most commonly these acute immune responses are mediated by the adaptive immune system when transplanted cells do not match the human leukocyte antigen (HLA) repertoire that is present in the recipient [23]. As a result, cell structures of allogeneic material is either directly recognized by immune cells or taken up by antigen presenting cells (APCs), which subsequently process and present the foreign antigens on their cell surface as HLA-class-II complexes to naive $CD4^+$ T cells in the lymph nodes. The successful activation of T cells involves at least two critical stimuli, as illustrated in **Figure 2**. First, interaction of the T cell receptor (TCR) on $CD4^+$ T cells with HLA-class-II complexes presented on the cell surface of APCs, or interaction of the

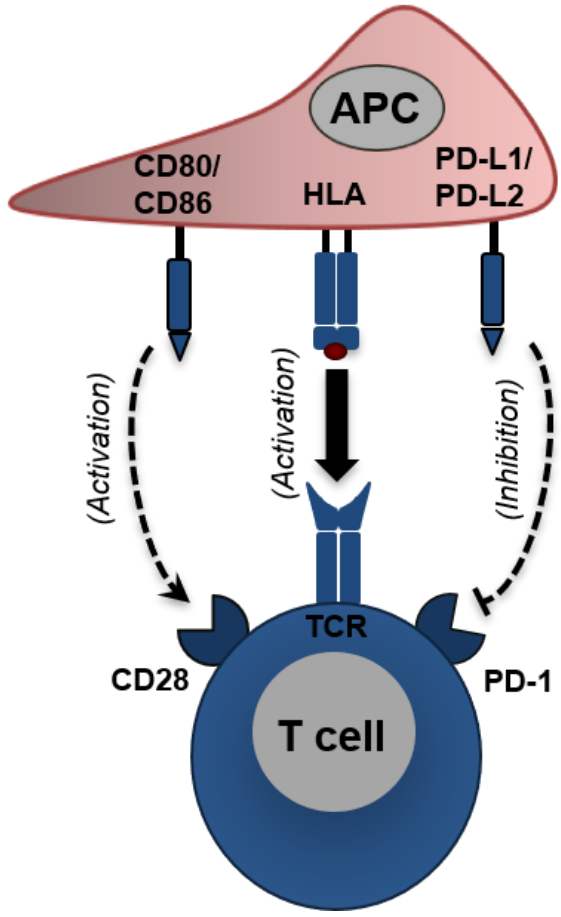

Figure 2. T cell interaction with APCs. Activation of T cells is a two-step process that requires a first recognition of foreign peptides presented by HLA on the surface of APCs through the TCR, as well as a second critical stimulus by the interaction of co-stimulatory molecules (e.g. CD80/CD86) with the CD28 family of receptors. The absence of the co-stimulatory signal prevents functional activation, clonal expansion, and cytokine secretion of the T cell. Checkpoint pathways, like the interaction of the regulatory ligands PD-L1/PD-L2 with PD-1 on T cells, delivers further inhibitory signals opposing the activation of T cells.

TCR on $CD8^+$ T cells with HLA-class-I complexes presented on the cell surface of all human nucleated cells. Second, a co-stimulatory signal that is provided by ligation of CD28 expressed on T cells with co-stimulatory molecules like CD80 or CD86. Additionally, there are also co-inhibitory pathways, that effectively suppress the activation of T cells. One example is the interaction of programmed cell death 1 ligand 1 (PD-L1) or programmed cell death 1 ligand 2 (PD-L2) with the receptor programmed cell death-1 (PD-1) on T cells. Upon successful T cell activation an inflammatory cascade is initiated that leads to a classic host-vs-graft-reaction characterized by T cell- and macrophage-dependent graft rejection as well as the secretion of allo-antibodies against the transplanted tissues or cells [23].

In search of a suitable allogeneic cell source, we previously identified the atrial appendage as a conveniently accessible and manageable tissue for the expansion of human atrial appendage-derived cells (hAACs) that feature similar properties compared to the endomyocardial CardAP cells [24]. The enhanced regenerative potential of hAACs is mediated, among other things, by expression of pro-angiogenic genes and the release of paracrine factors [24]. In addition, application of hAACs could already demonstrate improved left ventricular heart function and contractility as well as reduced collagen I expression in a mouse model of Coxsackievirus B3-induced myocarditis [25]. Most notably, to ensure a relatively pure cell product that excludes contamination with conventional MSCs or fibroblasts, the isolation procedure involves a negative selection step for CD90 [24]. A low expression of CD90 might be advantageous for the therapeutic efficacy of hAACs since it was established that reduction of cardiac fibrosis after CDC transplantation is inversely correlated with the expression of CD90 on the cell surface [26]. Moreover, the atrial appendage allows the generation of a sufficient number of $CD90^{low}$ hAACs for the treatment of at least 250 patients per tissue sample [24]. In summary, hAACs represent a preferable allogeneic cell-based therapy over the autologous CardAP cells, since an immediate “off-the-shelf” availability of a cryopreserved and pre-tested product allows less expensive and broad region-wide access. Nevertheless, induction of unwanted immune responses must be ruled out and the underlying mechanism of action in hAACs must be uncovered to ensure not only safety and efficacy for a future allogeneic transplantation but also discover novel approaches to enhance the regenerative capacity.

1.4. Aim

The extremely fast clinical translation of cell products over the past two decades reported only modest or insignificant efficacy to improve cardiac function after myocardial injury. Ultimately, the initial enthusiasm in regenerative cardiology weakened and there was a lack of scientific evidence and understanding of cell-based therapies regarding the observed effects and the underlying mode of action. Therefore, a return to the bench-side is urgently needed to characterize additional suitable cell sources and subtypes of cell populations like hAACs. It is critical to ensure their safety before allogeneic transplantation, and also expand our rudimentary knowledge on the fundamental mechanisms exerted by such promising candidates. This will ultimately lead to a fast and safe translation into the clinic and facilitates further possibilities to enhance the therapeutic efficacy of cell products in the future. To take these considerations into account, the aim of this thesis is divided into the following three sections:

1. Definition of the general characteristics of hAACs after long-term cryopreservation according to the ISCT criteria for MSCs.

2. Evaluation of the immune phenotype and interaction of hAACs with cells of the adaptive immune system in regular and inflammatory conditions *in vitro*.

3. Exploration of the underlying mechanism of action of the proven immunomodulatory capabilities of hAACs.

2. Materials and Methods

This detailed Materials and Methods section was adopted and modified from the preceding publication [1].

2.1. Isolation and Culture of Human Atrial Appendage-Derived Cells (hAACs)

Right atrial appendages, that were obtained during open-heart surgery at the German Heart Center Berlin from eight patients, were used to generate hAACs as previously described [24]. The procedure is succinctly depicted in **Figure 3**. Briefly, the right atrial appendages were reduced to fragments of 1 mm^3 and cultured in Iscove's Modified Dulbecco's Medium (IMDM; Biochrom, Berlin, Germany) containing 10 % allogeneic human serum (German Red Cross, Berlin, Germany), 100 U/mL penicillin and 100 µg/mL streptomycin (both from Biochrom). Outgrowing cells were harvested after about 13 days with 0.05 % trypsin / 0.02 % EDTA (Biochrom) and then subjected to immunomagnetic sorting (MACS) with CD90 microbeads (human CD90 MicroBeads kit, Miltenyi Biotec, Bergisch Gladbach, Germany). The resulting $CD90^{low}$ cell population was grown under standard culture conditions (37°C in 21 % O_2 and 5 % CO_2 atmosphere) at a density of 6000 cells/cm^2 in complete medium (cIDH) consisting of equal amounts of IMDM/DMEM/Ham's F12 (IDH; all Biochrom) and supplemented with 5 % male heat-inactivated human AB serum (Sigma-Aldrich, St. Louis, MO, USA), 100 U/mL penicillin and 100 µg/mL streptomycin (Gibco® Life Technologies, Grand Island, NY, USA), 20 ng/mL basic fibroblast growth factor and 10 ng/mL epithelial growth factor (both from Peprotech, Hamburg, Germany) for further expansion of the purified cell product. Subsequently, hAACs were cryopreserved in conventional

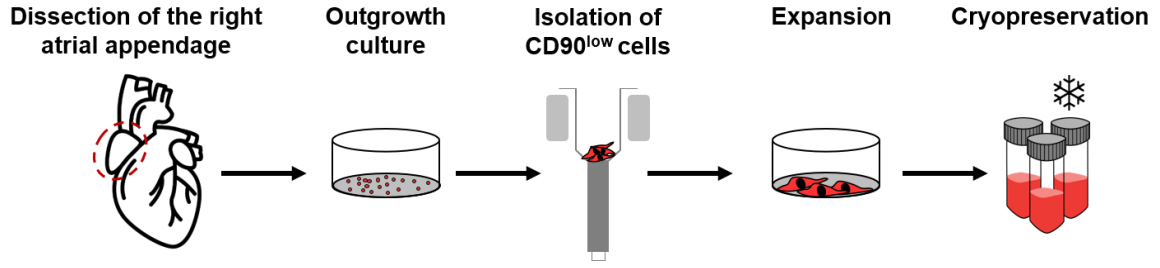

Figure 3. Overview of the isolation procedure for $CD90^{low}$ hAACs: Right atrial appendages were harvested from patients during open-heart surgery. The dissected tissue was minced into small pieces and placed into cell cultures. Subsequently, outgrowing cells from the fragments were harvested, immune-magnetically sorted as $CD90^{low}$ cells, and seeded again for further expansion of the desired, purified hAAC product. The hAACs were ultimately cryopreserved and long-term stored for later experimental use. This figure was adopted and modified from the preceding publication [1].

freezing medium (10 % dimethyl sulfoxide (DMSO; Sigma-Aldrich) / 90 % fetal calve serum (FCS; Biochrom)) for at least six months to mimic conditions of a cell bank. After thawing, cells were routinely passaged once in cIDH medium before performing assays and were used between passages 2 and 8. Tissues were obtained according to the local guidelines of the Charité - Universitätsmedizin Berlin as well as the Declaration of Helsinki and the study was approved by the ethics committee of the Charité - Universitätsmedizin Berlin (No. 4/028/12). HLA-typing of the cells were performed in the HLA-Laboratory of the Charité - Universitätsmedizin Berlin by SSO-PCR (low) for HLA-A, HLA-B and HLA-DR. A list of all HLA-typed cells is available in **Table 1**.

2.2. Culture of Human Umbilical Cord-Derived Mesenchymal Stromal Cells (MSCs) and Human Umbilical Vein Endothelial Cells (HUVECs)

Due to their known immunomodulatory potential human umbilical cord-derived MSCs were used as control cells in the immune cell co-culture experiments. Cells were kindly provided by Dirk Strunk´s laboratory from the Institute of Experimental and Clinical Cell Therapy and Spinal Cord & Tissue Regeneration Center, Paracelsus Medical University (PMU) Salzburg, Austria and were obtained for human cell and tissue sample collection from the Institutional Review Board of the Medical University of Graz (protocol 19-252 ex 07/08). Umbilical cord samples were collected from mothers that

Table 1. HLA genotypes for HLA-A, HLA-B, and DRB1 of different hAAC, MSC, and PBMC donor. This table was adopted and modified from the preceding publication [1].

Donor	HLA-A		HLA-B		DRB1	
hAAC1	02	23	40	49	11	13
hAAC2	03	32	07	57	07	15
hAAC3	03	11	15	50	07	09
hAAC4	03	-	35	49	01	07
hAAC5	01	03	27	57	07	15
hAAC6	01	03	07	08	01	03
hAAC7	02	26	18	37	11	13
hAAC8	01	02	08	57	15	16
MSC1	02	24	15	44	11	13
PBMC1	01	31	38	51	09	13
PBMC2	11	-	07	35	01	15
PBMC3	11	30	13	15	04	07
PBMC4	02	03	15	40	13	13
PBMC5	24	68	40	51	01	03
PBMC6	24	26	13	44	01	07
PBMC7	01	02	18	57	03	13
PBMC8	24	-	07	44	01	04

gave written informed consent after full-term pregnancies in accordance with the Declaration of Helsinki. After thawing, MSCs were grown in alpha-modified minimum essential medium (αMEM; Biochrom), supplemented with 5 % human male heat-inactivated AB serum (Sigma-Aldrich), 2 mM L-glutamine, 100 U/mL penicillin and 100 µg/mL streptomycin (both from Gibco® Life Technologies) at 37°C in 21 % O_2 and 5 % CO_2 atmosphere. HLA-typing of the donor cells was performed by SSP PCR using Olerup SSPTM low-resolution kits (GenoVision Inc., Philadelphia, PA, USA) and results are available in **Table 1**.

HUVECs with a known allo-immunogenicity were used as positive controls in the immune cell co-culture experiments (Cascade Biologics®, Thermo Fisher Scientific, Rochester, NY, USA and Lonza, Wakersville, MD, USA). After thawing, HUVECs were cultured in EGM-2 (Lonza) with 5 % human male heat-inactivated AB serum (Sigma-Aldrich), 100 U/mL penicillin and 100 µg/mL streptomycin (Gibco® Life Technologies) for further expansion.

Both cell types were passaged once before performing assays and were used between passages 2 and 8.

2.3. Peripheral Blood Mononuclear Cell (PBMC) Isolation

Human peripheral blood mononuclear cells (PBMCs) were isolated from buffy coats (German Red Cross, Berlin, Germany; approved by the local Ethical Committee, EA1/226/14) by using a Biocoll gradient (Biochrom). Briefly, following centrifugation at 800 g for 30 minutes without brake, PBMCs were harvested from the interphase and were washed three times with cold phosphate buffered saline solution (PBS; Biochrom). Cells were cryopreserved for later experimental use in liquid nitrogen. HLA-typing was performed in the HLA-Laboratory of the Charité - Universitätsmedizin Berlin by SSO-PCR (low) for HLA-A, HLA-B and HLA-DR, as listed in **Table 1**.

2.4. Bright-Field and Fluorescence-Based Microscopy of hAACs

hAACs were plated on 24 well dishes (Falcon, BD Biosciences, San Jose, CA, USA). After incubation overnight, wells were washed with PBS and fixed with 4 % paraformaldehyde (PFA; Roth, Karlsruhe, Germany) for ten minutes at room temperature for bright-field image acquisition using an Axio Observer Z1 microscope and the Axio Vision Software (both from Carl Zeiss, Jena, Germany).

For fluorescence-based microscopy, wells were washed three times with Hank's Balanced Salt Solution (HBSS; Gibco® Life Technologies) containing Mg^{2+} and Ca^{2+}, fixed with 4 % PFA (Roth) for ten minutes at room temperature and washed twice with HBSS. Subsequently, the cells were incubated with 5 µg/mL wheat germ agglutinin (WGA; Biotium, Fremont, CA, USA) for ten minutes at 37°C. After washing twice with HBSS, nuclei were counterstained for 15 minutes at room temperature with 4,6-diamidino-2-phenylindole (DAPI; Molecular probes™, Thermo Fisher). Images were taken with an Operetta® High Content Imaging System and image analysis performed by the Columbus™ Image Data Storage and Analysis System (both from Perkin Elmer, Waltham, MA, USA).

2.5. Fluorescence Staining of Cells and Fluorescence-Activated Cell Scanning (FACS)

Non-adherent PBMCs were collected by pipetting, and adherent hAACs were first harvested using a 0.05 % trypsin solution with EDTA (Gibco® Life Technologies) and transferred to 5 mL FACS tubes (Falcon, BD Biosciences). Cells were washed once with cold PBS, resuspended in a final volume of 50 µL antibody mix in cold FACS buffer

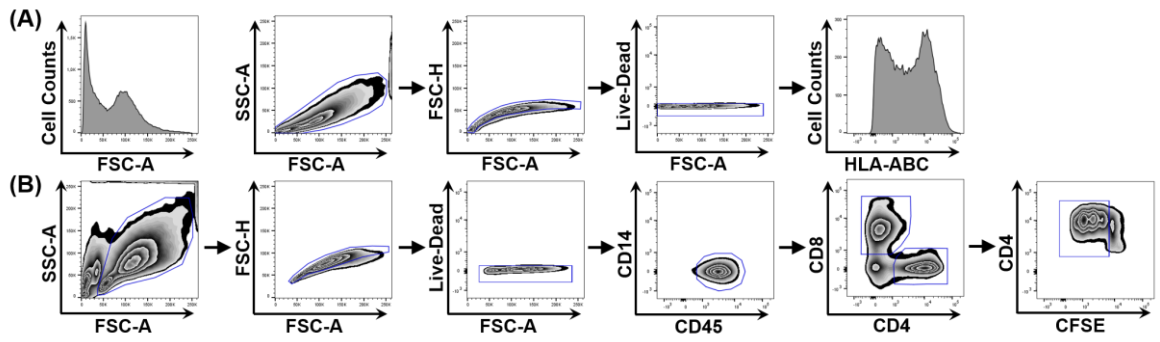

Figure 4. Flow cytometry gating strategies of mono-culture and co-culture experiments. **(A)** The hAAC product features a heterogonous size distribution in the forward-scatter area (FSC-A) histogram. Therefore, both distinct size-subsets were included in the pre-gating on the FSC-A against sideward-scatter area (SSC-A) to analyze the complete cell product. Next, the resulting cells were gated on FSC-A against forward-scatter height (FSC-H) to discriminate between doublets and single cells within the population. To exclude apoptotic or dead cells and assure the viability of hAACs, cells were gated on FSC-A against Live-Dead marker. In a last step, fluorescence intensities of various markers were analyzed, exemplarily shown here for HLA-ABC. **(B)** In human PBMC cultures the leukocyte population was defined according to size and granularity (FSC-A vs. SSC-A). Doublets (FSC-A vs. FCS-H) and apoptotic or dead cells (FCS-A vs. Live-Dead marker) were excluded from analysis. Monocytes and any possible debris from the adherent cells were gated out (CD14 vs. CD45). In a last gating step, T cell subsets were discriminated (CD4 vs. CD8), before proliferation, as seen in reduction of CFSE signal intensity, was determined for both subsets, exemplarily shown here for CFSE vs. CD4. This figure was adopted and modified from the preceding publication [1].

(PBS supplemented with 1 % FCS (both Biochrom)) and incubated for 30 minutes at 4°C in the dark. All antibodies and dyes used, and the respective dilutions are listed in **Table 2**. Antibody mixes also contained the Live/Dead® violet Staining Kit (Molecular probes™, Thermo Fisher Scientific) in order to exclude dead cells from the analysis. After antibody incubation, the samples were washed with cold FACS buffer and resuspended in 1 % PFA (Roth, Karlsruhe, Germany) in FACS buffer. Samples were kept at 4°C in the dark until measurement on a FACS Canto II device with FACS Diva software (Becton Dickinson, San Jose, CA, USA). Data analysis was performed using FlowJo software (TreeStar Inc., Ashland, OR, USA). Gating strategies for the FACS-analysis of hAACs and PBMCs are depicted in **Figure 4**. Expression of a marker is presented either as percentage of positive cells against the unlabeled control or as geometric mean of fluorescence intensity (MFI).

Table 2. Overview of antibodies and dyes used for staining. This table was adopted and modified from the preceding publication [1].

Antibody / Dye Name	Clone	Fluorochrome	Company	Dilution	Catalog#
HLA-ABC	W6/32	APCCy7	Biolegend	1:100	311425
HLA-E	3D12	APC	Biolegend	1:50	342605
HLA-DR	L243	PECy7	Biolegend	1:600	307616
CD3	SK7	PerCPCy5.5	BD Biosciences	1:20	332771
CD4	OKT4	APC	Biolegend	1:50	317416
CD8	BW135/80	PE	Miltenyi Biotec	1:200	130-091-084
CD14	MφP9	APCCy7	BD Biosciences	1:100	557831
CD25	BC96	PerCPCy5.5	Biolegend	1:50	302626
CD29	TS2/16	PE	Biolegend	1:100	303004
CD31	WM59	FITC	BD Biosciences	1:50	555445
CD34	4H11	FITC	Biolegend	1:50	316405
CD44	IM7	PECy7	Biolegend	1:3000	103030
CD45	HI30	PacificBlue	Biolegend	1:200	304022

Table 2. *(continued)*

Antibody / Dye Name	Clone	Fluorochrome	Company	Dilution	Catalog#
CD45	2D1	PerCP	BD Biosciences	1:100	345809
CD54	HCD54	FITC	Biolegend	1:1000	322720
CD73	AD2	APC	Biolegend	1:1000	344005
CD80	2D10	FITC	Biolegend	1:20	305206
CD86	IT2.2	PE	Biolegend	1:50	305406
CD90	5E10	PerCPCy5.5	Biolegend	1:400	328117
CD105	43A3	PE	Biolegend	1:50	323205
CD106	STA	PE	Biolegend	1:50	305806
c-Kit (CD117)	104D2	APC	Invitrogen	1:50	CD11705
CD166	3A6	PE	Biolegend	1:50	343903
CD166	3A6	PerCPCy5.5	BD Biosciences	1:50	562131
PD-L1 (CD274)	29E.2A3	PerCPCy5.5	Biolegend	1:100	329738
PD-L1 (CD274)	29E.2A3	-	Biolegend	1:100	329702
PD-L2 (CD273)	MIH18	APC	Biolegend	1:100	345508
PD-L2 (CD273)	MIH18	-	Biolegend	1:100	345502
Annexin-V	-	FITC	Biolegend	1:25	640906
CFSE	-	-	Biolegend	5 µM	423801
7-AAD	-	7-AAD	Biolegend	1:25	420404
Wheat Germ Agglutinin	-	CF488A	Biotium	1:400	29022-1

2.6. Kinetic Analysis of hAAC Surface Marker Expression

hAACs were seeded on 24 well-plates (Costar®, Corning Incorporated, Kennebunk, ME, USA) at a density of $3x10^5$ cells and were cultured in cIDH medium overnight. Afterwards, hAACs were either directly harvested for evaluation of constitutive MSC marker expression (CD90, CD29, CD44, CD73, CD105, CD166, CD14, CD31, CD45, c-Kit) or stimulated with 100 ng/mL of interferon-gamma (IFNγ; Miltenyi Biotec) for evaluation of the immunological (HLA-ABC, HLA-E, HLA-DR, CD80, CD86, PD-L1 and PD-L2) and MSC-typical markers (CD90, CD29, CD44, CD73, CD166). hAACs were stimulated and harvested after one, two and five days respectively for flow cytometric analysis as described before.

2.7. hAAC/Immune Cell Co-Cultures

The experimental setup is succinctly shown in **Figure 5**. In detail, hAACs from six different donors and control cultures with MSCs and HUVECs were seeded on rat tail collagen I-coated (BD Biosciences) 24 well plates (Costar®, Corning Incorporated) at a density of $2x10^5$ cells. After attachment overnight, the adherent cells were either stimulated with 100 ng/mL IFNγ (Miltenyi Biotec) or left unstimulated for 48 hours.

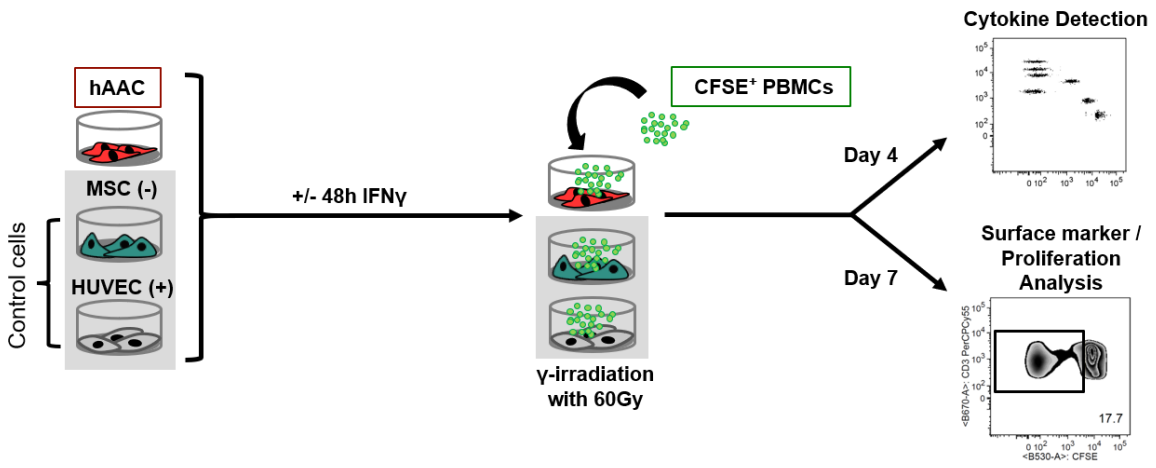

Figure 5. Overview of the experimental setup to analyze the immunogenicity of hAACs in immune cell-cocultures: Mesenchymal stromal cells from the umbilical cord (MSCs) as well as human umbilical vein endothelial cells (HUVECs) served as cellular controls, respectively (MSC (-); HUVEC (+)) and were cultured along with hAACs for 48 hours in the presence or absence of 100 ng/mL IFNγ. The cells were gamma-irradiated with 60 Gray before carboxyfluorescein succinimidyl ester (CFSE)-labeled, human leukocyte antigen (HLA)-mismatched peripheral blood mononuclear cells (PBMCs) were either added to the adherent cell cultures of all three cell types or left alone as control. After four days of incubation, supernatants were taken for cytokine detection using the Legendplex™ human inflammation panel and after seven days PBMCs were harvested, stained with human immune cell specific antibodies, and analyzed flow cytometrically. Levels of $CD4^+$ and $CD8^+$ T cell proliferation were detected by measuring reduced CFSE signal intensity (black square). This figure was adopted and modified from the preceding publication [1].

Afterwards, the confluent monolayers were irradiated with 60 Gray using a gamma-radiation source (GSM GmbH, Leipzig, Germany) to maintain a stable cell number throughout the assay. Human HLA-mismatched PBMCs were thawed, washed three times with cold PBS (Biochrom) and labeled with 5 µM carboxyfluorescein succinimidyl ester (CFSE; Biolegend, San Diego, CA, USA) for three minutes. The staining reaction was then stopped by incubating with cold heat-inactivated human AB serum (Sigma-Aldrich) for one minute. After washing three times with cold PBS, $3x10^5$ CFSE-labeled PBMCs were added to the hAAC, MSC and HUVEC cultures, which were a complete HLA-mismatch to the respective hAAC donor. The resulting co-cultures were maintained in 1 mL of very low endotoxin (VLE)-Roswell Park Memorial Institute (RPMI; Biochrom) medium, supplemented with 10 % human male heat-inactivated AB serum (Sigma-Aldrich), 100x L-glutamine solution, 100 U/mL penicillin and 100 µg/mL streptomycin (all from Gibco® Life Technologies). After four days, 250 µL of co-culture supernatant were taken for cytokine detection and 750 µL of fresh, completely supplemented VLE-RPMI were added to the cultures. Following seven days of incubation, PBMCs were harvested, stained for human immune cell defining surface markers and analyzed by flow cytometry.

2.8. Proliferation Based Immunomodulation Assay

Analogous to the hAAC/immune cell co-culture analysis, hAACs, MSCs and HUVECs were cultured on rat tail collagen I-coated (BD Biosciences) 24 well plates (Costar®, Corning Incorporated) at a density of $2x10^5$ cells in the presence or absence of 100 ng/mL IFNγ (Miltenyi Biotec) for 48 hours. Human PBMCs were CFSE-labeled as mentioned before and activated with a combination of 0.02 µg/mL anti-CD3 (OKT3 antibody, Janssen-Cilag, Neuss, Germany) and 0.03 µg/mL anti-CD28 (BD Biosciences) antibodies. Lastly, $1x10^6$ PBMCs were added to the cultures in 2 mL of completely supplemented VLE-RPMI medium. After 72 hours, supernatants were taken for cytokine detection and PBMCs were harvested, stained for human immune cell defining surface markers and analyzed by flow cytometry.

Experimental settings were repeated under transwell conditions. Here, hAACs were seeded at a density of $4x10^4$ cells at the bottom of rat tail collagen I-coated 24 well plates. After stimulation with IFNγ, polycarbonate transwell inserts with 0.4 µm pore size (Costar®, Corning Incorporated) were initially equilibrated for one hour at 37°C with RPMI and subsequently $2x10^5$ CFSE-labeled PBMCs were seeded into the

inserts. After a co-culture time of three days at 37°C in a 21 % O_2 and 5 % CO_2 atmosphere, PBMC were harvested for flow cytometric analysis of proliferation and surface marker expression.

To selectively analyze the effects of indoleamin-2,3-dioxygenase (IDO) and both PD-1 ligands (PD-L1 and PD-L2) in immune cell co-cultures with hAACs, the following blocking reagents were supplemented, as illustrated in **Figure 6**. For the specific blocking of IDO, 1 mM 1-methyl-L-tryptophan (1-MT; Sigma-Aldrich) was supplied two hours prior to the addition of CFSE-labeled or unlabeled PBMCs. For both PD-1 ligands (PD-L1 and PD-L2), 5 µg/mL of purified anti-PD-L1 and anti-PD-L2 antibodies (both Biolegend) were supplied 12 hours before CFSE-labeled or unlabeled PBMCs were added to the hAAC cultures. After 72 hours of co-culture, PBMCs were harvested for measurement of T cell proliferation rates in CFSE-labeled PBMCs as previously described. Unlabeled PBMC cultures were used to determine the proportion of late-apoptotic T cells by staining with Annexin-V and 7-aminoactinomycin D (7-AAD).

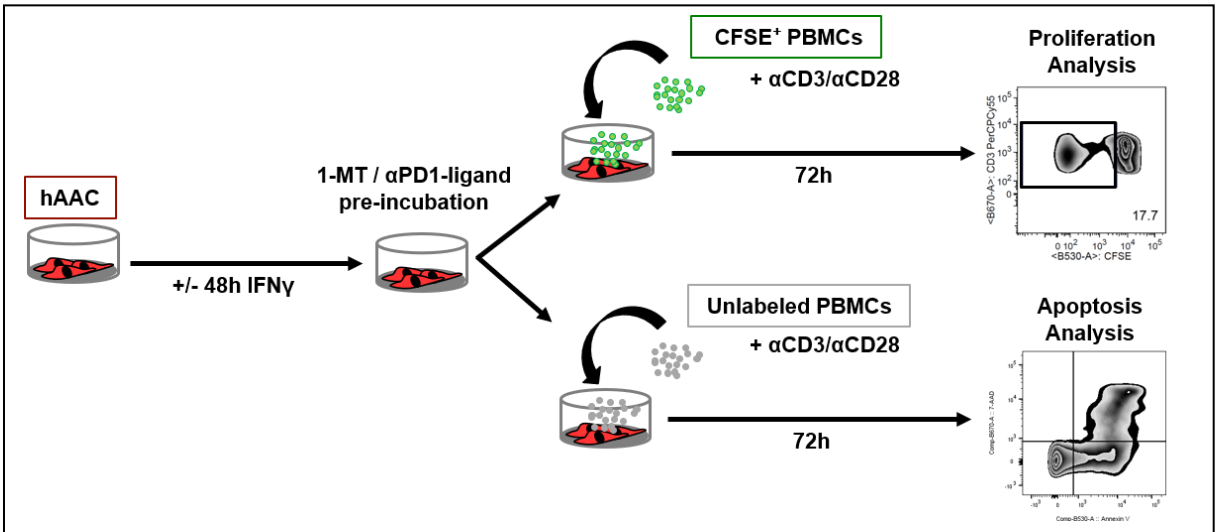

Figure 6. Overview of the experimental setup to evaluate the potential involvement of IDO and programmed death-1 (PD-1) ligands in hAAC effects on T cells: hAACs were seeded and stimulated with IFNγ or left unstimulated for 48 hours. Before co-cultivation with immune cells, 1-mehtyl-L-tryptophan (1-MT) as specific inhibitor of IDO or blocking antibodies against PD-L1 and PD-L2 (αPD1 ligands) were applied. Subsequently, either CFSE-labeled or unlabeled PBMCs were activated by adding a cocktail of anti-CD3/anti-CD28 (+αCD3/αCD28) antibodies and were left alone as controls or cultured with hAACs for 72 hours. $CD4^+$ or $CD8^+$ T cell proliferation levels as well as the percentage of Annexin-V^+ 7-AAD^+ late apoptotic cells were determined by flow cytometry. This figure was adopted and modified from the preceding publication [1].

2.9. Cytokine Detection Assays

Supernatants of mono- and co-cultures of hAACs, MSCs and HUVECs from the proliferation induction experiments were tested for IL-1β, IFNα, IFNγ, TNFα, MCP-1, IL-6, IL-8, IL-10, IL-12p70, IL-17A, IL-18, IL-23 and IL-33 using the Legendplex™ human inflammation 13-plex panel (Biolegend). The minimum detectable concentration of each cytokine is given as 0.6 – 2.1 pg/mL. Samples were treated following manufacturer's instructions and measured with a FACS Canto II device (Becton Dickinson).

Supernatants of hAAC co-cultures from the direct-contact immune modulation experiments were analyzed for their content of IL-10, IL-17A, TNFα, TNFβ and IFNγ by a multiplex assay using a Milliplex® human multi-analyte Luminex® kit (Merck KGaA, Darmstadt, Germany). Samples were treated following manufacturer's instructions and measured with a Bio-Plex® 200 multiplex analysis device (Bio-Rad®, California, USA).

2.10. Genome-Wide Gene Expression Profile

Human GeneChip U133 Plus 2.0 (Affymetrix, Santa Clara, CA, USA) was used for genome-wide gene expression profiling of hAAC samples covering over 47,000 transcripts (54,765 probes in total including double entries). RNA samples of unstimulated and IFNγ pre-stimulated hAACs were prepared with GeneChip® 3′ IVT Express Kit and GeneChip® Hybridisation, Wash and Stain Kit (Affymetrix) according to the manufacturer's instructions. In brief, 250 ng total RNA was used for cDNA synthesis and subsequent in vitro transcription (IVT) to amplified RNA (aRNA). 12.5 µg fragmented aRNA was used for hybridization on the chip for 16 h at 45°C. Finally, the chips were washed, stained, and scanned using the Affymetrix Gene Chip Scanner 3000. Affymetrix GeneChip Operating Software (GCOS) 1.4 was used to generate CEL data files, for raw data processing and for calculation of signal intensity, signal log ratio (SLR) and *p*-value of pairwise chip comparisons AF/NP. Quality control and pre-processing was done in R [2] with the package "affy". Raw data were normalized and log2-transformed using Robust Multi-array Average (RMA) algorithm implemented in this package. 1000 probe sets with the highest variances were selected in order to

[2] R Core Team (2018). R: A language and environment for statistical computing. R Foundation for Statistical Computing, Vienna, Austria. URL: https://www.R-project.org/

run a principle component analysis. Differentially expressed probe sets between the two treatment groups were selected by fitting linear models to the data and Bayesian statistics were run as implemented in the package "limma". False discovery rates were used to adjust raw p-values for multiple testing and a minimal absolute log2-Foldchange of 1 was used for probe set selection. Mapping of differentially expressed probesets to genes and functional annotations of the DAVID database was done using the package "clusterProfiler". Over-representation of differentially expressed genes in terms of the category "Biological Process" of the gene ontology system was done using the enrichDAVID()-function of this package. The eight top ranking results of this analysis were displayed as GOcirc-plot using the "GOplot"-package.

The technical assistance of Anja Fleischmann and statistical analysis of Dr. Karsten Jürchott were instrumental to obtain the presented results for this assay.

2.11. RNA Extraction, cDNA Synthesis and Quantitative Polymerase Chain Reaction (qPCR)

Total RNA was extracted from unstimulated and IFNγ pre-stimulated hAACs following 48 hours of incubation using the RNeasy® Mini Kit (QIAGEN, Venlo, Netherlands) according to the manufacturer's protocol. After measuring the RNA concentration with the NanoDrop 2000 spectrophotometer (Thermo Fisher Scientific), cDNA was synthesized. The reverse transcription reaction was performed using TaqMan™ Reverse Transcription Reagents Kit (Invitrogen™, Thermo Fisher Scientific). Briefly, the following components were combined to perform a 20 µL reaction volume: nuclease-free water plus total RNA (1000 ng/µL), RNase inhibitor (20 U/µL), Mg_2Cl, 10x RT Buffer, Random Hexamer Primer Mix (50 µM), dNTP Mixture (2.5 mM each dNTP) and Reverse Transcriptase (RT; 50 U/µL). Samples were incubated for 30 minutes at 48°C, 5 minutes at 95°C and subsequently cooled down at 4°C with a Thermo Flex Cycler Block (Analytik Jena, Jena, Germany). After the RT-PCR the concentration of the generated cDNA was measured with the NanoDrop 2000 to ensure a functional template for the subsequent qPCR. The qPCR was performed on a QuantStudio 6 Flex Real-Time PCR machine (Applied Biosystems, Thermo Fisher Scientific) using the SensiMix™ SYBR No-ROX kit (Bioline, London, UK). The thermal cycling conditions were comprised of a 95°C initial template denaturation for 20 seconds, followed by 40 cycles of PCR by applying 95°C for 15 seconds and 60°C for 20 seconds. Lastly, a final melt curve stage with 40 cycles comprising of 95°C for

15 seconds, 60°C for 60 seconds and 95°C for 15 seconds was performed. Three technical replicates of each sample were analyzed for gene expression of *IDO1, LGALS9, TLR3, PD-L1, PD-L2, PTGS1, HLA-G* and *VCAM1*. All the used primer sequences are provided in **Table 3**. The samples were normalized to the expression of the house-keeping gene *HPRT* and data were analyzed using the delta-delta Ct (ΔΔCt) method. The final results are therefore calculated as fold change of target gene expression in IFNγ pre-treated hAAC samples relative to the unstimulated hAAC reference samples to demonstrate upregulation of differentially expressed genes.

2.12. Statistical Analysis

Statistical analysis and graph generation was performed with GraphPad Prism 8.0 (Graphpad Software, La Jolla, USA). Since all data sets in this thesis were n ≤ 10, statistical analyses were chosen that do rely on non-parametric distribution. Therefore, statistical differences between two groups with only one variable were analyzed using the Mann-Whitney non-parametric t test. For more than two groups with multiple variables, Kruskal Wallis one-way analysis of variance (ANOVA) with Dunn's post tests were applied. Statistical differences between two or more groups with more than two variables were analyzed using an ordinary two-way ANOVA with the Sidak's post test. All results are shown as mean ± SEM and asterisks were assigned to the *p* values in the following order: *$*p \leq .05$; ** $p \leq .01$; ***$p \leq .001$; ****$p \leq .0001$*.

Table 3. Overview of primer sequences for selected immunomodulatory genes. This table was adopted from the preceding publication [1].

Gene	Forward Primer (5' → 3')	Reverse Primer (3' → 5')
IDO1	CGGTCTGGTGTATGAAGG	CTAATGAGCACAGGAAGTTC
LGALS9	CACACATGCCTTTCCAGAAG	AAGAGGATCCCGTTCACCAT
TLR3	ATCTGTCTCATAATGGCTT	AGAAAGTTGTATTGCTGGT
PD-L1	GGCATCCAAGATACAAACTCAA	CAGAAGTTCCAATGCTGGATTA
PD-L2	GAGCTGTGGCAAGTCCTCAT	GCAATTCCAGGCTCAACATTA
PTGS1	TGTTCGGTGTCCAGTTCCAATA	ACCTTGAAGGAGTCAGGCATG AG
HLA-G	TTGGGAAGAGGAGACACGGAACA	AGGTCGCAGCCAATCATCCAC
VCAM1	CGTCTTGGTCAGCCCTTCCT	ACATTCATATACTCCCGCATCCTTC
HPRT	AGTCTGGCTTATATCCAACACTTC	GACTTTGCTTTCCTTGGTCAGG

3. Results

The following results and discussion sections of this thesis are revised, partial results of the preceding publication [1].

3.1. Cryopreserved hAACs Show Stable and Unique Properties for a Mesenchymal Stromal-Like Cell Subset

The limited success of cell-based therapies for cardiac repair over the last decades underlines the serious need for a thorough pre-clinical characterization of new cell products before clinical translation. Therefore, hAACs, generated from eight human atrial appendages, were cryopreserved for at least six months to mimic conditions of a cell bank and were subsequently defined according to the ISCT classification criteria for MSCs.

Firstly, thawed hAACs adhered to plastic after 12 hours in standard cell culture conditions and revealed the typical morphology of cells from mesenchymal origin with elongated cell bodies and fibroblast-like appearance (**Figure 7**).

Secondly, all tested hAAC donors expressed most of the known mesenchymal stem- and progenitor cell surface markers including CD29, CD44, CD73, CD105 and CD166.

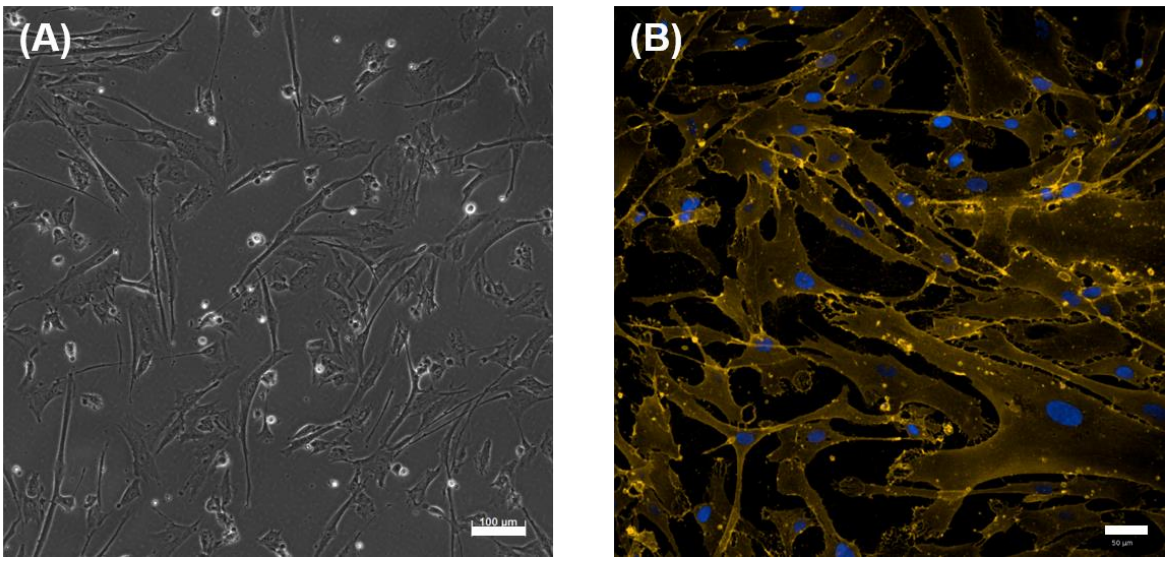

Figure 7. Representative bright-field and fluorescence microscopy images reveal the characteristic morphology of one hAAC donor in a cell culture plate after 12 hours of incubation. Cells were left unstained for bright-field image acquisition **(A)**, while cell membranes (orange) were stained with wheat germ agglutinin (WGA) and nuclei (blue) with 4,6-diamidin-2-phenylindol (DAPI) for fluorescence-based microscopy **(B)**. Scale bar for the bright-field image represents 100 µm **(A)** and for the fluorescence image 50 µm **(B)**. This figure was partly adopted and modified from the preceding publication [1].

Conversely, hAACs lacked expression of endothelial (CD31) and hematopoietic (CD14, CD34, CD45) surface markers as well as of the cardiac progenitor marker c-kit (CD117) (**Figure 8A**). However, divergent from the ISCT criteria for MSCs, only a small percentage of cells in the hAAC product expressed the surface marker Thy-1 (CD90) (**Figure 8B**). Interestingly, this unique surface marker

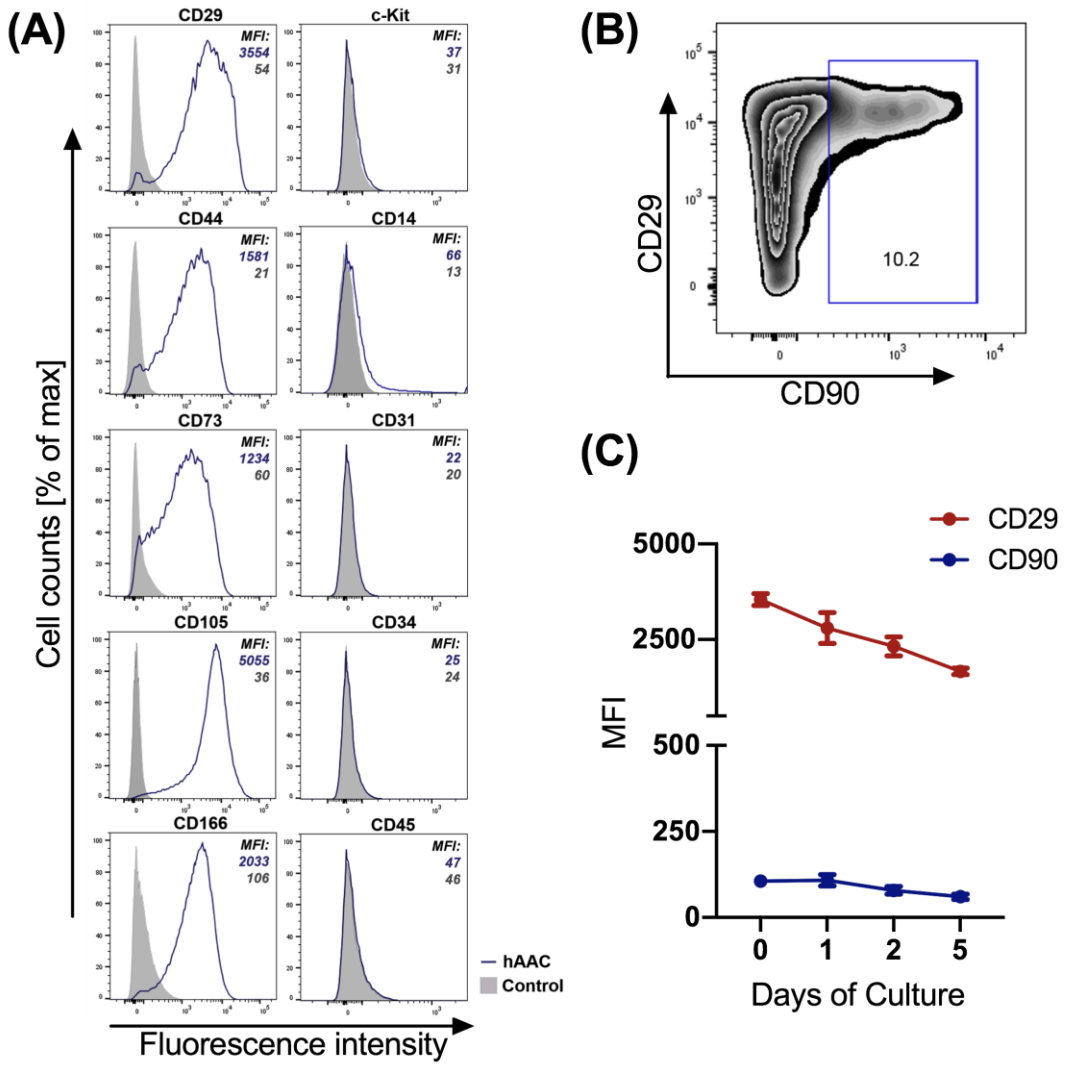

Figure 8. Expression of characteristic MSC markers on hAACs. **(A)** Expanded hAACs were harvested by treatment with trypsin after passage four and stained with human-specific antibodies against surface markers characteristic for cells of mesenchymal origin (CD29, CD44, CD73, CD105, CD166), markers for exclusion of hematopoietic contaminants (CD14, CD31, CD34, CD45) and the cardiac progenitor marker c-kit (CD117). Representative flow cytometry histograms of one hAAC donor are shown as fluorescence intensity against cell counts for all tested markers, indicating the mean of fluorescence intensity (MFI) of marker positive cells (blue) compared to the unlabeled controls (grey). **(B)** The percentage of remaining $CD90^+$ cells in the hAAC cell product is shown for one representative donor in a dot plot of CD90 against CD29. **(C)** Cells were either stained directly after thawing (day 0) or were cultured for one, two and five days. After harvest by application of trypsin, cells were stained with human-specific antibodies against CD29 (red) and CD90 (blue) and were analyzed by flow cytometry. The MFI of marker expression is presented as mean ± SEM for all time points (n = 6; three independent experiments with six different hAAC donor). This figure was partly adopted and modified from the preceding publication [1].

profile remained relatively stable in all donors for five days in standard cell culture conditions, as exemplarily shown for the expression of CD29 and CD90, respectively (**Figure 8C**).

Lastly, conventional MSCs commonly feature a tri-lineage differentiation potential. However, our collaboration partners extensively investigated hAACs after isolation and could thereby prove the principal inability of these cells to differentiate into osteoblasts, chondroblasts, or adipocytes *in vitro* (data not shown).

3.2. Inflammatory Priming Conserves the Low Allogenicity and Enhances the Immunomodulatory Potential of hAACs

To assess the immunological properties of the novel hAAC product *in vitro*, the following mono- and co-culture experiments were carried out in standard cell culture conditions, and after 48 hours of pro-inflammatory pre-conditioning with 100 ng/mL IFNγ. To mimic the environmental site after cardiac injury, IFNγ was selected as one of the most potent pro-inflammatory cytokines. Besides, “licensing” with IFNγ is a commonly exploited strategy to alter the immune phenotype and enhance the immunosuppressive potential of cell products prior to clinical application. The experimental focus was divided into: (I) detection of the immune phenotype by FACS, (II) monitoring of the induction of allogeneic T cell responses, and (III) examination of the immunomodulatory capacity of hAACs in PBMC co-cultures.

(I) To determine the capacity of hAACs to induce allogeneic immune responses, the expression of a set of immunologically relevant surface markers – including HLA-class-I and class-II, as well as co-stimulatory molecules – was analyzed. Stimulation of all six hAAC donors with IFNγ for 48 hours caused similar changes in their surface marker expression profile as seen in the FACS overlay plots for one representative donor (**Figure 9A**), summarized data displayed as normalized MFI values (**Figure 9B**), as well as percentages of marker positive cells (**Figure 9C)**. In standard cell culture conditions, all donors expressed HLA-class-I (HLA-ABC and partly HLA-E), were negative for HLA-class-II (HLA-DR) and lacked expression of the co-stimulatory molecules CD80 and CD86 (**Figure 9B,C**). Notably, all hAAC donors expressed the co-inhibitory molecules PD-L1 and PD-L2 on a specific proportion of their cells (**Figure 9B,C**). Treatment with IFNγ significantly upregulated the expression of HLA-class-I and class-II molecules, as well as of the co-inhibitory molecules PD-L1

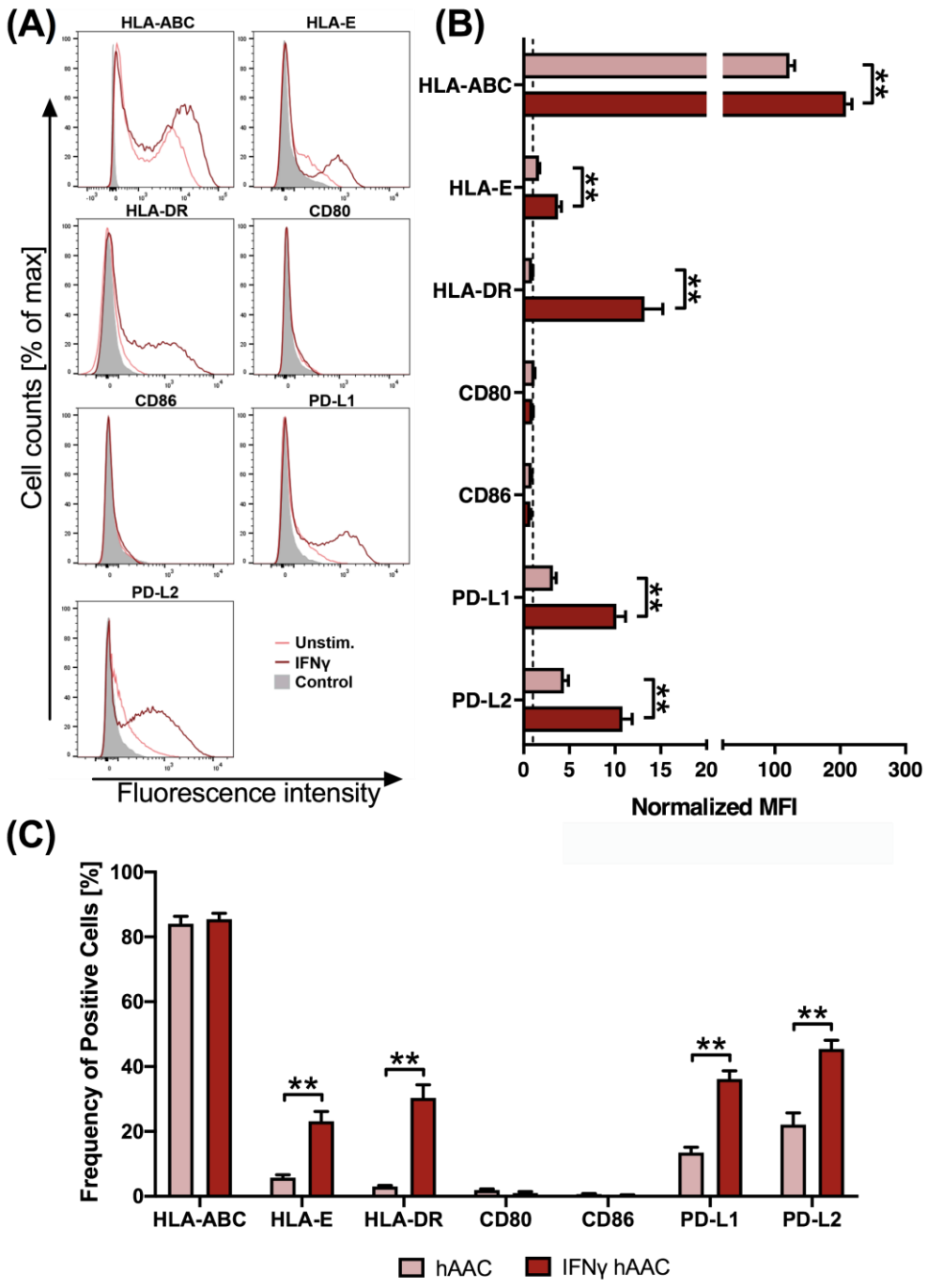

Figure 9. Immune phenotype of cryopreserved hAACs under constitutive and inflammatory conditions. **(A)** Representative histogram overlays for one hAAC donor display the expression pattern for immunologically relevant surface markers (HLA-ABC, HLA-E, HLA-DR, CD80, CD86, PD-L1, PD-L2). Cells were cultured for 48 hours without additional stimulation (hAAC; light red line) or in presence of 100 ng/mL human interferon-gamma (IFNγ hAAC; dark red line). After harvest by application of trypsin, cells were stained with human-specific antibodies and analyzed by flow cytometry. Fluorescence intensity of marker expression is presented compared to the unlabeled control (Control; filled grey curve). Summarized hAAC surface marker expression data are either presented as normalized mean of fluorescence intensities (MFI), that are calculated based on the respective controls (set to one; dashed black line) **(B)**, or as percentage of marker positive cells **(C)**. Results are shown as mean + SEM (n = 6; three independent experiments with six different hAAC donors). Differences between unstimulated hAACs and IFNγ hAACs were considered significant when $**p \leq .01$ with the Mann-Whitney t-test. This figure was adopted and modified from the preceding publication [1].

and PD-L2 (**Figure 9B,C**). Interestingly, the pre-conditioning with IFNγ did not increase the expression of the co-stimulatory molecules CD80 and CD86 (**Figure 9B,C**).

(II) To investigate whether hAACs induce allogeneic T cell responses, HLA-mismatched PBMCs were co-cultured *in vitro* with hAACs from six different donors. Since the T cell responses triggered by MSCs and HUVECs have been well-described in the literature, both cell types were used in this assay as cellular reference controls for absent or induced immune responses, respectively. In standard cell culture conditions, HUVECs induced proliferation of $CD8^+$ T cells, but had indeed no significant effect on the induction of the $CD4^+$ T cell fraction (**Figure 10A,B)**. As expected, pre-conditioning with IFNγ for 48 hours resulted in greatly elevated levels of $CD4^+$ and $CD8^+$ T cell proliferation. In accordance with the considerable proliferation after IFNγ pre-treatment, T cells also show a stronger activation, which is indicated by the significantly increased percentage of HLA-DR^+ T cells (**Figure 10C**). Contrarily, presence of MSCs caused no detectable T cell proliferation, regardless of whether MSCs have been pre-conditioned with IFNγ or were left unstimulated (**Figure 10A,B**). Analogous to the tested MSCs, unstimulated and IFNγ pre-conditioned hAACs also demonstrated low immunogenic characteristics due to the absence of induced allogeneic $CD4^+$ or $CD8^+$ T cell responses (**Figure 10A,B**). Furthermore, both, MSCs and hAACs, did not lead to an activation of T cells, which is shown by the missing HLA-DR expression (**Figure 10C**).

In addition, concentration levels of the cytokines TNFα, IL-10, IL-1β and IL-33 were quantified in supernatants of all co-culture experiments after four days of incubation (**Figure 11)**. In line with the strikingly elevated proliferation, co-cultures of IFNγ pre-conditioned HUVECs revealed significantly increased release of the pro-inflammatory cytokine TNFα. Interestingly, only co-cultures with unstimulated hAACs showed slightly increased levels of IL-10, which significantly decreased when IFNγ pre-conditioned hAACs were used as stimulators. Moreover, hAAC co-cultures in unstimulated and IFNγ pre-treated conditions also showed significantly higher levels for the cytokines IL-1β and IL-33.

(III) Inflammation is considered one of the leading risk factors for the development of cardiac fibrosis and is consequently partially responsible for the onset of chronic heart disease in patients. Therefore, hAACs were tested *in vitro* for their capacity to modulate already ongoing T cell responses in co-cultures with αCD3/αCD28 activated PBMCs.

Again, MSCs and HUVECs were used as reference controls in this assay due to their well-known immunomodulatory capacity or absence of it, respectively. As anticipated, HUVECs, whether IFNγ pre-treated or left unstimulated, did not significantly alter the

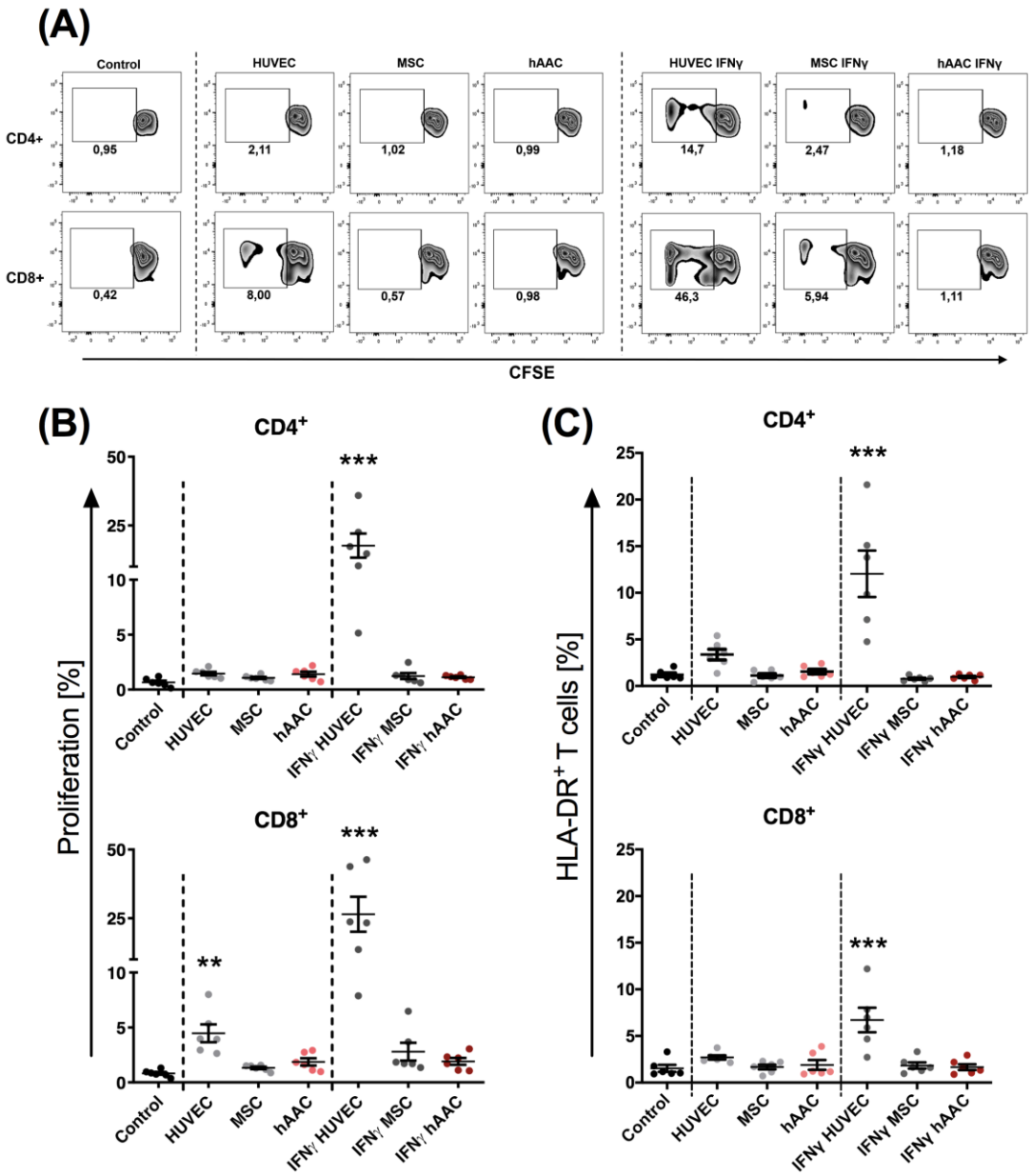

Figure 10. Immunogenicity of hAACs in comparison to MSCs and HUVECs. MSCs as well as HUVECs served as cellular controls and were cultured along with hAACs for 48 hours in the presence or absence of 100 ng/mL IFNγ. HLA-mismatched PBMCs were either added to the adherent cell cultures of all three cell types or left alone as controls. After seven days of co-culture PBMCs were harvested, stained with human immune cell specific antibodies, and analyzed flow cytometrically. **(A)** Representative flow cytometry plots of proliferated $CD4^+$ and $CD8^+$ T cells are shown for all PBMC co-culture groups and PBMCs only (Control). Summarized proliferation data for $CD4^+$ and $CD8^+$ T cells **(B)** as well as the percentage of HLA-DR^+ T cells **(C)** are presented as mean ± SEM (n = 6; three independent experiments with six different hAAC donor). Groups were considered significantly different compared to the Control when $^{***}p \leq .001$ with Kruskal Wallis ANOVA and Dunn's post-test. This figure was adopted and modified from the preceding publication [1].

proliferation rates of activated $CD4^+$ or $CD8^+$ T cells after 72 hours of co-incubation (**Figure 12A,B**). Although, the presence of MSCs and hAACs in standard cell culture conditions caused a slight reduction of T cell proliferation, these effects were indeed not significant. In contrast, the pre-treatment with IFNγ facilitated MSCs and hAACs to dramatically suppress the proliferation of both, $CD4^+$ and $CD8^+$ T cells, well below 10 % (**Figure 12A,B**). To analyze whether the observed immunomodulatory effects were mediated through contact-dependent mechanisms, experiments were repeated exclusively for hAACs under transwell conditions. While no change in T cell proliferation was detectable in the presence of untreated hAACs in transwell settings, IFNγ pre-conditioning induced a significant decrease in proliferation of both T cell subsets to 20 % in average (**Figure 12C)**.

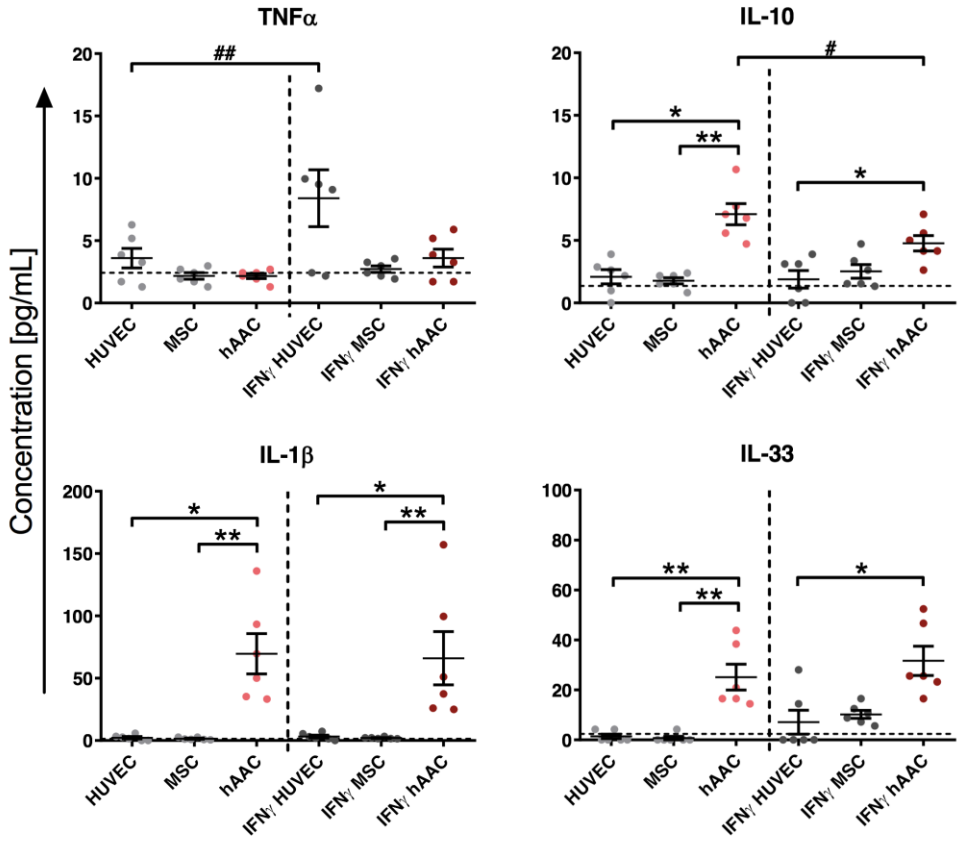

Figure 11. Quantification of cytokine release from hAAC, MSC and HUVEC co-cultures with HLA-mismatched PBMCs after four days of incubation. Cytokine levels in [pg/mL] for TNFα, IL-10, IL-1β and IL-33 were measured using the Legendplex™ human inflammation panel and are shown as mean ± SEM (n = 6; three independent experiments with six different hAAC donor). Cytokine levels of the PBMC control groups are depicted as dotted grey line. Groups were considered significantly different when *$p \leq .05$; **$p \leq .01$ with Kruskal Wallis ANOVA and Dunn's post-test. Differences between treatments were considered significant when #$p \leq .05$; ##$p \leq .01$ with ordinary two-way ANOVA and Sidak's post-test. This figure was adopted and modified from the preceding publication [1].

Additionally, supernatants of the hAAC co-culture experiments in direct-contact settings were measured after 72 hours to analyze the composition of secreted cytokines (**Figure 13**). Presence of untreated hAACs already lowered the concentration of the pro-inflammatory cytokines IFNγ and TNFβ significantly. These effects were further enhanced in co-cultures with IFNγ-licensed hAACs that also showed significantly diminished levels of the pro-inflammatory cytokines TNFα and IL-17A as well as of the immunomodulatory cytokine IL-10.

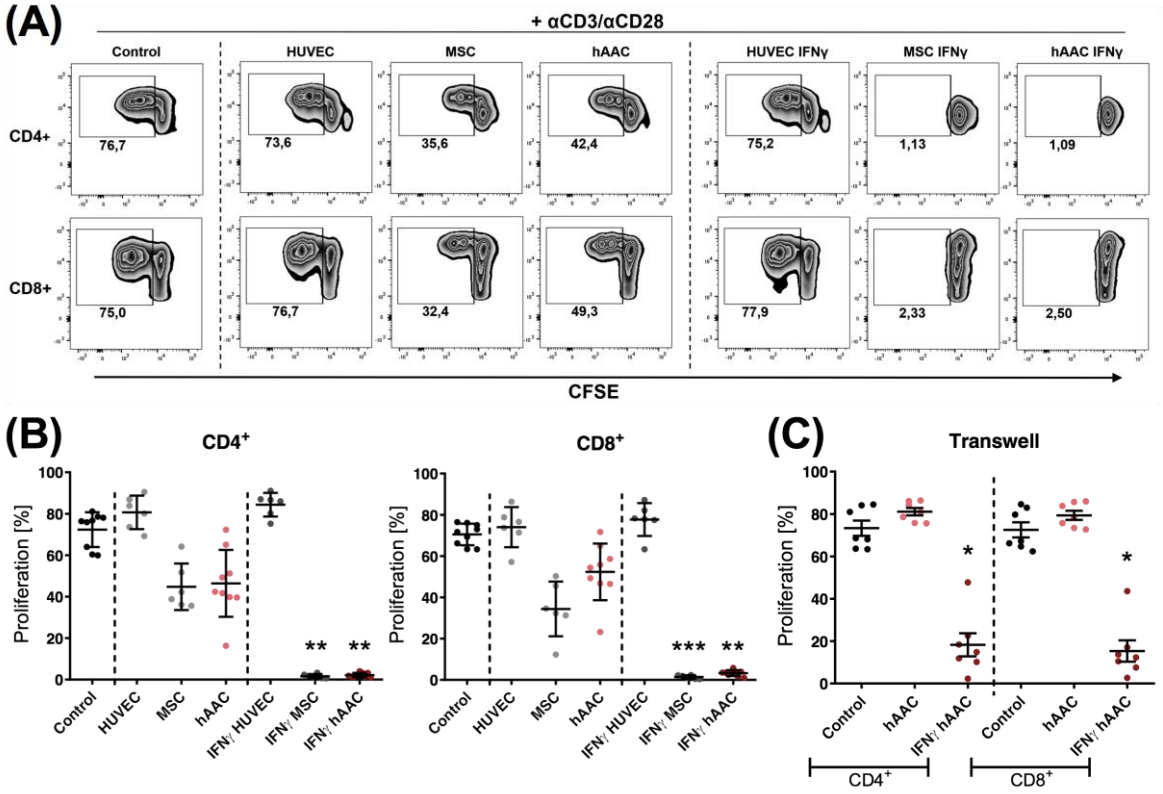

Figure 12. Immunomodulatory capacity of hAACs in comparison to MSCs and HUVECs. CFSE-labeled PBMCs were activated with anti-CD3/anti-CD28 antibodies (+αCD3/αCD28) and cultured alone (Control) or in the presence of unstimulated or IFNγ pre-stimulated hAACs, HUVECs or MSCs for 72 hours. Cells were harvested, stained with human-specific antibodies, and analyzed by flow cytometry for T cell proliferation, based on reduced CFSE signal intensity. Percentages of $CD4^+$ or $CD8^+$ proliferated cells for all experimental groups are shown as representative zebra plots **(A)** and as summarized data with mean ± SEM **(B)** (n = 6 – 9; four independent experiments with seven different hAAC donors). **(C)** Experimental settings were repeated with hAACs under transwell culture conditions to evaluate a contact-dependent mode of action in the observed immune-modulatory effects (n = 7; three independent experiments with six different hAAC donors). Groups were considered significantly different when *$p \leq .05$; **$p \leq .01$; ***$p \leq .001$ with Kruskal Wallis ANOVA and Dunn's post-test. This figure was adopted and modified from the preceding publication [1].

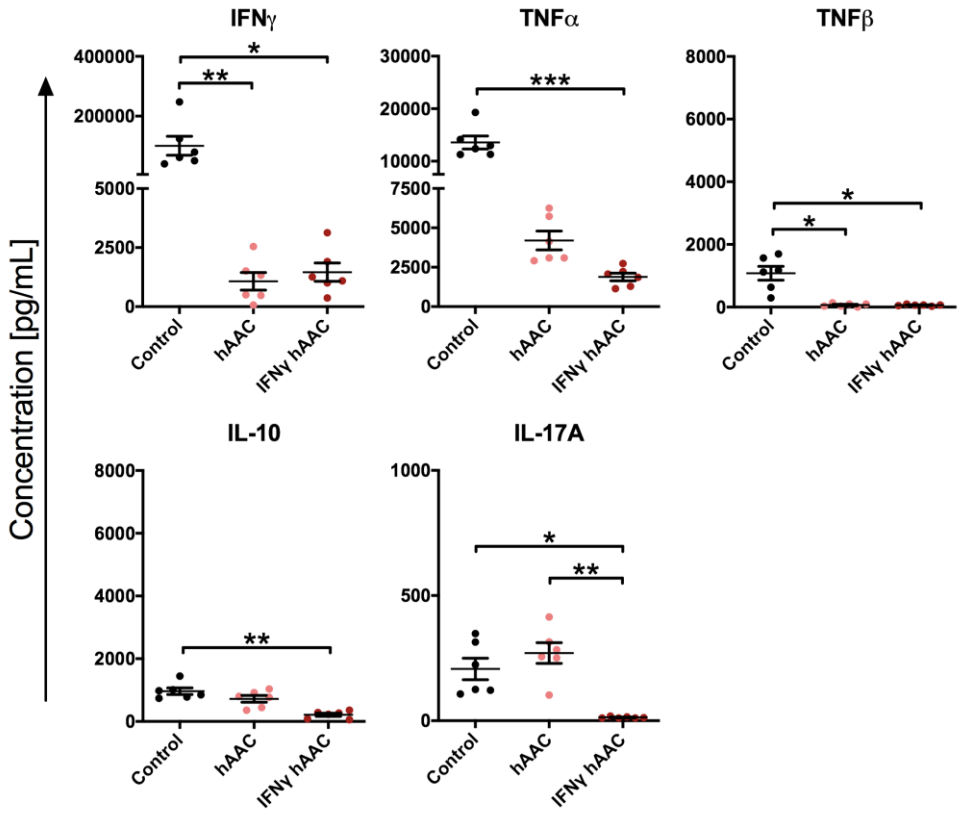

Figure 13. Quantification of cytokine release from hAAC co-cultures with αCD3/αCD28-activated PBMCs after 72 hours. Supernatants of the direct immune cell co-cultures with either unstimulated or IFNγ-treated hAACs were analyzed with a Luminex bead assay for their content of IFNγ, TNFα, TNFβ, IL-10 and IL-17A. Summarized data for cytokine concentrations [pg/mL] are presented as mean ± SEM (n = 6; three independent experiments with six different hAAC donors). Groups were considered significantly different when *$p \leq .05$; **$p \leq .01$; ***$p \leq .001$ with Kruskal Wallis ANOVA and Dunn's post-test. This figure was adopted and modified from the preceding publication [1].

3.3. The Expression of IDO Is Essential for the Immunomodulatory Function of IFNγ-Licensed hAACs

It is vital to gain profound insights into the observed immunomodulatory function of promising cell types like hAACs to understand their underlying mode of action and thereby discover new possibilities to enhance the therapeutic efficacy in the future. To identify involved molecular candidates, whole genome gene expression of hAACs from three different donors were screened after 48 hours in standard cell culture conditions or after IFNγ treatment on human hgu133plus2 microarrays. Normalized data with the 1000 most variable probe sets revealed a strong separation of unstimulated and IFNγ pre-treated samples in the first principal component, as anticipated. The differences of hAAC donors in the principal component two indicate some biological heterogeneity in gene expression between the unrelated donors (**Figure 14A**). Despite those differences in individually expressed genes, all donors predominantly shared a

universal response to the stimulation with IFNγ as illustrated in the heatmap (**Figure 14B**). Subsequently, differently expressed probe sets were used in an overrepresentation analysis with the gene ontology system. Interestingly, the eight top-ranking results of the category “biological process” were all related to the immune

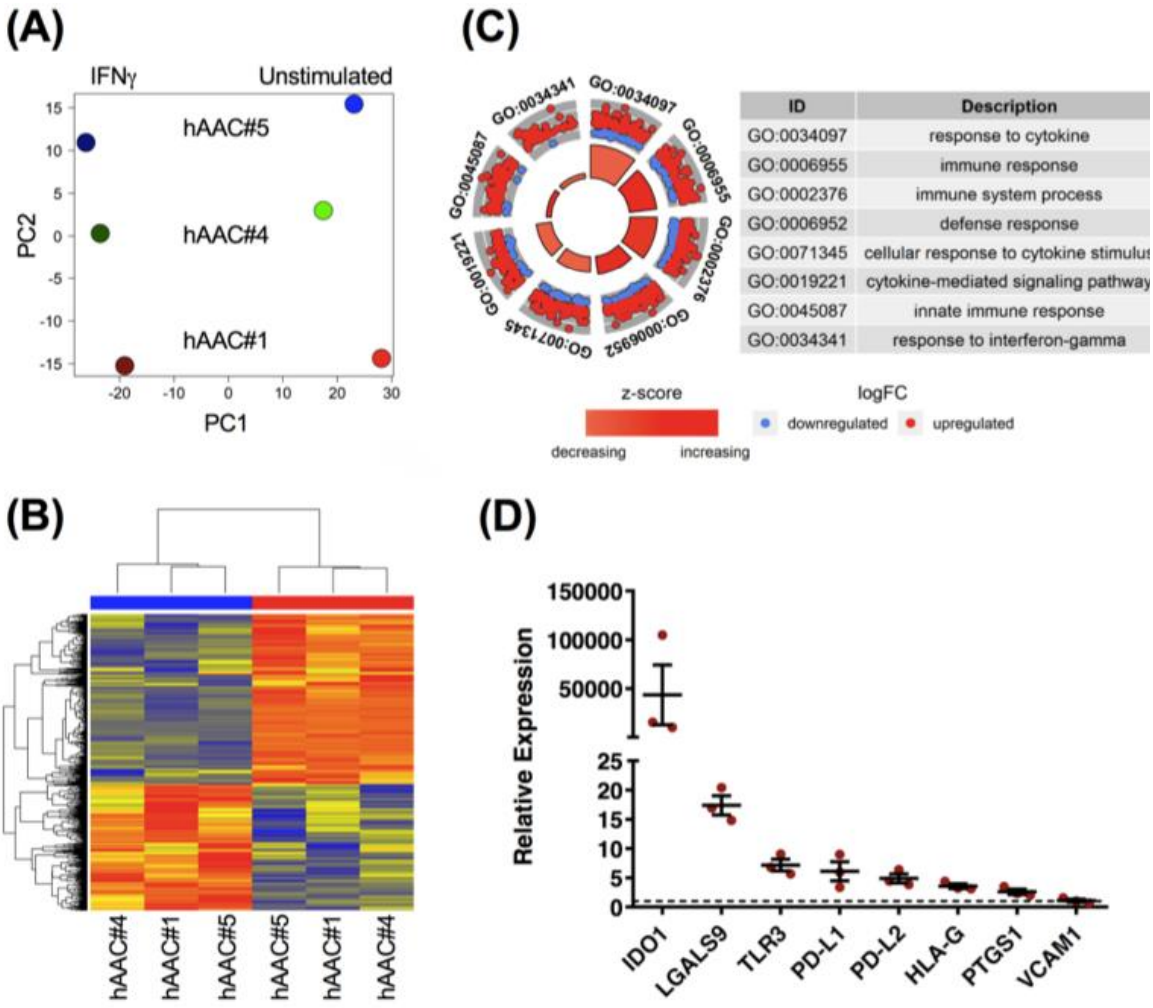

Figure 14. Whole genome gene expression analysis and quantitative verification of immunomodulatory gene expression of unstimulated and IFNγ pre-treated hAACs. **(A)** Microarray expression data of unstimulated and IFNγ-stimulated hAACs were normalized and log2-transformed. 1000 probe sets with the highest variances across all samples were selected and used in a principle component analysis, showing PC1 versus PC2 for n = 3 hAAC donors (#1, #4, #5). **(B)** Differentially expressed probe sets were determined by fitting linear models to the data and apply Bayesian statistics. P-values were adjusted for multiple testing using false discovery rate. Probe sets with an adjusted p-value below .05 and a minimal absolute log2-foldchange of 1 are shown in the heatmap. The blue column bar indicates the unstimulated and the red bar the IFNγ pre-stimulated hAACs of donors #1, #4, #5. **(C)** Differentially expressed probe sets were used in an overrepresentation analysis utilizing the gene ontology system. The eight top-ranking results of the category biological process are shown. **(D)** The differentially expressed immunomodulatory genes *IDO1, LGALS9, TLR3, PD-L1, PD-L2, HLA-G, PTGS1* and *VCAM1*, identified in the global microarray analysis, were validated by qPCR. Values of IFNγ pre-stimulated hAACs were normalized to the unstimulated samples (set to 1; black dotted line) by means of a ΔΔCt analysis and upregulation is shown as mean of relative expression ± SEM for n = 3 hAAC donors (#1, #4, #5). This figure was adopted and modified from the preceding publication [1].

system, cytokine signaling and, understandably, the IFNγ-response with much more up-regulated than down-regulated genes (**Figure 14C**). In a final step, probe sets were checked for differential expression of genes known to be involved in the immunomodulatory function of MSCs. In this process *IDO1*, *LGALS9*, *TLR3*, *PD-L1*, *PD-L2*, *PTGS1*, *HLA-G*, and *VCAM1* were exposed as differently expressed genes among all three donors that were ultimately validated by qPCR. Strikingly, only *IDO1* showed a remarkable 50.000-fold increase in relative expression on average. In comparison, the upregulation of relative gene expression for *LGALS9*, *TLR3*, *PD-L1*, *PD-L2*, *HLA-G, PTGS1*, and *VCAM1* ranged between 20- and 1-fold increases, respectively (**Figure 14D**).

To prove the mechanistic involvement of *IDO1* and *PD-L1/PD-L2*, which were previously described as one key mechanism in cardiac-derived cells [27] and MSCs [28] likewise, immunomodulatory co-culture experiments were repeated. This time, unstimulated and IFNγ pre-treated hAACs were incubated with blocking reagents against IDO (*i.e.* 1-MT) or against PD-L1/PD-L2 (*i.e.* blocking antibodies; αPD-1 ligands) prior to the supplementation of PBMCs. After 72 hours of co-culture, proliferation as well as apoptosis rates of $CD4^+$ and $CD8^+$ T cells were measured. The presence of unblocked hAACs confirmed the previously described findings by significantly reducing the proliferation of $CD4^+$ and $CD8^+$ T cells after IFNγ pre-treatment (**Figure 15A**). Furthermore, the frequencies of late-apoptotic Annexin-V^+/7-AAD^+ T cells were significantly increased with IFNγ pre-treated hAACs as modulators (**Figure 15B**). Intriguingly, pre-incubation with blocking antibodies against both PD-1 ligands had neither a significant effect on the proliferation nor on the apoptosis rates of both T cell subsets relative to the unblocked hAAC controls (**Figure 15A,B**). Blocking with 1-MT, as specific inhibitor of IDO, on the other hand caused a significant restoration of T cell proliferation in presence of IFNγ pre-treated hAACs compared to the unblocked controls **(Figure 15A)**. Concurrently, unstimulated 1-MT treated hAAC co-cultures displayed reduced proliferation rates for both T cell subsets (**Figure 15A**). Inversely, 1-MT pre-incubation resulted in lowered apoptosis rates for the IFNγ-hAAC cultures in contrast to the unblocked controls **(Figure 15B)**. 1-MT treatment also reduced the levels of $CD8^+$ T cell apoptosis in unstimulated and IFNγ-treated co-cultures to non-significant levels (**Figure 15B**).

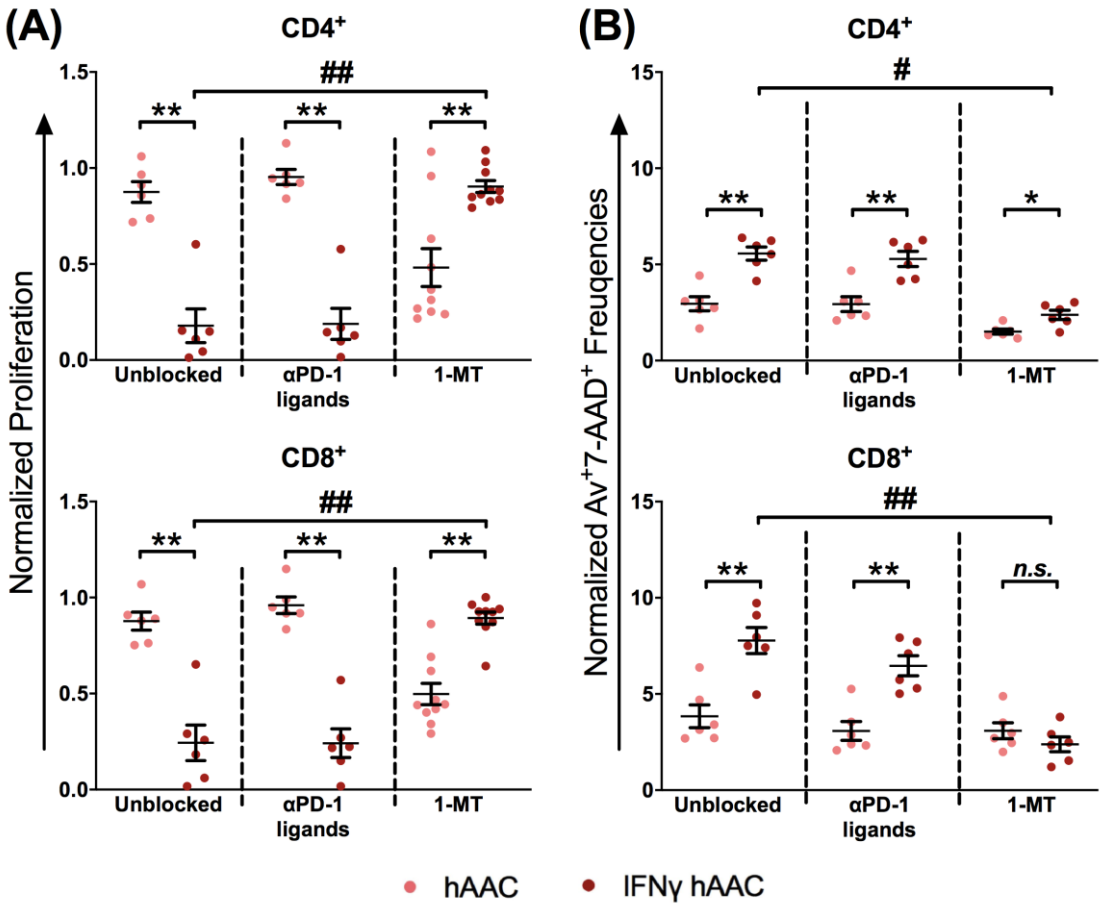

Figure 15. Analysis of the involvement of indolamine-2,3-dioxygenase (IDO) and both programmed death-1 (PD-1) ligands in hAAC-mediated immunosuppression of T cells and their induction of apoptosis. For this, hAACs were pre-treated with 1-mehtyl-L-tryptophan (1-MT) as specific inhibitor of IDO or blocking antibodies against PD-L1 and PD-L2 (αPD1 ligands). Subsequently, αCD3/αCD28-activated PBMCs were either left alone as controls or cultured with hAACs for 72 hours. $CD4^+$ or $CD8^+$ T cell proliferation levels as well as the percentage of Annexin-V^+ 7-AAD^+ late apoptotic cells were determined by flow cytometry. **(A)** The normalized proliferation values for $CD4^+$ or $CD8^+$ T cell subsets were calculated based on the respective PBMC controls and are presented as mean ± SEM (n = 6 – 10; four independent experiments with seven different hAAC donors). **(B)** The normalized percentages of late-apoptotic Annexin-V^+ 7-AAD^+ cells within the $CD4^+$ and $CD8^+$ T cell subsets were calculated based on the respective PBMC controls and are presented as mean ± SEM (n = 6; two independent experiments with six different hAAC donors). Unstimulated (hAAC) and IFNγ-stimulated hAACs (IFNγ hAAC) within the same treatment group were considered significantly different when *$p \leq .05$; **$p \leq .01$ with the Mann-Whitney t-test. Differences between treatments were considered significant when #$p \leq .05$; ##$p \leq .01$ with Kruskal Wallis ANOVA and Dunn's post-test. This figure was adopted and modified from the preceding publication [1].

4. Discussion

Even though, the development of cell-based therapies could demonstrate modest improvements after cardiac injury over the last years, the absence of a revolutionary success story strongly discouraged further and modern innovations to the field [13]. While the extremely fast and premature clinical translation might be one of the major reasons for the shortcomings of cell-based therapies, many scientific questions, particularly regarding the basic understanding of observed positive effects, remained unexplored [13]. Therefore, it is crucial to return to the bench-side and characterize promising cell sources and their subsets to gain a profound understanding of how these cells mediate their regenerative features [16]. The comparison to established cell populations like MSCs from defined sources, might help in this context to classify any measured effects [16]. Furthermore, the development of new approaches for patient selection, time of administration, choosing of appropriate application routes, combination with scaffold-based approaches as well as cell pre-conditioning or genetic manipulation are important scientific avenues that need to be considered for an effective clinical translation of any novel cell product in the future [13,16]. Since an allogeneic application is preferable for its broad availability and comparatively low manufacturing costs, it is indispensable to exclude any unwanted immunogenicity of promising cell types, especially under inflammatory and disease-related conditions [13,22].

In this thesis, the aforementioned issues were addressed by characterizing the allogeneic hAAC product, evaluating the immune phenotype as well as the interaction with cells of the adaptive immune system, and lastly, uncovering the underlying mode of action in the observed immunomodulatory function of hAACs. The presented results provide the first direct evidence for the immunological implications of a $CD90^{low}$ subtype of MSC-like cells derived from the right atrial appendage (hAACs). The hAAC product displayed an inherently low immunogenicity that is maintained or even enhanced under inflammatory conditions. Strikingly, hAACs also exerted strong immunomodulatory effects like MSCs. Pre-treatment with the pro-inflammatory cytokine IFNγ potentiated the mostly paracrine mode of immunosuppression and led to the identification of IDO as the main player of the observed effects. Altogether, hAACs represent a promising allogeneic cellular treatment option for a future therapeutic application in cardiovascular diseases.

To date, mainly stem cell-derived cardiomyocytes, CPCs and MSCs have been used in clinical studies for the treatment of cardiac injury. To ensure comparability of novel cell types to those previously published ones, it is necessary to thoroughly characterize the cellular properties according to standardized protocols [16]. Here, the hAAC product was checked for principal MSC hallmarks according to the ISCT criteria [17]. Although, hAACs share a similar and stable surface marker profile with MSCs, they are in contrast intrinsically unable to differentiate into osteoblasts, chondroblasts, or adipocytes *in vitro* (data not shown). The absence of a tri-lineage differentiation potential was recently reported by Oldershaw and colleagues for another MSC-like subpopulation derived from the atrial appendage [29]. Yet, hAACs uniquely express the surface marker CD90 only on a low level due to the required negative selection process. Interestingly, absence of CD90 was already shown to be directly involved in the inability of MSCs to differentiate into specific lineages [30]. Besides, a clinical trial with cardiosphere-derived CPCs could negatively correlate the expression of CD90 with a worsened clinical outcome, as seen in enhanced cardiac fibrosis of patients [26]. In addition, hAACs lacked the expression of cardiac progenitor markers like c-kit that are thought to be key mediators of the regenerative function of conventional CPC products [12]. In conclusion, hAACs should be considered a novel and unique MSC-like cell subset that might have comparable or enhanced beneficial effects in future clinical applications for cardiac disease.

The immune phenotype of an allogeneic cell product contributes to its immunogenicity after cell transplantation [31]. Consequently, it is necessary to evaluate expression of immunological-relevant surface markers under basal and inflammatory conditions for every potential cell type. In this thesis, the FACS analysis of the hAAC product revealed a low immunogenic phenotype by expression of HLA-class-I (HLA-ABC and partly HLA-E) and absence of HLA-class-II (HLA-DR) as well as of co-stimulatory molecules (CD80 and CD86). However, the *de novo* induction of HLA-DR and further increase of HLA-ABC expression, after pre-treatment with the pro-inflammatory cytokine IFNγ, might pose the risk of allorecognition by the recipient's immune system after cell transplantation [31]. Then again, the co-stimulatory molecules remained absent and hAACs additionally expressed and upregulated the co-inhibitory molecules PD-L1 and PD-L2 under inflammatory stimulation that might enable evasion of immune cell detection [28]. This specific surface marker profile is consistent with previously characterized MSCs [14,28] and related CPCs [27,32], but also demands the

continuous investigation for induction of unwanted allogeneic immune responses. There is one notable limitation of all performed *in vitro* experiments with artificial pre-treatment: The inflammatory microenvironment surrounding cardiac injury *in vivo* might have more complex implications on hAACs than the effects of IFNγ as a singular cytokine alone. However, preliminary experiments with a complex and more disease-related cytokine stimulation mix, generated from activated PBMCs, induced a comparable shift of surface marker expression on hAACs as described before (data not shown). Strikingly, this mixture contained a variety of different cytokines, including IFNγ, TNFα, IL-1, IL-6, IL-8, and IL-10. Yet, the quantitative level of IFNγ was comparable to the concentrations used in this thesis, thereby suggesting that IFNγ dominates the inflammatory licensing of hAACs in this particular context.

The subsequent analysis of immune responses in HLA-mismatched PBMC co-cultures revealed that unstimulated and IFNγ pre-treated hAACs efficiently evaded an adaptive immune response, as seen in the low induction of $CD4^+$ and $CD8^+$ T cell proliferation. This observation confirms the low immunogenicity of hAACs that was already assumed by the measured surface marker profile. Even though the exposed T cell response pattern was similar to the in parallel tested MSCs, both cell types clearly differed in their profile of secreted cytokines. Hence, it might be likely that hAACs exert their immune evasive effects through a differing mode of action, despite their common mesenchymal heritage. While only pre-stimulated HUVEC co-cultures induced release of the pro-inflammatory cytokine TNFα, as a “proof-of-principle” in this assay, hAAC co-cultures alone demonstrated slightly elevated levels of the anti-inflammatory cytokine IL-10. Certainly, it suggests that the appearance of IL-10 might be linked to the induction of a $FoxP3^+$ regulatory T cell subset. However, no evidence for this assumption could be uncovered in preliminary experiments (data not shown). Our speculation, as of now, is that non-classically activated monocytes might be responsible for the observed IL-10 secretion, as already described for other MSC sources [33]. Moreover, exclusively hAAC co-cultures exhibited elevated levels of the pro-inflammatory cytokines IL-1β and IL-33. Further mono-culture experiments revealed that both cytokines were in fact self-produced and secreted by hAACs (data not shown). Apart from a classical inflammatory role, cytokines of the IL-1 family seem to also fulfill some regulatory functions. IL-1β release of MSCs, for instance, was shown to be linked to the monocyte-dependent regulation of T cell activation [34]. Whereas IL-33 might be involved in promoting the establishment of immune evasive

environments as reported for specific tumor entities [35]. The low induction of allogeneic T cell responses in hAAC co-cultures are in accordance with previous studies that analyzed the immunological properties of c-kit sorted $CD90^+$ CPCs [27]. Therefore, the expression of CD90 seems to play an inferior role in the immunological function of cardiac-derived cell products. Unlike Lauden and colleagues, who suggested induction of regulatory $FoxP3^+$ T cells as the main mode of immune cell evasion in c-kit^+ CPCs [27], we hypothesize that the hAAC product might mediate its effects through activation of non-classical monocytes. This claim is further substantiated by a study of our group which demonstrated that extracellular vesicles, derived from the related CardAP cells, prime $CD14^+$ monocytes towards a regulatory phenotype with immunosuppressive functions [36].

Since cardiac inflammation has gained increasing interest as an independent risk factor for the development of heart disease [4], it is imperative to determine the immunomodulatory capacity of promising candidates for cell-based therapies. In this thesis, it could be shown that hAACs are potent modulators of ongoing adaptive immune responses, analogous to the also tested MSCs. However, one limitation of the utilized *in vitro* co-cultures is that the defined ratios of modulator cells to responder PBMCs notably influence the effectiveness of the tested modulator cell type. Despite this limitation, the applied study design has the key advantage that MSCs and HUVECs have been used as reference control cells, which enables the comprehensible classification of observed effects and allows inferences to its clinical significance. Comparatively, the sharp suppression of $CD4^+$ and $CD8^+$ T cell proliferation in presence of IFNγ-licensed hAACs have been already described for MSC populations from other tissues [14,37]. Although, the results presented in this thesis indicate that hAACs and umbilical cord-derived MSCs share equally strong immunosuppressive tendencies, no clear similarities between human c-kit^+ CPCs and bone marrow-derived MSCs were detectable as reported by Lauden and colleagues [27]. The apparent discrepancies may be due to the different cell sources or the diverging experimental setup, including the dissimilar T cell stimulation or mixed lymphocyte reaction settings. The outlined downregulation of T cell proliferation in hAAC co-cultures was additionally accompanied by a strong suppression of the pro-inflammatory cytokines IFNγ, TNFα, TNFβ, and IL-17A. Again, these effects were greatly enhanced with IFNγ pre-treated hAACs as modulators. The common shift from a pro-inflammatory secretion profile towards an anti-inflammatory one upon IFNγ-stimulation was previously described for

various MSCs [14] and CPCs [22]. Contrary to the reported factor release of MSCs in activated immune cell co-cultures, hAACs rather lowered the levels of anti-inflammatory cytokines like IL-10 [14]. We hypothesize that the strong decrease of IL-10 to comparatively low levels is due to the efficient suppression of highly activated effector immune cell subsets, instead of the absence of regulatory cell types. However, this speculation can only be verified by an intracellular cytokine staining. Moreover, to test for contact-dependency in the performed immunomodulation assays, co-culture experiments were repeated under transwell settings. In this context, IFNγ-licensed hAACs suppressed the ongoing T cell responses in direct contact as well as transwell settings almost to the same extent, implying a paracrine mode of action in an inflammatory milieu. A surprising finding was that the suppressive tendencies of unstimulated hAACs completely receded to the control levels under transwell conditions. These findings add weight to the notion that additional contact-dependent mechanisms might contribute in a minor but insignificant manner to the overall modulatory potency. While some evidence for c-kit$^+$ CPCs suggest a primarily contact-dependent mechanism of immunomodulation [27], hAACs seem to exert their modulatory functions predominantly through secretion of soluble factors and/or vesicles after IFNγ-licensing. Similar conclusions were also reported for MSCs from various tissues [14].

Lastly, to gain a more profound understanding of the specific mediators involved in the observed immunomodulatory activity, three hAAC donors were screened for molecular changes in a global genome gene expression microarray after IFNγ pre-treatment. The analysis revealed that all three donors responded evenly to the stimulation, despite natural biological heterogeneities in their individual RNA expression profiles. Interestingly, mostly immunological pathways of immune system response, cytokine signaling, and, obviously, IFNγ-response were mainly upregulated among the donors. By comparing differentially expressed genes from the microarray analysis with known immunomodulatory molecules from the literature, several interesting target genes were identified that were ultimately measured for their expression by qPCR. Surprisingly, hAACs showed only for *IDO1* an exceptionally intense upregulation of RNA expression after IFNγ pre-treatment. However, other interesting candidates, such as *LGALS9* (Galectin-9), *TLR3*, *HLA-G*, *PD-L1/PD-L2*, and *PTGS1* (Cyclooxygenase-1), were distinctively upregulated after inflammatory licensing of hAACs, too. Especially IDO is one of the most discussed molecules in the immunoregulatory function of MSCs that

has been shown to moderate T cell function by depletion of tryptophan and accumulation of metabolites like kynurenin [38]. In this thesis, the involvement of IDO in the hAAC-mediated suppression of T cell proliferation and induction of their apoptosis could be conclusively proven by application of the specific inhibitor 1-MT in our mechanistic co-culture experiments. This observation is in line with a recent study that correlated the immunosuppressive capacity of IFNγ-licensed MSCs to the enhanced expression of IDO and PD-L1 [39]. In fact, hAACs also demonstrated intensified expression of the co-inhibitory molecules PD-L1 and PD-L2 on protein and RNA level after inflammatory treatment. Yet, blocking of both PD-1 ligands could neither reverse the suppression of T cell proliferation nor prevent the induction of their apoptosis in our experimental settings. Conclusively, PD-L1 and PD-L2 expression seem to reinforce the immunosuppressive capability of hAACs only in an inferior and insignificant way. This deduction contrasts a recent report of bone marrow-derived MSCs that have been shown to suppress activation and induce anergy as well as apoptosis in T cells through the expression and secretion of PD-L1 and PD-L2 [28]. In addition, Lauden and colleagues also propose a more contact-dependent mode of immunosuppression through the induction of regulatory T cells by the PD-L1/PD-1 axis in c-kit$^+$ CPCs [27]. These results lend further credence to the earlier hypothesis that hAACs represent a unique and distinct MSC-like cell subset with atypical but clinically interesting features.

The results presented in this thesis clearly confirm IDO as the main mechanism of action in hAACs that mediates the efficient immunosuppression of T cells, whereas the role of the immune system's other cell types remain elusive. Therefore, future research should take the interaction of antigen-presenting cells into account to broaden our knowledge on the hAAC/immune cell interplay. The profound understanding of the interaction with the immune system after transplantation will help to discover new scientific avenues for the therapeutic enhancement of cell products like hAACs. In this context, specifically monocytes have been reported to be important players in the establishment of anti-inflammatory environments after interaction with MSCs [33]. Besides, c-kit$^+$ CPCs were already described as potent attractors of monocytes that additionally induced changes in the differentiating macrophages towards a more reparative and immunosuppressive phenotype [40]. Data by our own group also argues for an important contribution of CD14$^+$ monocytes in the immunosuppressive function of cardiac-derived cells. Indeed, the uptake of CardAP-derived extracellular

vesicles induced a shift in monocytes towards a regulatory phenotype with immunosuppressive functions [36]. Moreover, the observed paracrine mode of action in the hAAC product encourages further investigation of its secretome, including the isolation, characterization and use of extracellular vesicles for a clinical application.

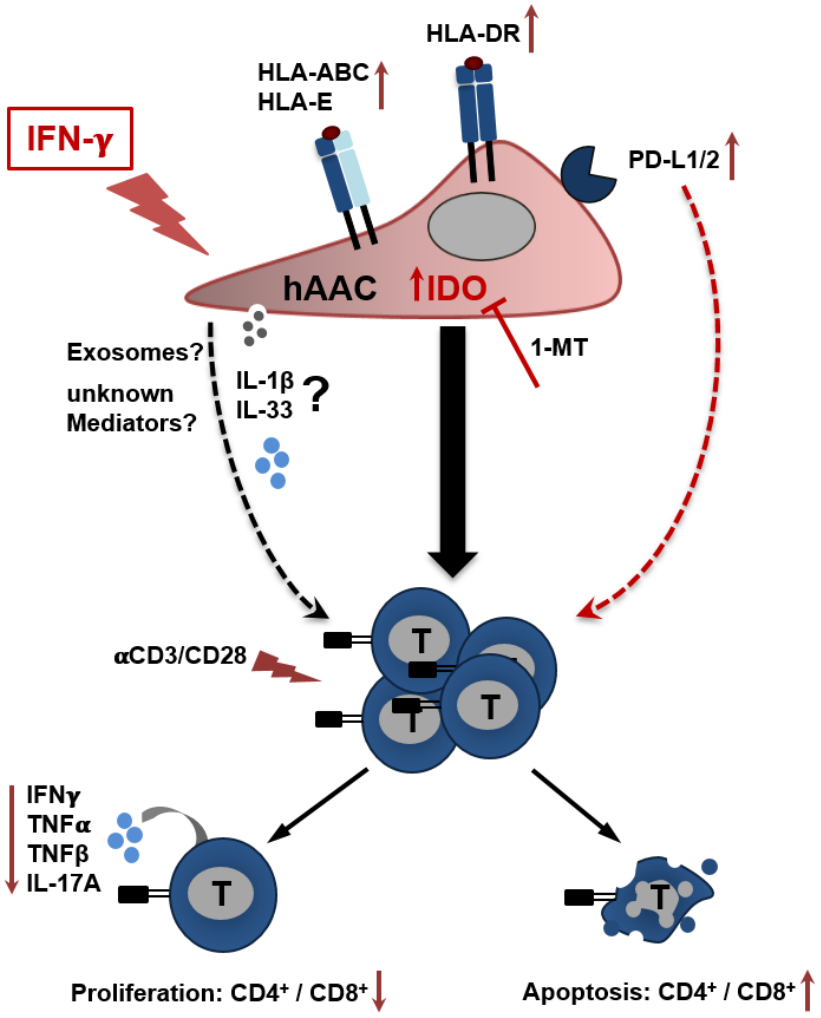

Figure 16. Potential crosstalk between hAACs and T cells in an inflammatory milieu. The scheme illustrates the impact of IFNγ stimulation on CD90^{low} hAACs and its implication on the interplay with αCD3/αCD28 activated human T cells. Stimulation of hAACs alone induces upregulation of HLA-class I (HLA-ABC, HLA-E) and *de novo* expression of HLA-class II molecules (HLA-DR). Even though expression of the inhibitory co-stimulatory molecules PD-L1 and PD-L2 is enhanced on the cell surface, no specific effects in the interaction with activated T cells were detectable. Similarly, the role of the specific secretion of IL-1 family cytokines (IL-1β, IL-33) by hAACs and additional unknown mediators like exosomes remain unclear. However, a global genome-wide expression profile analysis revealed IDO as one of the strongest expressed genes in IFNγ stimulated hAACs. Specific blocking with 1-MT proved the essential involvement of IDO in the interaction with T cells. It mediates the suppression of CD4$^+$ and CD8$^+$ T cell proliferation, reduces the secretion of pro-inflammatory cytokines (IFNγ, TNFα, TNFβ, IL-17A) and induces apoptosis of both T cell subsets. We hypothesize, that this mode of hAAC interaction might contribute to the resolution of immune responses and limit thereby the effects of adverse remodeling after cardiac injury. This figure was adopted from the preceding publication [1].

Ultimately, development of innovative solutions that combine well-described cell products, such as hAACs, with modern approaches, like tissue engineered scaffolds or genetic cell manipulation, are needed to ensure a safe and effective translation of cell-based therapies in the future [13,16].

The present thesis provides the first direct evidence for the immunological implications of a so-far unrecognized $CD90^{low}$ MSC-like cell subset with clinically interesting features, such as a potential allogeneic “off-the-shelf” availability. Most importantly, hAACs do not induce allogeneic immune responses based on their low immunogenic phenotype after IFNγ-licensing, as seen by moderately low expression of HLA-DR and absence of co-stimulatory molecules. Moreover, hAACs are potent modulators of ongoing immune responses especially in inflammatory environments. Lastly, we could identify IDO as the key molecule of action in the observed immunomodulatory function of hAACs after IFNγ pre-treatment (**Figure 16**). Thus, the presented data not only suggests the safety of the hAAC product for an allogeneic application, but also indicates its compelling potential to limit adverse remodeling after cardiac injury by effectively modulating the misdirected immune system. We therefore recommend the novel hAAC product, as a promising allogeneic treatment option, for the future application in patients suffering from cardiac disease.

5. References

[1] Diedrichs F, Stolk M, Jürchott K, Haag M, Sittinger M, & Seifert M. Enhanced Immunomodulation in Inflammatory Environments Favors Human Cardiac Mesenchymal Stromal-Like Cells for Allogeneic Cell Therapies. Front Immunol 2019;10. https://doi.org/10.3389/fimmu.2019.01716.

[2] Uygur A, & Lee RT. Mechanisms of Cardiac Regeneration. Dev Cell 2016;36:362–74. https://doi.org/10.1016/j.devcel.2016.01.018.

[3] Bergmann O, Bhardwaj RD, Bernard S, Zdunek S, Barnabé-Heider F, Walsh S, Zupicich J, Alkass K, Buchholz BA, Druid H, Jovinge S, & Frisén J. Evidence for Cardiomyocyte Renewal in Humans. Science (80-) 2009;324:98–102. https://doi.org/10.1126/science.1164680.

[4] Prabhu SD, & Frangogiannis NG. The Biological Basis for Cardiac Repair After Myocardial Infarction. Circ Res 2016;119:91–112. https://doi.org/10.1161/CIRCRESAHA.116.303577.

[5] Buckley LF, & Shah AM. Recent advances in the treatment of chronic heart failure. F1000Research 2019;8. https://doi.org/10.12688/f1000research.20447.1.

[6] Giwa S, Lewis JK, Alvarez L, Langer R, Roth AE, Church GM, Markmann JF, Sachs DH, Chandraker A, Wertheim JA, Rothblatt M, Boyden ES, Eidbo E, Lee WPA, Pomahac B, Brandacher G, Weinstock DM, Elliott G, Nelson D, Acker JP, Uygun K, Schmalz B, Weegman BP, Tocchio A, Fahy GM, Storey KB, Rubinsky B, Bischof J, Elliott JAW, Woodruff TK, Morris GJ, Demirci U, Brockbank KGM, Woods EJ, Ben RN, Baust JG, Gao D, Fuller B, Rabin Y, Kravitz DC, Taylor MJ, & Toner M. The promise of organ and tissue preservation to transform medicine. Nat Biotechnol 2017;35:530–42. https://doi.org/10.1038/nbt.3889.

[7] Orlic D, Kajstura J, Chimenti S, Jakoniuk I, Anderson SM, Li B, Pickel J, McKay R, Nadal-Ginard B, Bodine DM, Leri A, & Anversa P. Bone marrow cells regenerate infarcted myocardium. Nature 2001;410:701–5. https://doi.org/10.1038/35070587.

[8] Murry CE, Soonpaa MH, Reinecke H, Nakajima H, Nakajima HO, Rubart M, Pasumarthi KBS, Virag JI, Bartelmez SH, Poppa V, Bradford G, Dowell JD, Williams DA, & Field LJ. Haematopoietic stem cells do not transdifferentiate into cardiac myocytes in myocardial infarcts. Nature 2004;428:664–8. https://doi.org/10.1038/nature02446.

[9] Tzahor E, & Poss KD. Cardiac regeneration strategies: Staying young at heart. Science (80-) 2017;356:1035–9. https://doi.org/10.1126/science.aam5894.

[10] Duran A, Reidell O, Stachelscheid H, Klose K, Gossen M, Falk V, Röll W, & Stamm C. Regenerative Medicine/Cardiac Cell Therapy: Pluripotent Stem Cells. Thorac Cardiovasc Surg 2018;66:053–62. https://doi.org/10.1055/s-0037-1608761.

[11] Zhang Y, Mignone J, & MacLellan WR. Cardiac Regeneration and Stem Cells. Physiol Rev 2015;95:1189–204. https://doi.org/10.1152/physrev.00021.2014.

[12] Nigro P, Perrucci GL, Gowran A, Zanobini M, Capogrossi MC, & Pompilio G. c-kit+ cells: the tell-tale heart of cardiac regeneration? Cell Mol Life Sci 2015;72:1725–40. https://doi.org/10.1007/s00018-014-1832-8.

[13] Fernández-Avilés F, Sanz-Ruiz R, Climent AM, Badimon L, Bolli R, Charron D, Fuster V, Janssens S, Kastrup J, Kim HS, Lüscher TF, Martin JF, Menasche P, Simari RD, Stone GW, Terzic A, Willerson JT, Wu JC, Joseph CW, Weny T, Broughton K, DiFede DL, Dimmeler S, Madonna R, Penn MS, Sussman MA, Sluijter JPG, Woller KC, Balkan W, Chamuleau S, Charron D, Fernández-Santos ME, Goliasch G, Gyöngyösi M, Hare JM, Tompkins BA, Winkler J, Bayés-Genis A, Henry TD, Taylor DA, Lerman A, Pelacho B, Prosper F, Perin EC, Pompilio G, Gersh B, Bartunek J, Duckers E, Ferdinandy P, Losordo DW, Čanchez PL, Sherman W, Wojakowski W, Zeiher A, Roncalli J, Mathur A, Crea F, D'Amario D, Povsic TJ, Traverse J, & Yla-Herttuala S. Global position paper on cardiovascular regenerative medicine. Eur Heart J 2017;38:2532–46. https://doi.org/10.1093/eurheartj/ehx248.

[14] Ferreira JR, Teixeira GQ, Santos SG, Barbosa MA, Almeida-Porada G, & Gonçalves RM. Mesenchymal Stromal Cell Secretome: Influencing Therapeutic Potential by Cellular Pre-conditioning. Front Immunol 2018;9:2837. https://doi.org/10.3389/fimmu.2018.02837.

[15] Rezaie J, Rahbarghazi R, Pezeshki M, Mazhar M, Yekani F, Khaksar M, Shokrollahi E, Amini H, Hashemzadeh S, Sokullu SE, & Tokac M. Cardioprotective role of extracellular vesicles: A highlight on exosome beneficial effects in cardiovascular diseases. J Cell Physiol 2019;234:21732–45. https://doi.org/10.1002/jcp.28894.

[16] Najar M, Bouhtit F, Melki R, Afif H, Hamal A, Fahmi H, Merimi M, & Lagneaux L. Mesenchymal Stromal Cell-Based Therapy: New Perspectives and Challenges. J Clin Med 2019;8:626. https://doi.org/10.3390/jcm8050626.

[17] Dominici M, Le Blanc K, Mueller I, Slaper-Cortenbach I, Marini FC, Krause DS, Deans RJ, Keating A, Prockop DJ, & Horwitz EM. Minimal criteria for defining multipotent mesenchymal stromal cells. The International Society for Cellular Therapy position statement. Cytotherapy 2006;8:315–7. https://doi.org/10.1080/14653240600855905.

[18] Lalu MM, Mazzarello S, Zlepnig J, Dong YY (Ryan), Montroy J, McIntyre L, Devereaux PJ, Stewart DJ, David Mazer C, Barron CC, McIsaac DI, & Fergusson DA. Safety and Efficacy of Adult Stem Cell Therapy for Acute Myocardial Infarction and Ischemic Heart Failure (SafeCell Heart): A Systematic Review and Meta-Analysis. Stem Cells Transl Med 2018;7:857–66. https://doi.org/10.1002/sctm.18-0120.

[19] Li TS, Cheng K, Malliaras K, Smith RR, Zhang Y, Sun B, Matsushita N, Blusztajn A, Terrovitis J, Kusuoka H, Marbán L, & Marbán E. Direct comparison of different stem cell types and subpopulations reveals superior paracrine potency and myocardial repair efficacy with cardiosphere-derived cells. J Am Coll Cardiol 2012;59:942–53. https://doi.org/10.1016/j.jacc.2011.11.029.

[20] Haag M, Van Linthout S, Schröder SEA, Freymann U, Ringe J, Tschöpe C, & Sittinger M. Endomyocardial biopsy derived adherent proliferating cells - A potential cell source for cardiac tissue engineering. J Cell Biochem 2010;109:564–75. https://doi.org/10.1002/jcb.22433.

[21] Miteva K, Van Linthout S, Pappritz K, Müller I, Spillmann F, Haag M, Stachelscheid H, Ringe J, Sittinger M, & Tschöpe C. Human Endomyocardial Biopsy Specimen-Derived Stromal Cells Modulate Angiotensin II-Induced Cardiac Remodeling. Stem Cells Transl Med 2016;5:1707–18. https://doi.org/10.5966/sctm.2016-0031.

[22] Al-Daccak R, & Charron D. Allogenic benefit in stem cell therapy: cardiac repair and regeneration. Tissue Antigens 2015;86:155–62. https://doi.org/10.1111/tan.12614.

[23] Wood KJ, & Goto R. Mechanisms of Rejection: Current Perspectives. Transplantation 2012;93:1–10. https://doi.org/10.1097/TP.0b013e31823cab44.

[24] Detert S, Stamm C, Beez C, Diedrichs F, Ringe J, Van Linthout S, Seifert M, Tschöpe C, Sittinger M, & Haag M. The atrial appendage as a suitable source to generate cardiac-derived adherent proliferating cells for regenerative cell-based therapies. J Tissue Eng Regen Med 2018;12:e1404–17. https://doi.org/10.1002/term.2528.

[25] El-Shafeey M, Pappritz K, Diedrichs F, Seifert M, Stamm C, Haag M, Sittinger M, Tschöpe C & Van Linthout S. Cardioprotective and immunomodulatory effects of endomyocardial biopsy and atiral appendage-derived stromal cells in an acute model of Coxsackievirus B3-induced myocarditis. Eur J Heart Fail 2018;20(Suppl. S1):517; P1982.

[26] Cheng K, Ibrahim A, Hensley MT, Shen D, Sun B, Middleton R, Liu W, Smith RR, & Marbán E. Relative Roles of CD90 and c-Kit to the Regenerative Efficacy of Cardiosphere-Derived Cells in Humans and in a Mouse Model of Myocardial Infarction. J Am Heart Assoc 2014;3. https://doi.org/10.1161/JAHA.114.001260.

[27] Lauden L, Boukouaci W, Borlado LR, López IP, Sepúlveda P, Tamouza R, Charron D, & Al-Daccak R. Allogenicity of Human Cardiac Stem/Progenitor Cells Orchestrated by Programmed Death Ligand 1. Circ Res 2013;112:451–64. https://doi.org/10.1161/CIRCRESAHA.112.276501.

[28] Davies LC, Heldring N, Kadri N, & Le Blanc K. Mesenchymal Stromal Cell Secretion of Programmed Death-1 Ligands Regulates T Cell Mediated Immunosuppression. Stem Cells 2017;35:766–76. https://doi.org/10.1002/stem.2509.

[29] Oldershaw R, Owens WA, Sutherland R, Linney M, Liddle R, Magana L, Lash GE, Gill JH, Richardson G, & Meeson A. Human cardiac-mesenchymal stem cell-like cells, a novel cell population with therapeutic potential. Stem Cells Dev 2019;28:593–607. https://doi.org/10.1089/scd.2018.0170.

[30] Saalbach A, & Anderegg U. Thy-1: more than a marker for mesenchymal stromal cells. FASEB J 2019;33:6689–96. https://doi.org/10.1096/fj.201802224R.

[31] Lohan P, Treacy O, Griffin MD, Ritter T, & Ryan AE. Anti-Donor Immune Responses Elicited by Allogeneic Mesenchymal Stem Cells and Their Extracellular Vesicles: Are We Still Learning? Front Immunol 2017;8:1626. https://doi.org/10.3389/fimmu.2017.01626.

[32] Di Trapani M, Bassi G, Ricciardi M, Fontana E, Bifari F, Pacelli L, Giacomello L, Pozzobon M, Féron F, De Coppi P, Anversa P, Fumagalli G, Decimo I, Menard C, Tarte K, & Krampera M. Comparative Study of Immune Regulatory Properties of Stem Cells Derived from Different Tissues. Stem Cells Dev 2013;22:2990–3002. https://doi.org/10.1089/scd.2013.0204.

[33] de Witte SFH, Luk F, Sierra Parraga JM, Gargesha M, Merino A, Korevaar SS, Shankar AS, O'Flynn L, Elliman SJ, Roy D, Betjes MGH, Newsome PN, Baan CC, & Hoogduijn MJ. Immunomodulation By Therapeutic Mesenchymal Stromal Cells (MSC) Is Triggered Through Phagocytosis of MSC By Monocytic Cells. Stem Cells 2018;36:602–15. https://doi.org/10.1002/stem.2779.

[34] Groh ME, Maitra B, Szekely E, & Koç ON. Human mesenchymal stem cells require monocyte-mediated activation to suppress alloreactive T cells. Exp Hematol 2005;33:928–34. https://doi.org/10.1016/j.exphem.2005.05.002.

[35] Afferni C, Buccione C, Andreone S, Galdiero MR, Varricchi G, Marone G, Mattei F, & Schiavoni G. The Pleiotropic Immunomodulatory Functions of IL-33 and Its Implications in Tumor Immunity. Front Immunol 2018;9:2601. https://doi.org/10.3389/fimmu.2018.02601.

[36] Beez CM, Haag M, Klein O, Van Linthout S, Sittinger M, & Seifert M. Extracellular vesicles from regenerative human cardiac cells act as potent immune modulators by priming monocytes. J Nanobiotechnology 2019;17. https://doi.org/10.1186/s12951-019-0504-0.

[37] Sivanathan KN, Gronthos S, Rojas-Canales D, Thierry B, & Coates PT. Interferon-Gamma Modification of Mesenchymal Stem Cells: Implications of Autologous and Allogeneic Mesenchymal Stem Cell Therapy in Allotransplantation. Stem Cell Rev Reports 2014;10:351–75. https://doi.org/10.1007/s12015-014-9495-2.

[38] Kyurkchiev D, Bochev I, Ivanova-Todorova E, Mourdjeva M, Oreshkova T, Belemezova K, & Kyurkchiev S. Secretion of immunoregulatory cytokines by mesenchymal stem cells. World J Stem Cells 2014;6:552. https://doi.org/10.4252/wjsc.v6.i5.552.

[39] Guan Q, Li Y, Shpiruk T, Bhagwat S, & Wall DA. Inducible indoleamine 2,3-dioxygenase 1 and programmed death ligand 1 expression as the potency marker for mesenchymal stromal cells. Cytotherapy 2018;20:639–49. https://doi.org/10.1016/j.jcyt.2018.02.003.

[40] Dam N, Hocine HR, Palacios I, DelaRosa O, Menta R, Charron D, Bensussan A, El Costa H, Jabrane-Ferrat N, Dalemans W, Lombardo E, & Al-Daccak R. Human Cardiac-Derived Stem/Progenitor Cells Fine-Tune Monocyte-Derived Descendants Activities toward Cardiac Repair. Front Immunol 2017;8. https://doi.org/10.3389/fimmu.2017.01413.

Statutory Declaration

“I, Falk Diedrichs, by personally signing this document in lieu of an oath, hereby affirm that I prepared the submitted dissertation on the topic “Defining the Role of Cardiac-Derived Cells as Modulators of Major Immune Responses in Inflammatory Environments” / “Die Rolle Kardial-Abgeleiteter Zellen als Potente Modulatoren von Immunreaktionen unter Inflammation”, independently and without the support of third parties, and that I used no other sources and aids than those stated.

All parts which are based on the publications or presentations of other authors, either in letter or in spirit, are specified as such in accordance with the citing guidelines. The sections on methodology (in particular regarding practical work, laboratory regulations, statistical processing) and results (in particular regarding figures, charts and tables) are exclusively my responsibility.

Furthermore, I declare that I have correctly marked all of the data, the analyses, and the conclusions generated from data obtained in collaboration with other persons, and that I have correctly marked my own contribution and the contributions of other persons (cf. declaration of contribution). I have correctly marked all texts or parts of texts that were generated in collaboration with other persons.

My contributions to any publications to this dissertation correspond to those stated in the below declaration. All publications created within the scope of the dissertation comply with the guidelines of the ICMJE (International Committee of Medical Journal Editors; www.icmje.org) on authorship. In addition, I declare that I shall comply with the regulations of Charité – Universitätsmedizin Berlin on ensuring good scientific practice.

I declare that I have not yet submitted this dissertation in identical or similar form to another Faculty.

The significance of this statutory declaration and the consequences of a false statutory declaration under criminal law (Sections 156, 161 of the German Criminal Code) are known to me.”

Date Signature

Declaration of Contribution

Publication 1: Falk Diedrichs, Meaghan Stolk, Karsten Jürchott, Marion Haag, Michael Sittinger und Martina Seifert, „Enhanced Immunomodulation in Inflammatory Environments Favors Human Cardiac Mesenchymal Stromal-Like Cells for Allogeneic Cell Therapies“, Frontiers in Immunology, published 23.07.2019.

Contribution: I led the project and was responsible for study design, execution of experiments, collection and assembly of data, data analysis and interpretation, as well as manuscript writing. The following figures and tables were generated by my own statistical analysis: **Figures 1**, **2**, **3**, **4**, **5D**, **6** and **7**, **Supplementary Figures 1**, **2**, **3**, **4**, **5**, **6** and **7**, as well as **Tables 1**, **2,** and **3**, as well as **Supplementary Tables 1** and **2**.

I would like to acknowledge the excellent technical assistance of **Anja Fleischmann** and the help with statistical analysis of **Dr. Karsten Jürchott**, who also created **Figures 5A**, **B**, and **C**, as well as **Supplementary Table 3**.

Furthermore, Raman trapping microscopy analysis and creation of **Supplementary Figure 8** were performed by **CellTool GmbH** (Tutzing, Germany).

_____

Signature of doctoral candidate

Publication 1: Diedrichs F, Stolk M, Jürchott K, Haag M, Sittinger M, & Seifert M. Enhanced Immunomodulation in Inflammatory Environments Favors Human Cardiac Mesenchymal Stromal-Like Cells for Allogeneic Cell Therapies. Front Immunol 2019;10:1716. https://doi.org/10.3389/fimmu.2019.01716.

Journal Data Filtered By: **Selected JCR Year: 2018** Selected Editions: SCIE,SSCI
Selected Categories: **"Immunology"** Selected Category Scheme: WoS
Gesamtanzahl: 158 Journale

Rank	Full Journal Title	Total Cites	Journal Impact Factor	Eigenfactor Score
1	NATURE REVIEWS IMMUNOLOGY	41,499	44.019	0.080220
2	NATURE IMMUNOLOGY	44,298	23.530	0.094250
3	IMMUNITY	51,051	21.522	0.126090
4	Annual Review of Immunology	17,013	21.429	0.022210
5	Lancet HIV	2,417	14.753	0.014270
6	JOURNAL OF ALLERGY AND CLINICAL IMMUNOLOGY	51,978	14.110	0.076250
7	TRENDS IN IMMUNOLOGY	12,153	13.000	0.025470
8	IMMUNOLOGICAL REVIEWS	15,517	11.292	0.027050
9	JOURNAL OF EXPERIMENTAL MEDICINE	63,983	10.892	0.071790
10	Science Immunology	1,292	10.551	0.007580
11	CLINICAL INFECTIOUS DISEASES	64,031	9.055	0.119010
12	Journal for ImmunoTherapy of Cancer	2,716	8.676	0.011350
13	Cancer Immunology Research	5,420	8.619	0.025380
14	Cellular & Molecular Immunology	4,058	8.213	0.009160
15	AUTOIMMUNITY REVIEWS	9,127	7.716	0.018220
16	CURRENT OPINION IN IMMUNOLOGY	9,164	7.667	0.017440
17	Journal of Allergy and Clinical Immunology-In Practice	4,196	7.550	0.013090
18	JOURNAL OF AUTOIMMUNITY	6,900	7.543	0.015050
19	SEMINARS IN IMMUNOLOGY	5,016	7.358	0.010290
20	Mucosal Immunology	6,990	7.352	0.020730
21	CLINICAL REVIEWS IN ALLERGY & IMMUNOLOGY	3,149	7.328	0.006390

Rank	Full Journal Title	Total Cites	Journal Impact Factor	Eigenfactor Score
22	Clinical & Translational Immunology	998	7.271	0.003770
23	EMERGING INFECTIOUS DISEASES	30,311	7.185	0.059420
24	Seminars in Immunopathology	3,337	6.804	0.007890
25	ALLERGY	17,873	6.771	0.024250
26	EXERCISE IMMUNOLOGY REVIEW	754	6.455	0.000890
27	Emerging Microbes & Infections	1,941	6.212	0.006720
28	BRAIN BEHAVIOR AND IMMUNITY	14,533	6.170	0.025700
29	Advances in Immunology	2,544	5.771	0.004220
30	Journal of Neuroinflammation	11,767	5.700	0.023240
31	OncoImmunology	7,790	5.333	0.025470
32	Journal of the International AIDS Society	4,530	5.192	0.018770
33	JOURNAL OF INFECTIOUS DISEASES	45,452	5.045	0.076010
34	Allergy Asthma & Immunology Research	1,599	5.026	0.003240
35	npj Vaccines	282	5.020	0.001120
36	BIODRUGS	1,685	4.903	0.003370
37	CANCER IMMUNOLOGY IMMUNOTHERAPY	7,779	4.900	0.012870
38	Virulence	3,557	4.775	0.009120
39	Vaccines	1,077	4.760	0.003910
40	INFECTIOUS DISEASE CLINICS OF NORTH AMERICA	2,765	4.757	0.005160
41	CLINICAL AND EXPERIMENTAL ALLERGY	11,312	4.741	0.012900
42	JOURNAL OF IMMUNOLOGY	127,940	4.718	0.124400
43	Frontiers in Immunology	27,827	4.716	0.085880
44	EUROPEAN JOURNAL OF IMMUNOLOGY	22,037	4.695	0.024730

2

Selected JCR Year: 2018; Selected Categories: "IMMUNOLOGY"

frontiers in Immunology

ORIGINAL RESEARCH
published: 23 July 2019
doi: 10.3389/fimmu.2019.01716

Enhanced Immunomodulation in Inflammatory Environments Favors Human Cardiac Mesenchymal Stromal-Like Cells for Allogeneic Cell Therapies

Falk Diedrichs[1,2], *Meaghan Stolk*[2], *Karsten Jürchott*[2,3], *Marion Haag*[2,4], *Michael Sittinger*[2,4] *and Martina Seifert*[2,3]*

[1] Berlin Institute of Health (BIH), Berlin, Germany, [2] BIH Center for Regenerative Therapies (BCRT), Charité-Universitätsmedizin Berlin, Corporate Member of Freie Universität Berlin, Humboldt-Universität zu Berlin, and Berlin Institute of Health, Berlin, Germany, [3] Institute of Medical Immunology, Charité-Universitätsmedizin Berlin, Corporate Member of Freie Universität Berlin, Humboldt-Universität zu Berlin, and Berlin Institute of Health, Berlin, Germany, [4] Tissue Engineering Laboratory, Charité-Universitätsmedizin Berlin, Corporate Member of Freie Universität Berlin, Humboldt-Universität zu Berlin, and Berlin Institute of Health, Berlin, Germany

OPEN ACCESS

Edited by:
Martin Johannes Hoogduijn, Erasmus University Rotterdam, Netherlands

Reviewed by:
Ralf Dressel, University Medical Center Göttingen, Germany
Lagneaux Laurence, Free University of Brussels, Belgium
Mehdi Najar, Free University of Brussels, Belgium

***Correspondence:**
Martina Seifert
martina.seifert@charite.de

Specialty section:
This article was submitted to Alloimmunity and Transplantation, a section of the journal Frontiers in Immunology

Received: *14 February 2019*
Accepted: *09 July 2019*
Published: *23 July 2019*

Citation:
Diedrichs F, Stolk M, Jürchott K, Haag M, Sittinger M and Seifert M (2019) Enhanced Immunomodulation in Inflammatory Environments Favors Human Cardiac Mesenchymal Stromal-Like Cells for Allogeneic Cell Therapies. Front. Immunol. 10:1716. doi: 10.3389/fimmu.2019.01716

Rising numbers of patients with cardiovascular diseases and limited availability of donor hearts require new and improved therapy strategies. Human atrial appendage-derived cells (hAACs) are promising candidates for an allogeneic cell-based treatment. In this study, we evaluated their inductive and modulatory capacity regarding immune responses and underlying key mechanisms *in vitro*. For this, cryopreserved hAACs were either cultured in the presence of interferon-gamma (IFNγ) or left unstimulated. The expression of characteristic mesenchymal stromal cell markers (CD29, CD44, CD73, CD105, CD166) was revealed by flow cytometry that also highlighted a predominant negativity for CD90. A low immunogeneic phenotype in an inflammatory milieu was shown by lacking expression of co-stimulatory molecules and upregulation of the inhibitory ligands PD-L1 and PD-L2, despite *de novo* expression of HLA-DR. Co-cultures of hAACs with allogeneic peripheral blood mononuclear cells, proved their low immunogeneic state by absence of induced T cell proliferation and activation. Additionally, elevated levels of IL-1β, IL-33, and IL-10 were detectable in those cell culture supernatants. Furthermore, the immunomodulatory potential of hAACs was assessed in co-cultures with αCD3/αCD28-activated peripheral blood mononuclear cells. Here, a strong inhibition of T cell proliferation and reduction of pro-inflammatory cytokines (IFNγ, TNFα, TNFβ, IL-17A, IL-2) were observable after pre-stimulation of hAACs with IFNγ. Transwell experiments confirmed that mostly soluble factors are responsible for these suppressive effects. We were able to identify indolamin-2,3-dioxygenase (IDO) as a potential key player through a genome-wide gene expression analysis and could demonstrate its involvement in the observed immunological responses. While the application of blocking antibodies against both PD-1 ligands did not affect the immunomodulation by hAACs, 1-methyl-L-tryptophan as specific inhibitor of IDO was able to restore proliferation and to lower apoptosis of T cells. In conclusion, hAACs

represent a cardiac-derived mesenchymal stromal-like cell type with a high potential for the application in an allogeneic setting, since they do not trigger T cell responses and even increase their immunomodulatory potential in inflammatory environments.

Keywords: cardiac-derived cells, immunogenicity, immunomodulation, inflammation, IFNγ, IDO

INTRODUCTION

Cardiovascular diseases are the leading cause of morbidity and mortality worldwide with ischemic heart disease alone being responsible for almost 1.8 million deaths per year in Europe (20% of all deaths; European Heart Network, 2017[1]). Even though there is a range of existing therapeutic strategies available, which have beneficial effects on the improvement of life quality and the extension of lifespan in cardiovascular patients, they often leave them with no other causal therapy option than heart transplantation (1, 2).

Numerous attempts using a variety of different cell sources were initiated over the last 20 years for development of new therapeutic treatments to induce cardiac regeneration (3). Particularly autologous cell sources, ranging from hematopoietic cells (4), over mesenchymal stromal cells (MSCs) from different tissues (5–7), to various cardiac progenitor cells (CPCs) (8–11) have been heavily investigated in this context. Specifically, the use of CPCs led to promising results: animal models of myocardial infarction demonstrated improved cardiac function after cell transplantation (12) and even first clinical studies in humans (SCIPIO and CADUCEUS trials) were able to show moderately increased regeneration of cardiac tissue (13–16).

An alternative mesenchymal-like cardiac cell type for an autologous therapeutic application in heart injury, are so called cardiac-derived adherent proliferating cells (CardAPs). This unique cell type derived from endomyocardial biopsies shares typical characteristics with MSCs but clearly distinguishes itself from all other cell types used so far in cell therapeutic application. CardAPs are positive for CD44, CD73, CD105, and CD166 but express neither the hematopoietic markers CD14, CD34 and are strikingly low for the marker CD90, which is otherwise characteristic for MSCs and fibroblasts (17). These cardiac-derived cells demonstrated increased regenerative potency by mediating angiogenesis and cardiomyogenesis, reducing cardiac hypertrophy and exhibiting immunomodulatory capacities to induce an anti-inflammatory environment (18–20). Our own immunological *in vitro* tests with these mesenchymal-like CardAPs proved their low immunogeneic status as well as the capacity to modulate the immune system toward an anti-inflammatory state (21). However, recent clinical phase-I studies with mesenchymal cell types highlighted some of the fundamental limitations of autologous cell sources (22). Manufacturing a sufficient amount of a patient-specific cell product is time consuming, thus preventing immediate availability in acute situations. Additionally, harvesting from elderly diseased patients with co-morbidities raised further concerns regarding the functional integrity and overall survival of obtained cells (23). Furthermore, it is the recent scientific consensus that every stromal cell source has to be considered as an independent entity and requires a comprehensive phenotypical and functional characterization using standardized protocols, with a particular focus on their immunological properties and immunomodulatory potency (24). This would help to identify an adequate cell source or cell subset and to promote the appropriate and safe application as a cell therapeutic or even as cell free products based on paracrine released vesicles or mediators.

For that reason, it is essential to evaluate the potential use of allogeneic cardiac-derived cells, since they can be harvested from healthy donors, have the benefit of being available at any time and can be assessed and manipulated in advance to fit the patient's needs (25). This might be important, since the transplantation of allogeneic cells or tissues always poses the risk of recognition by the recipient's immune system and induction of unwanted inflammatory responses by secretion of allo-antibodies (26, 27) or even T cell-mediated rejection responses (28, 29).

Experimental data by others with a cardiac-derived mesenchymal-like cell type indicated that those cryopreserved c-Kit$^+$ CPCs displaying low immunogeneic properties, were able to reduce local inflammatory processes and limit T cell proliferation in already ongoing immunoreactions *in vitro* (30). Additionally, the phase-I/-II CAREMI trial already proved the principal safety of allogeneic cell transplantation with previously mentioned c-Kit$^+$ selected CPCs by absence of major adverse effects after intracoronary injection (31). However, the overall benefit in cardiac improvement remains ambiguous and demands the evaluation of additional allogeneic cell sources.

Our group recently described the atrial appendage as a potential new cell source for human atrial appendage-derived cells (hAACs) that are a CD90^{low} cell product with similar pro-angiogenic characteristics compared to the endomyocardial-derived CardAPs (32). hAACs can be easily isolated from cardiac tissue and would allow allogeneic treatment for a substantial number of patients. These cells represent a mesenchymal-like cardiac-derived cell type based on the expression of the characteristic markers CD29, CD44, CD73, CD105, and CD166, but predominantly lack expression of CD90 at the same time. Precisely, this CD90^{low} phenotype could provide

[1]European Cardiovascular Disease Statistics 2017 edition. *CVD Statistics 2017* (2017). Available online at: http://www.ehnheart.org/cvd-statistics/cvd-statistics-2017.html (accessed: February 02, 2019).

Abbreviations: 1-MT, 1-methyl-L-tryptophan; CardAPs, cardiac-derived adherent proliferating cells; CD, cluster of differentiation; CFSE, carboxyfluorescein succinimidyl ester; COX-1, cyclooxygenase 1; CPCs, cardiac progenitor cells; hAACs, human atrial appendage-derived cells; HLA, human leukocyte antigen; HUVECs, human umbilical vein endothelial cells; IDO, indolamine-2,3-dioxygenase; IFNγ, interferon-gamma; IL, interleukin; MFI, mean fluorescence intensity; MSCs, mesenchymal stromal cells; PBMCs, peripheral blood mononuclear cells; PD-L, programmed death ligand; TGFβ, transforming growth factor beta; TLR3, toll-like receptor 3; TNF, tumor necrosis factor.

a beneficial tool for the enhanced repair capacity of a cell product, since it was shown that CD90 expression on cardiosphere-derived cells is negatively correlated with the scar size of injured heart tissue after cell application in myocardial infarction (33). In addition, first studies with hAACs in a mouse model of Coxsackievirus B3 (CVB3)-induced myocarditis could demonstrate, that intravenous application was able to improve the left ventricular heart function and contractility as well as to decrease tissue collagen I expression. In this experimental mouse study, immunomodulatory effects were also confirmed by detecting reduced levels of TGFβ-producing $CD68^+$ cells and regulatory T cells in the spleen of treated animals (34).

To ensure the safety and efficacy of this new hAAC product for an allogeneic transplantation in humans, it is crucial to determine whether these cells trigger immune responses in an inflammatory scenario, as seen in cell transplantation. Therefore, we aimed to assess the immunological properties of this defined cell product, test their interaction with cells from the adaptive immune system *in vitro* and gain insights into the underlying mechanism of action. First, we confirmed a mesenchymal-like surface marker expression profile after cryopreservation and assessed changes of the immune phenotype under inflammatory conditions. Second, hAACs were evaluated in immune cell co-cultures to study potential immunogeneic properties and the capacity to modulate adaptive immune responses. We could identify several potential molecules explaining the observed immune modulatory effects by a genome-wide gene expression analysis. Finally, our data revealed that indolamine-2,3-dioxygenase (IDO) is a key player of the immunomodulation by hAACs mediating the inhibition of T cell proliferation and the induction of their apoptosis.

MATERIALS AND METHODS

Isolation and Culture of Human Atrial Appendage-Derived Cells (hAACs)

Right atrial appendages, that were obtained during open-heart surgery at Deutsches Herzzentrum Berlin from eight patients, were used to generate hAACs as previously described (32). Briefly, the right atrial appendages were reduced to fragments of 1 mm^3 and cultured in Iscove's Modified Dulbecco's Medium (IMDM; Biochrom, Berlin, Germany) containing 10% allogeneic human serum (German Red Cross, Berlin, Germany), 100 U/mL penicillin and 100 µg/mL streptomycin (both from Biochrom). Outgrowing cells were harvested after about 13 days with 0.05% trypsin/0.02% EDTA (Biochrom) and then subjected to immunomagnetic sorting with CD90 microbeads (MACS; human CD90 MicroBeads kit, Miltenyi Biotec, Bergisch Gladbach, Germany). The resulting $CD90^{low}$ cell population was grown under standard culture conditions (37°C in 21% O_2 and 5% CO_2 atmosphere) at a density of 6000 cells/cm^2 in complete medium (cIDH) consisting of equal amounts of IMDM/DMEM/Ham's F12 (IDH; all Biochrom) and supplemented with 5% male heat-inactivated human AB serum (Sigma-Aldrich, St. Louis, MO, USA), 100 U/mL penicillin and 100 µg/mL streptomycin (Gibco® Life Technologies, Grand Island, NY, USA), 20 ng/mL basic fibroblast growth factor and 10 ng/mL epithelial growth factor (both from Preprotech, Hamburg, Germany) for further expansion of the purified cell product. Subsequently, hAACs were cryopreserved for at least 6 months to mimic conditions of a cell bank. After thawing, cells were routinely passaged once in cIDH medium before performing assays and were used between passages 2 and 8. Tissues were obtained according to the local guidelines of the Charité - Universitätsmedizin Berlin as well as the Declaration of Helsinki and the study was approved by the ethics committee of the Charité - Universitätsmedizin Berlin (No. 4/028/12). Human leukocyte antigen (HLA)-typing of the cells were performed in the HLA-Laboratory of the Charité - Universitätsmedizin Berlin by SSO-PCR (low) for HLA-A, HLA-B and HLA-DR. A list of all HLA-typed cells is available in the **Supplementary Table 1**.

Culture of Human Umbilical Cord-Derived Mesenchymal Stromal Cells (MSCs) and Umbilical Vein Endothelial Cells (HUVECs)

Due to their known immunomodulatory potential as previously described (35), human umbilical cord-derived MSCs were used as control cells in the immune cell co-culture experiments. Cells were kindly provided by Dirk Strunk's laboratory at the Institute of Experimental and Clinical Cell Therapy and Spinal Cord & Tissue Regeneration Center, Paracelsus Medical University (PMU) Salzburg, Austria and were obtained for human cell and tissue sample collection from the Institutional Review Board of the Medical University of Graz (protocol 19-252 ex 07/08) as described (36). Umbilical cord samples were collected from mothers that gave written informed consent after full-term pregnancies in accordance with the Declaration of Helsinki. After thawing, MSCs were grown in alpha-modified minimum essential medium (alpha-MEM; Biochrom), supplemented with 5% human male heat-inactivated AB serum (Sigma-Aldrich), 2 mM L-glutamine, 100 U/mL penicillin and 100 µg/mL streptomycin (both from Gibco® Life Technologies) at 37°C in 21% O_2 and 5% CO_2 atmosphere. HLA-Typing of the donor cells was performed by SSP PCR using Olerup SSPTM low-resolution kits (GenoVision Inc., Philadelphia, PA, USA).

HUVECs were used as positive controls in the immune cell co-culture experiments (Cascade Biologics®, Thermo Fisher Scientific, Rochester, NY, USA and Lonza, Wakersville, MD, USA). After thawing, HUVECs were cultured in EGM-2 (Lonza) with 5% human male heat-inactivated AB serum (Sigma-Aldrich), 100 U/mL penicillin and 100 µg/mL streptomycin (Gibco® Life Technologies) for further expansion.

Both cell types were passaged once before performing assays and were used between passages 2 and 8.

PBMC Isolation

Human peripheral blood mononuclear cells (PBMCs) were isolated from buffy coats (German Red Cross, Berlin, Germany; approved by the local Ethical Committee, EA1/226/14) by using a Biocoll gradient (Biochrom), as previously described (37). Briefly, following centrifugation at 800 g for 30 min without brake, PBMCs were harvested from the interphase and were

washed three times with cold phosphate buffered saline solution (PBS; Biochrom). Cells were cryopreserved for later experimental use in liquid nitrogen. HLA-typing was performed in the HLA-Laboratory of the Charité - Universitätsmedizin Berlin by SSO-PCR (low) for HLA-A, HLA-B and HLA-DR.

Immunocytochemistry Analysis of hAACs

hAACs were plated on collagen I-coated (BD Biosciences, San Jose, CA, USA) 24 well dishes (Falcon, BD Biosciences). After incubation overnight, wells were washed three times with Hank's Balanced Salt Solution (HBSS; Gibco® Life Technologies) containing Mg^{2+} and Ca^{2+}, fixed with 4% paraformaldehyde (PFA; Roth, Karlsruhe, Germany) for 10 min at room temperature and washed twice with HBSS. Subsequently, the cells were incubated with 5 μg/mL wheat germ agglutinin (WGA; Biotium, Fremont, CA, USA) for 10 min at 37°C. After washing twice with HBSS, nuclei were counterstained for 15 min at room temperature with 4,6-diamidino-2-phenylindole (DAPI; Molecular probes™, Thermo Fisher). Images were taken with an Operetta® High Content Imaging System and image analysis performed by the Columbus™ Image Data Storage and Analysis System (both from Perkin Elmer, Waltham, MA, USA).

Fluorescence Staining of Cells and Flow Cytometry (FACS)

Non-adherent PBMCs were resuspended by pipetting, and adherent hAACs were first harvested using a 0.05% trypsin solution with EDTA (Gibco® Life Technologies) and transferred to 5 mL FACS tubes (Falcon, BD Biosciences). Staining procedure was performed as previously described (37). Briefly, cells were washed once with cold PBS, resuspended in a final volume of 50 μL antibody mix in cold FACS buffer [PBS supplemented with 1% fetal calve serum (FCS; both Biochrom)] and incubated for 30 min at 4°C in the dark. A list of all used antibodies and dyes as well as the respective dilution is available in the online **Supplementary Table 2**. Antibody mixes also contained the Live/Dead® violet Staining Kit (Molecular probes™, Thermo Fisher Scientific) in order to exclude dead cells from the analysis. After antibody incubation, the samples were washed with cold FACS buffer and resuspended in 1% PFA (Roth, Karlsruhe, Germany) in FACS buffer. Samples were kept at 4°C in the dark until measurement on a FACS Canto II device with FACS Diva software (Becton Dickinson, San Jose, CA, USA). Data analysis was performed using FlowJo software (TreeStar Inc., Ashland, OR, USA; RRID:SCR_008520). Gating strategies for the FACS-analysis of hAACs and PBMCs are shown in **Supplementary Figure 1**. Expression of a marker is presented either as percentage of positive cells against the unlabeled control or as geometric mean of fluorescence intensity (MFI).

Kinetic Analysis of hAAC Surface Marker Expression

hAACs were seeded on 24 well-plates (Costar®, Corning Incorporated, Kennebunk, ME, USA) at a density of 3×10^5 cells and were cultured in cIDH medium overnight. Afterwards, hAACs were either directly harvested for evaluation of constitutive MSC marker expression (CD90, CD29, CD44, CD73, CD105, CD166, CD14, CD31, CD45, c-Kit) or stimulated with 100 ng/mL of interferon-gamma (IFNγ) or a combination of 100 ng/mL IFNγ and 100 ng/mL tumor necrosis factor alpha (TNFα; both from Miltenyi Biotec) for evaluation of the immunological (HLA-ABC, HLA-E, HLA-DR, CD80, CD86, PD-L1 and PD-L2) and characteristic MSC markers (CD90, CD29, CD44, CD73, CD166). hAACs were stimulated and harvested after one, 2 and 5 days, respectively for flow cytometric analysis as described before.

hAAC/Immune Cell Co-cultures

hAACs from six different donors and control cultures with MSCs and HUVECs were seeded on rat tail collagen I-coated (BD Biosciences) 24 well plates (Costar®, Corning Incorporated) at a density of 2×10^5 cells. After attachment overnight, the adherent cells were either stimulated with 100 ng/mL IFNγ (Miltenyi Biotec) or left unstimulated for 48 h. Afterwards, the confluent monolayers were irradiated with 60 Gray using a gamma-radiation source (GSM GmbH, Leipzig, Germany) to maintain a stable cell number throughout the assay. Human HLA-mismatched PBMCs were thawed, washed three times with cold PBS (Biochrom) and labeled with 5 μM carboxyfluorescein succinimidyl ester (CFSE; Biolegend, San Diego, CA, USA) for 3 min. The staining reaction was then stopped by incubating with cold heat-inactivated human AB serum (Sigma-Aldrich) for 1 min. After washing three times with cold PBS, 3×10^5 CFSE-labeled PBMCs, that were a complete mismatch to the respective hAAC donor, were added to the hAAC, MSC and HUVEC cultures. The resulting co-cultures were maintained in 1 mL of very low endotoxin (VLE)-Roswell Park Memorial Institute (RPMI; Biochrom), supplemented with 10% human male heat-inactivated AB serum (Sigma-Aldrich), 100x L-glutamine solution, 100 U/mL penicillin and 100 μg/mL streptomycin (all from Gibco® Life Technologies). After 4 days, 250 μL of co-culture supernatant were taken for cytokine detection and 750 μL of completely supplemented VLE-RPMI were added to the cultures. Following seven days of incubation, PBMCs were harvested, stained for human immune cell defining surface markers and analyzed by flow cytometry.

Proliferation Based Immunomodulation Assay

Analogous to the hAAC/immune cell co-culture analysis, hAACs, MSCs and HUVECs were cultured on rat tail collagen I-coated (BD Biosciences) 24 well plates (Costar®, Corning Incorporated) at a density of 2×10^5 cells in the presence or absence of 100 ng/mL IFNγ (Miltenyi Biotec) for 48 h. Human PBMCs were CFSE-labeled as mentioned before and activated with a combination of 0.02 μg/mL anti-CD3 (OKT3 antibody, Janssen-Cilag, Neuss, Germany) and 0.03 μg/mL anti-CD28 (BD Biosciences). Lastly, 1×10^6 PBMCs were added to the cultures in 2 mL of completely supplemented VLE-RPMI medium. After 3 days, supernatants were taken for cytokine detection and PBMCs were harvested, stained for human immune cell defining surface markers and analyzed by flow cytometry.

Experimental settings were repeated under transwell conditions. Here, hAACs were seeded at a density of 4×10^4

cells at the bottom of rat tail collagen I-coated 24 well plates. After stimulation with IFNγ, polycarbonate transwell inserts with 0.4 μm pore size (Costar®, Corning Incorporated) were initially equilibrated for 1 h at 37°C with RPMI and subsequently 2×10^5 CFSE-labeled PBMCs were seeded into the inserts. After a co-culture time of 3 days at 37°C in a 21% O_2 and 5% CO_2 atmosphere, PBMC were harvested for flow cytometric analysis of proliferation and surface marker expression.

To selectively analyze the effects of either indoleamin-2,3-dioxygenase (IDO) or both programmed death-1 (PD-1) ligands (PD-L1 and PD-L2) in immune cell co-cultures with hAACs, 1 mM 1-methyl-L-tryptophan (1-MT; Sigma-Aldrich) was provided 2 h prior to addition of CFSE-labeled or unlabeled PBMCs and 5 μg/mL of purified anti-PD-L1 and anti-PD-L2 antibodies (both Biolegend) were added 12 h before CFSE-labeled or unlabeled PBMCs were added to the hAAC cultures.

Cytokine Detection Assays

Supernatants of mono- and co-cultures of hAACs, MSCs and HUVECs from the proliferation induction experiments were tested for IL-1β, IFNα, IFNγ, TNFα, MCP-1, IL-6, IL-8, IL-10, IL-12p70, IL-17A, IL-18, IL-23, and IL-33 using the Legendplex™ human inflammation 13-plex panel (Biolegend). The minimum detectable concentration of each cytokine is given as 0.6–2.1 pg/mL. Samples were treated following manufacturer's instructions and measured with a FACS Canto II device (Becton Dickinson).

Supernatants of hAAC co-cultures from the direct-contact immune modulation experiments were analyzed for their content of IL-1β, IL-2, IL-5, IL-10, IL-13, IL-17A, TNFα, TNFβ, IFNγ, and MDC by a multiplex assay using a Milliplex® human multi-analyte Luminex® kit (Merck KGaA, Darmstadt, Germany). Samples were treated following manufacturer's instructions and measured with a Bio-Plex® 200 multiplex analysis device (Bio-Rad®, California, USA).

Genome-Wide Gene Expression Profile

Human GeneChip U133 Plus 2.0 (Affymetrix, Santa Clara, CA, USA) was used for genome-wide gene expression profiling of hAAC samples covering over 47,000 transcripts (54,765 probes in total including double entries). RNA samples of unstimulated and IFNγ pre-stimulated hAACs were prepared with GeneChip® 3′ IVT Express Kit and GeneChip® Hybridisation, Wash and Stain Kit (Affymetrix) according to the manufacturer's instructions. In brief, 250 ng total RNA was used for cDNA synthesis and subsequent *in vitro* transcription (IVT) to amplified RNA (aRNA). 12.5 μg fragmented aRNA was used for hybridization on the chip for 16 h at 45°C. Finally, the chips were washed, stained and scanned using the Affymetrix Gene Chip Scanner 3000. Affymetrix GeneChip Operating Software (GCOS) 1.4 was used to generate CEL data files, for raw data processing and for calculation of signal intensity, signal log ratio (SLR) and *p*-value of pairwise chip comparisons AF/NP. Quality control and pre-processing was done in R[2] with the package "affy" (38). Raw data were normalized and log2-transformed using Robust Multi-array Average (RMA) algorithm implemented in this package. Thousand probe sets with the highest variances were selected in order to run a principle component analysis. Differentially expressed probe sets between the two treatment groups were selected by fitting linear models to the data and Bayesian statistics were run as implemented in the package "limma" (39). False discovery rates were used to adjust raw *p*-values for multiple testing and a minimal absolute log2-Foldchange of 1 was used for probe set selection. Mapping of differentially expressed probesets to genes and functional annotations of the DAVID database (40, 41) was done using the package "clusterProfiler" (42). Over-representation of differentially expressed genes in terms of the category "Biological Process" of the gene ontology system was done using the enrichDAVID()-function of this package. The eight top ranking results of this analysis were shown as GOcirc-plot using the "GOplot"-package (43).

RNA Extraction, cDNA Synthesis and Quantitative Polymerase Chain Reaction (qPCR)

Total RNA was extracted from unstimulated and IFNγ pre-stimulated hAACs following 48 h of incubation using the RNeasy® Mini Kit (QIAGEN, Venlo, Netherlands) according to the manufacturer's protocol. After measuring the RNA concentration with the NanoDrop 2000 spectrophotometer (Thermo Fisher Scientific), cDNA was synthesized. The reverse transcription reaction was performed using TaqMan™ Reverse Transcription Reagents Kit (Invitrogen™, Thermo Fisher Scientific). Briefly, the following components were combined to perform a 20 μL reaction volume: nuclease-free water plus total RNA (1000 ng/μL), RNase inhibitor (20 U/μL), Mg_2Cl, 10x RT Buffer, Random Hexamer Primer Mix (50 μM), dNTP Mixture (2.5 mM each dNTP) and Reverse Transcriptase (RT; 50 U/μL). Samples were incubated for 30 min at 48°C, 5 min at 95°C and subsequently cooled down at 4°C with a Thermo Flex Cycler Block (Analytik Jena, Jena, Germany). After the RT-PCR the concentration of the generated cDNA was measured with the NanoDrop 2000 to ensure a functional template for the subsequent qPCR. The qPCR was performed on a QuantStudio 6 Flex Real-Time PCR machine (Applied Biosystems, Thermo Fisher Scientific) using the SensiMix™ SYBR No-ROX kit (Bioline, London, UK). The thermal cycling conditions were comprised of a 95°C initial template denaturation for 20 s, followed by 40 cycles of PCR by applying 95°C for 15 s and 60°C for 20 s. Lastly, a final melt curve stage with 40 cycles comprising of 95°C for 15 s, 60°C for 60 s and 95°C for 15 s was performed. Three technical replicates of each sample were analyzed for gene expression of *IDO1, LGALS9, TLR3, PD-L1, PD-L2, PTGS1, HLA-G*, and *VCAM1*. All of the used primer sequences are listed in **Table 1**. The samples were normalized to the expression of the

[2]R Core Team. *R: A Language and Environment for Statistical Computing*. Vienna: R Foundation for Statistical Computing (2018). Available online at: https://www.R-project.org/

TABLE 1 | The Primer sequences of selected immunomodulatory genes.

Gene	Forward primer (5′→3′)	Reverse primer (3′→5′)
IDO1	CGGTCTGGTGTATGAAGG	CTAATGAGCACAGGAAGTTC
LGALS9	CACACATGCCTTTCCAGAAG	AAGAGGATCCCGTTCACCAT
TLR3	ATCTGTCTCATAATGGCTT	AGAAAGTTGTATTGCTGGT
PD-L1	GGCATCCAAGATACAAACTCAA	CAGAAGTTCCAATGCTGGATTA
PD-L2	GAGCTGTGGCAAGTCCTCAT	GCAATTCCAGGCTCAACATTA
PTGS1	TGTTCGGTGTCCAGTTCCAATA	ACCTTGAAGGAGTCAGGCATGAG
HLA-G	TTGGGAAGAGGAGACACGGAACA	AGGTCGCAGCCAATCATCCAC
VCAM1	CGTCTTGGTCAGCCCTTCCT	ACATTCATATACTCCCGCATCCTTC
HPRT	AGTCTGGCTTATATCCAACACTTC	GACTTTGCTTTCCTTGGTCAGG

house keeping gene *HPRT* and data were analyzed using the delta-delta Ct ($\Delta\Delta$Ct) method. The final results are therefore calculated as fold change of target gene expression in IFNγ pre-stimulated hAAC samples relative to the unstimulated hAAC reference samples to demonstrate upregulation of differentially expressed genes.

Raman Trapping Microscopy

Raman spectral acquisition was conducted using a BioRam® system (CellTool GmbH, Tutzing, Germany) equipped with an excitation laser wavelength of 785 nm and a laser power of 80 mW. The laser was focused through a 60x (NA 0.7) air objective. In all samples, 500 single cells were randomly selected under bright-field illumination and pinpointed for automatic spectra retrieval. Raman spectra were taken from the cytoplasm using accumulated scans of 3 × 10 s. Together with the spectra the x-y-z coordinates as well as bright-field images of each measured cell were stored. As control, 10 background measurements were taken from each sample. To assess acquired Raman spectra, multivariate data analysis was performed. Principal Component Analysis (PCA) was used for visualizing the datasets. PCA was implemented in Python 2.7, using the scikit-learn package (44). PCA score plots were used to look for clusters among the data. Circles in 2D scores plot depict 95% confidence intervals.

Statistical Analysis

Statistical Analysis and graph generation was performed with GraphPad Prism 8.0 (Graphpad Software, La Jolla, USA; RRID:SCR_002798). Statistical analyses were chosen that do rely on non-parametric distribution, since all data sets were $n \leq 10$. Statistical differences between two groups with only one variable were analyzed using the Mann-Whitney non-parametric *t*-test. For more than two groups with multiple variables, Kruskal Wallis one-way analysis of variance (ANOVA) with Dunn's post tests were applied. Statistical differences between two or more groups with more than two variables were analyzed using an ordinary two-way ANOVA with the Sidak's post-test. All results are shown as mean ± SEM and asterisks were assigned to the *p*-values in the following order: $^{*}p \leq 0.05$; $^{**}p \leq 0.01$; $^{***}p \leq 0.001$; $^{****}p \leq 0.0001$.

RESULTS

Cryopreserved hAACs Show Typical Characteristics for Cells of Mesenchymal Origin

It is crucial for a potential allogeneic application of hAACs to determine the general characteristics of these cells after long-term cryopreservation. hAACs from eight right atrial appendages were generated from outgrowth cultures by negative immunoselection for CD90, expanded in cell culture and cryopreserved for at least 6 months (**Figure 1A**). Thawed cells after 24 h in cell culture showed their distinctive morphology with long elongated cell bodies and fibroblast-like appearance (**Figure 1B**). Flow cytometry analysis for characteristic surface markers of mesenchymal cells confirmed the distinguishing marker profile of these cells. The hAAC cell product expressed most of the known mesenchymal stem- and progenitor markers (e.g., CD29, CD44, CD73, CD105, and CD166), while lacking the expression of the endothelial marker CD31, the hematopoietic markers CD14, CD34, and CD45 as well as the cardiac progenitor marker c-Kit (CD117) (**Figure 1C**). Yet, in contrast to classical fibroblasts and mesenchymal stromal cells, only a small proportion of cells was positive for CD90 (**Figure 1D**).

Inflammatory Priming Alters the Immune Phenotype of hAACs

To investigate the surface marker profile in an inflammatory milieu, that mimics the environmental site of cardiac injury, hAACs were stimulated with 100 ng/mL of IFNγ for 48 h. Initial experiments with stimulation by pro-inflammatory cytokines (IFNγ or a combination with TNFα) for 1, 2, and 5 days, showed an increase in surface marker expression in the majority of tested markers (HLA-ABC, HLA-DR, PD-L1) with an overall maximum of up-regulation after 2 days (**Supplementary Figure 2**). Hence, the time point of 48-h stimulation with an appropriate IFNγ concentration of 100 ng/mL was chosen to determine the relative expression levels as normalized mean fluorescence intensities (MFI) for a set of immunologically-relevant markers. Stimulation of hAACs induced similar changes in the surface marker expression of all six donors as shown in FACS histogram overlays (**Figure 2A**) of one representative donor and summarized as

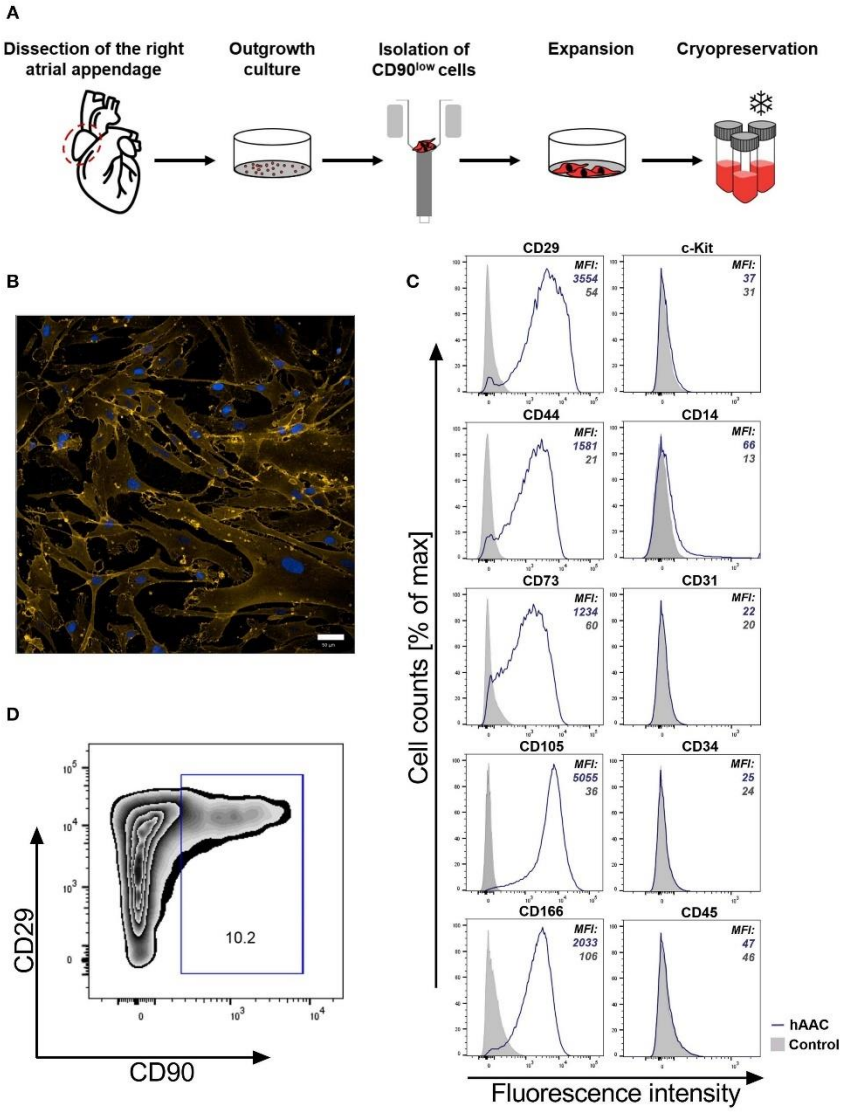

FIGURE 1 | Characteristics of human atrial appendage-derived cells (hAAC). **(A)** The general procedure to generate hAACs is shown: right atrial appendages were harvested from patients during open-heart surgery. The dissected tissue was minced into small pieces and cultured. Subsequently, the fragment's outgrowth was harvested, immuno-magnetically sorted as $CD90^{low}$ cells and seeded again for further expansion of the desired purified hAAC product. The cells were cryopreserved and long-term stored for later experimental use. **(B)** Representative immunofluorescence images show the characteristic morphology of one hAAC donor in a cell culture plate after 12 h of incubation. Cell membranes (orange) were stained with wheat germ agglutinin (WGA) and nuclei (blue) with 4,6-diamidin-2-phenylindol (DAPI). Scale bar represents 50 μm. **(C)** Generated hAACs were harvested by treatment with trypsin after passage four and stained with human-specific antibodies against surface markers characteristic for cells of mesenchymal origin (CD29, CD44, CD73, CD105, CD166), markers for exclusion of hematopoietic contaminants (CD14, CD31, CD34, CD45) and the cardiac progenitor marker c-Kit (CD117). Representative flow cytometry histograms of one hAAC donor are shown as fluorescence intensity against cell counts for all tested markers, indicating the mean of fluorescence intensity (MFI) of positive cells (blue) compared to the unlabeled controls (gray) for each marker. **(D)** The percentage of remaining $CD90^{+}$ cells in the hAAC cell product is shown for one representative donor in a dot plot of CD90 against CD29.

normalized MFI values (**Figure 2B**) as well as percentages of marker positive cells (**Supplementary Figure 3**). All donors expressed HLA-class I (HLA-ABC, and partly HLA-E) and low or negligible levels of HLA class II (HLA-DR) constitutively, but significantly up-regulated both HLA-molecule classes under IFNγ-stimulation. In contrast, co-stimulatory molecules such as CD80 and CD86 were completely absent, even under stimulation. Additionally, a significant increase of the

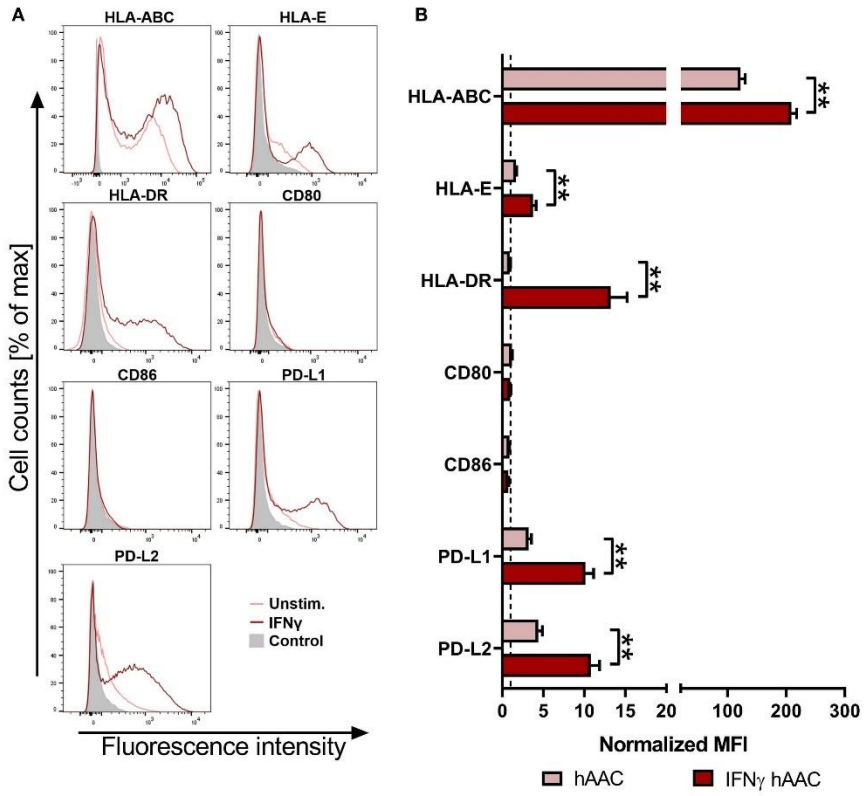

FIGURE 2 | Immune phenotype of cryopreserved hAACs under constitutive and inflammatory conditions. **(A)** Representative histogram overlays for one hAAC donor display the expression pattern for immunologically-relevant surface markers (HLA-ABC, HLA-E, HLA-DR, CD80, CD86, PD-L1, PD-L2). Cells were cultured for 48 h without additional stimulation (hAAC; light red line) or in presence of 100 ng/mL human interferon-gamma (IFNγ hAAC; dark red line). After harvest by application of trypsin, cells were stained with human-specific antibodies and analyzed by flow cytometry. Fluorescence intensity of marker expression is presented compared to the unlabeled control (Control; filled gray curve). **(B)** Summarized hAAC surface marker expression data are presented as normalized mean of fluorescence intensities (MFI), that are calculated based on the respective controls (set to one; dashed black line), and shown as mean + SEM ($n = 6$; three independent experiments with six different hAAC donors). Differences between unstimulated hAACs and IFNγ hAACs were considered significant when $^{**}p \leq 0.01$ with the Mann-Whitney *t*-test.

MFI for the immunomodulatory PD-1 ligands (PD-L1 and PD-L2) could be determined after stimulation with IFNγ (**Figure 2B**). Both markers were shown to be expressed on a considerable proportion of cells (**Supplementary Figure 3**). However, stimulation with IFNγ did not led to alterations in MFI or frequency of mesenchymal marker expression (CD29, CD44, CD73) on hAACs and even CD90 remained unchanged (**Supplementary Figure 4**).

hAACs Evade Recognition by Allogeneic T Cells *in vitro* Even in an Inflammatory Milieu

Next, we were interested in the response of T cells against allogeneic hAACs due to their key role as mediators of allo-recognition and rejection in adaptive immune responses. Accordingly, we mimicked the *in vivo* situation by co-culturing HLA-mismatched PBMCs with hAACs from six different donors and investigated the induction of allogeneic T cell responses by monitoring their activation as well as proliferation. The T cell immune responses induced by MSCs and HUVECs have been well-described in the literature and therefore both cell types were used as controls for absent or induced responses, respectively. As shown in the experimental setup (**Figure 3A**) hAACs as well as MSCs and HUVECs were cultured with or without pre-stimulation by IFNγ for 48 h, thereupon CFSE-labeled PBMCs from healthy donors were added to the cultures. After 7 days of co-culture, the surface marker expression and proliferation of T cells were analyzed by flow cytometry. Compared to the unstimulated PBMC control cultures, the presence of unstimulated HUVECs significantly induced proliferation of $CD8^+$ T cells but had no effect on the $CD4^+$ T cell compartment (**Figures 3B,C**). However, pre-stimulation with IFNγ led to highly elicited levels of both $CD4^+$ and $CD8^+$ T cell proliferation.

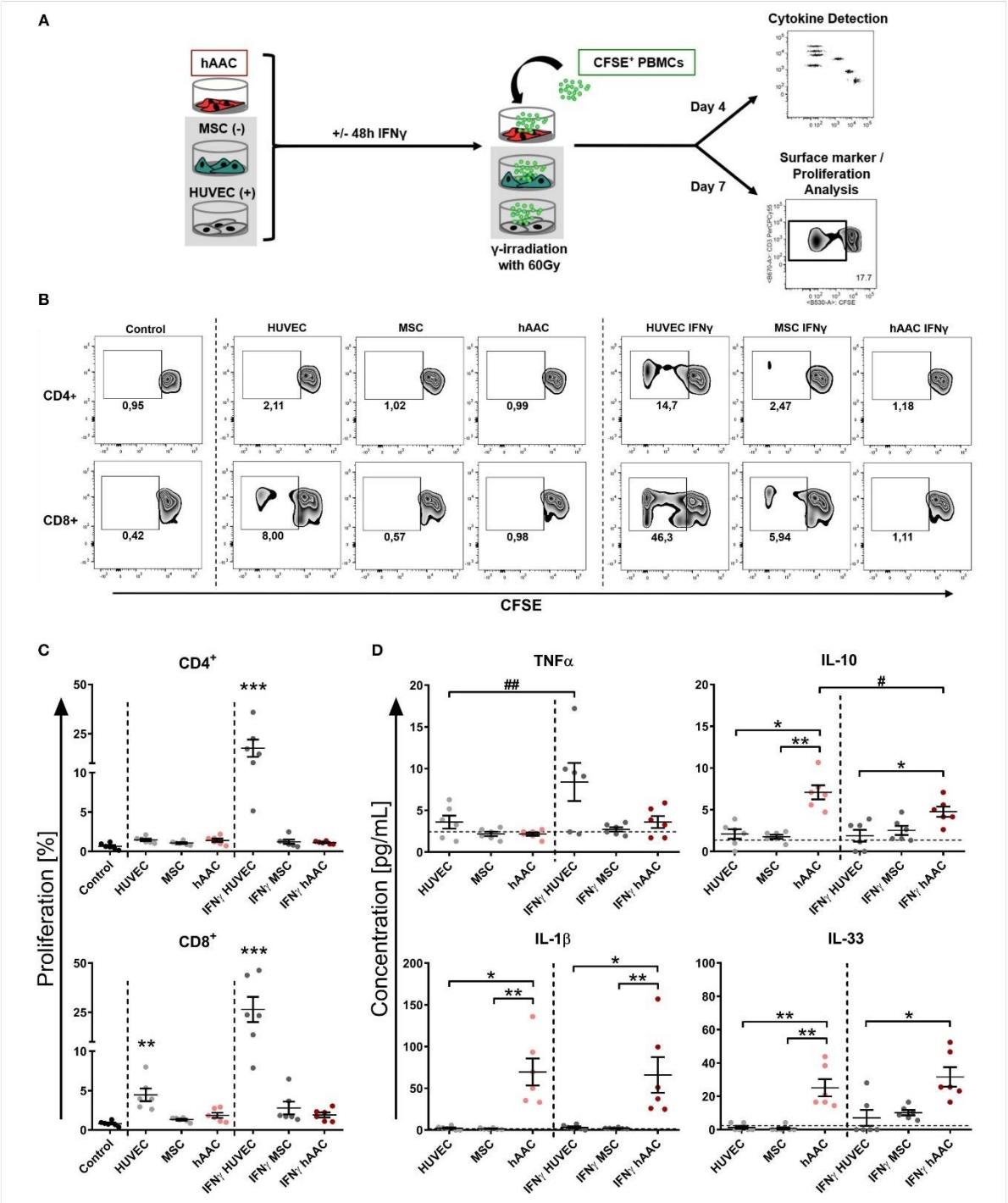

FIGURE 3 | hAACs maintain a low-immunogeneic profile even in an inflammatory environment. **(A)** The experimental setup for analyzing hAACs immunogenicity in immune cell co-cultures is illustrated: mesenchymal stromal cells from the umbilical cord (MSCs) as well as human umbilical vein endothelial cells (HUVECs) served,

(Continued)

FIGURE 3 | respectively, as cellular controls [MSC (-); HUVEC (+)] and were cultured along with hAACs for 48 h in the presence or absence of 100 ng/mL IFNγ. The cells were gamma-irradiated with 60 Gray before carboxyfluorescein succinimidyl ester (CFSE)-labeled, human leukocyte antigen (HLA)-mismatched peripheral blood mononuclear cells (PBMCs) were either added to the adherent cell cultures of all three cell types or left alone as control. After 4 days of incubation, supernatants were taken for cytokine detection using the Legendplex™ human inflammation panel and after 7 days PBMCs were harvested, stained with human immune cell specific antibodies and analyzed flow cytometrically. Levels of $CD4^+$ and $CD8^+$ T cell proliferation were detected by determining reduced CFSE signal intensity (black square). **(B)** Representative flow cytometry plots of proliferated $CD4^+$ and $CD8^+$ T cells are shown for all PBMC co-culture groups and PBMCs only (Control). **(C)** Summarized proliferation data for $CD4^+$ and $CD8^+$ T cells are presented as mean ± SEM ($n = 6$; three independent experiments with six different hAAC donor). Groups were considered significantly different compared to the Control when $^*p \leq 0.05$; $^{**}p \leq 0.01$; $^{***}p \leq 0.001$ with Kruskal Wallis ANOVA and Dunn's post-test. **(D)** Measured cytokine levels in [pg/mL] for TNFα, IL-10, IL-1β, and IL-33 are shown as mean ± SEM ($n = 6$). Cytokine levels of the PBMC control groups are depicted as dotted gray line. Groups were considered significantly different when $^*p \leq 0.05$; $^{**}p \leq 0.01$; $^{***}p \leq 0.001$ with Kruskal Wallis ANOVA and Dunn's post-test. Differences between treatments were considered significant when $\#p \leq 0.05$; $\#\#p \leq 0.01$ with ordinary two-way ANOVA and Sidak's post-test.

A similar trend was observed in the activation status that was revealed by significantly increased percentages of HLA-DR^+ T cells in the $CD4^+$ and $CD8^+$ subsets after IFNγ pre-stimulation (**Supplementary Figure 5**). hAACs on the other hand displayed low-immunogeneic properties analogous to the moderate levels of induced T cell proliferation detected in MSC co-cultures. Both, hAACs and MSCs did not induce significant changes in $CD4^+$ or $CD8^+$ T cell proliferation after IFNγ pre-stimulation as well as under unstimulated conditions (**Figures 3B,C**), neither did both cell types lead to increased expression levels of the activation marker HLA-DR on T cells (**Supplementary Figure 5**).

Additionally, supernatants were taken from co-cultures after 4 days of incubation and were evaluated for their content of various cytokines. Summarized data for TNFα, IL-10, IL-1β, and IL-33 are presented in **Figure 3D**. The amount of the pro-inflammatory cytokine TNFα significantly increased in IFNγ-stimulated HUVEC co-cultures. Contrarily, unstimulated hAAC co-cultures exclusively showed elevated levels of IL-10 release, that significantly decreased with IFNγ pre-stimulation. Significant increases of IL-1β concentrations were detected in co-cultures of unstimulated and IFNγ-stimulated hAACs. While the concentration of IL-33 also increased in unstimulated hAAC cultures, IFNγ-triggered co-cultures only showed a significant elevation compared to the cytokine levels secreted by HUVECs. Contrary to TNFα and IL-10, mono-cultures of hAACs already constitutively produced the cytokines IL-1β and IL-33 (**Supplementary Figure 6**). Other cytokines measured, like MCP-1 and IL-8, were also produced at a basal level by the adherent cells and showed no inordinate changes in PBMC co-cultures (**Supplementary Figure 7**). IFNα, IFNγ, IL-12p70, IL-17A, IL-18, and IL-23 were not detectable or only at negligible levels (data not shown).

Immunomodulatory Efficiency of hAACs Is Considerably Enhanced After IFNγ Treatment

Activation of T cells and the resulting inflammatory responses after cardiac injury largely contribute to adverse remodeling and development of chronic heart diseases in patients. We therefore examined the ability of hAACs, either unstimulated or IFNγ pre-stimulated, to modulate an already ongoing T cell response in co-cultures with αCD3/αCD28 activated PBMCs. In parallel PBMC co-cultures with both control cell types (HUVECs and MSCs) were performed. After 72 h of co-culture, proliferation rates of $CD4^+$ and $CD8^+$ T cells and cytokine release were analyzed.

As expected, the presence of HUVECs did not significantly affect the proliferation rates of T cells (**Figures 4A,B**). Contrarily, hAACs and MSCs efficiently reduced the percentage of proliferating $CD4^+$ and $CD8^+$ cells, exclusively after IFNγ triggering, below 10% (**Figures 4A,B**). A slight reduction in T cell proliferation was observed with unstimulated adherent cells, but these changes were in fact not significant. Experimental settings were repeated with hAACs under transwell conditions to test for contact-dependency of the observed immunomodulatory effects. No changes in proliferation of $CD4^+$ and $CD8^+$ T cells were detectable with unstimulated hAACs in the transwell setting. Pre-stimulation with IFNγ on the other hand caused significant reduction of proliferation levels in both T cell subsets (**Figure 4C**). The same trend was observed with a significant decrease of the activation marker CD25 on $CD4^+$ and particularly $CD8^+$ T cells after IFNγ pre-stimulation (**Supplementary Figure 8**).

Furthermore, a significant decrease of IFNγ and TNFβ concentration was measured in co-cultures with unstimulated and IFNγ-stimulated hAACs, but only the latter showed a significant reduction in the amount of released TNFα, MDC, IL-10, and IL-17A. Interestingly, co-cultures with unstimulated hAACs produced significantly more IL-1β and less IL-2 (**Figure 4D**). Other cytokines measured like IL-5 and IL-13 showed significantly lower levels in IFNγ stimulated co-cultures (data not shown).

Stimulation by IFNγ Leads to Specific Changes in the Gene Expression Profile of hAACs

Whole genome gene expression of unstimulated and IFNγ pre-stimulated hAACs were analyzed on human hgu133plus2 microarrays (Affymetrix). Data were normalized and the 1000 most variable probe sets were used in a principle component analysis. This unbiased analysis revealed a strong separation of unstimulated and IFNγ pre-stimulated samples along the first principle component reflecting the experimental design. In addition, samples were separated according to different hAAC donors in the principle component two, indicating some heterogeneity of gene expression (**Figure 5A**). Although showing these individual characteristics in gene expression, additional analyses with Raman spectroscopy revealed a

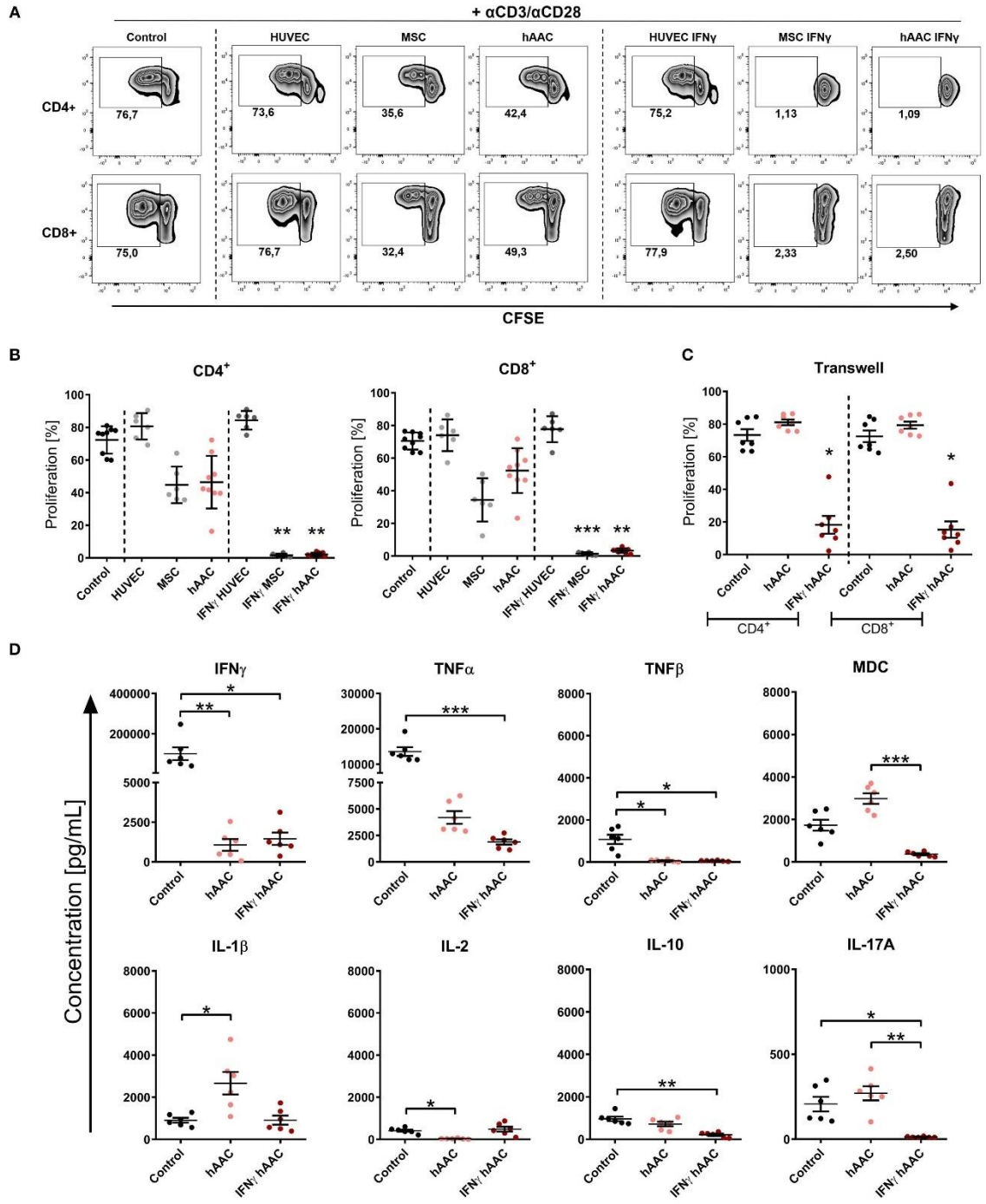

FIGURE 4 | IFNγ pre-stimulation enhances the immune-modulatory capacity of hAACs. CFSE-labeled PBMCs were activated with anti-CD3/anti-CD28 antibodies (+αCD3/αCD28) and cultured alone (Control) or in the presence of unstimulated or IFNγ-stimulated hAACs, HUVECs or MSCs for 72 h. Cells were harvested, stained

(Continued)

FIGURE 4 | with human-specific antibodies and analyzed by flow cytometry for T cell proliferation, based on reduced CFSE signal intensity. Percentages of $CD4^+$ or $CD8^+$ proliferated cells for all experimental groups are shown as representative dot plots **(A)** and as summarized data with mean ± SEM **(B)** ($n = 6–9$; four independent experiments with seven different hAAC donors). **(C)** Experimental settings were repeated with hAACs under transwell culture conditions to evaluate a contact-dependent mode of action in the observed immune-modulatory effects ($n = 7$; three independent experiments with six different hAAC donors). **(D)** Supernatants of the direct immune cell co-cultures with either unstimulated or IFNγ-treated hAACs were analyzed with a Luminex bead kit for their content of IFNγ, TNFα, TNFβ, MDC, IL-1β, IL-2, IL-10, and IL-17A. Summarized data for cytokine concentrations [pg/mL] are presented as mean ± SEM ($n = 6$; three independent experiments with six different hAAC donors). Groups were considered significantly different when $^*p \leq 0.05$; $^{**}p \leq 0.01$; $^{***}p \leq 0.001$ with Kruskal Wallis ANOVA and Dunn's post-test.

similar global phenotype of the hAAC cell product with no detectable differences in the molecular composition of cells derived from three hAAC donors (**Supplementary Figure 9**). Next, differentially expressed genes between the unstimulated and IFNγ pre-stimulated groups were determined by fitting linear models to the data and running a Bayesian statistic. Despite the genetic heterogeneity of the donors, a common response to IFNγ can be identified as shown in the heatmap (**Figure 5B**). Differentially expressed genes were subjected to an overrepresentation analysis utilizing the gene ontology system. The eight top-ranking results of the category "biological process" are shown in **Figure 5C** and were related to the immune system, cytokine-signaling and according to the experimental setup to the IFNγ-response. Remarkably, much more genes were up-regulated as down-regulated in the gene sets matched to these GO-terms. The whole results of the overrepresentation analysis are summarized in **Supplementary Table 3**. To identify a common mode of action among the hAAC donors after IFNγ pre-stimulation, the results of the genome-wide gene expression profile were checked for differential expression of known immunomodulatory genes in MSCs, including: *IDO1, PD-L1, PD-L2, NT5E, TGFB1, PTGES2, HGF, IGF, TNFAIP6, JAG1, ICOSLG, HLA-G, PGE2, IL-10, LDHB, LDHA, LGALS1, LGALS9, TLR3, ANXA1, VCAM1, PTGS1, PTGS2* and *LIF*. However, only *IDO1, LGALS9, TLR3, PD-L1, PD-L2, PTGS1, HLA-G*, and *VCAM1* were differentially expressed among all three donors and were therefore validated by qPCR. The analysis of the relative gene expression normalized to the corresponding unstimulated hAAC sample showed a very strong upregulation of *IDO1* expression in IFNγ-triggered hAACs. Yet, other immune regulatory genes like *LGALS9* (Galectin-9), *TLR3, HLA-G, PTGS1* (COX-1) as well as *PD-L1* and *PD-L2* also showed a distinct upregulation in the presence of IFNγ, but admittedly to a much lesser extent (**Figure 5D**).

IDO Predominantly Mediates Immunomodulation by IFNγ-Triggered hAACs and Acts Through Apoptosis of T Cells

Since *IDO1* was by far the most upregulated gene in IFNγ pre-stimulated hAACs (**Figure 5D**) and PD-L1/PD-L2 were already described in the literature as a key mechanism of action in cardiac-derived cells (30) and MSCs (45), we selected them as promising molecules that might be involved in the observed immunomodulatory potential of hAACs (**Figure 4B**). As illustrated in **Figure 6A**, hAACs were cultured for 48 h in the presence or absence of IFNγ. Following 2 h of pre-incubation with 1-MT as a specific inhibitor of IDO or 12 h with blocking antibodies against PD-L1 and PD-L2 (αPD1-ligand), either CFSE labeled or unlabeled PBMCs were added to the cultures and were subsequently activated with a cocktail of αCD3/αCD28 antibodies. After 72 h, PBMCs were analyzed by flow cytometry to determine proliferation and apoptosis of T cells.

hAACs without treatment by blocking agents confirmed the observed immunomodulatory effects by significantly inhibiting T cell proliferation after IFNγ pre-stimulation, shown as relative proliferation normalized to the αCD3/αCD28 PBMC control (**Figure 6B**). Additionally, significantly higher levels of late-apoptotic T cells occurred in IFNγ pre-stimulated co-cultures, shown as relative percentages of Annexin-V^+7-AAD^+ T cells normalized to the αCD3/αCD28 PBMC control (**Figure 6C**). Treatment with blocking antibodies against both PD-1 ligands neither had a significant effect on proliferation (**Figure 6B**), nor on apoptosis rates (**Figure 6C**) of $CD4^+$ and $CD8^+$ T cells when compared to the untreated control group. Notably, treatment with 1-MT, mediating the blocking of IDO, resulted in significant restoration of T cell proliferation in IFNγ-stimulated hAAC co-cultures. However, unstimulated cultures displayed rather reduced proliferation rates for both T cell subsets (**Figure 6B**). Complementary to the proliferation, treatment with 1-MT also caused significant reduction of Annexin-V^+7-AAD^+ late-apoptotic T cells for the IFNγ hAAC group relative to the untreated control group (**Figure 6C**). Yet, comparing unstimulated hAACs with IFNγ hAAC under 1-MT treatment illustrates, that levels were still elevated for apoptotic $CD4^+$ cells, but were in fact not significantly different for the $CD8^+$ subset (**Figure 6C**).

DISCUSSION

Based on the limited treatment options for cardiovascular diseases, the development of new and potent cellular therapeutics has emerged in the past decade as a promising new strategy aimed at preventing or even reversing myocardial damage.

A huge variety of cell therapy studies had been conducted with MSCs of different tissue origins, which reported only modest or no significant efficacy to improve cardiac function (46). The initial enthusiasm faded and a multitude of scientific questions remained unanswered (47). Apart from developing solutions for patient selection, timing of administration and appropriate application routes including scaffold-based approaches, efficient cell pre-conditioning or genetic manipulation (24), the most pressing task is the identification of an isolation procedure for a

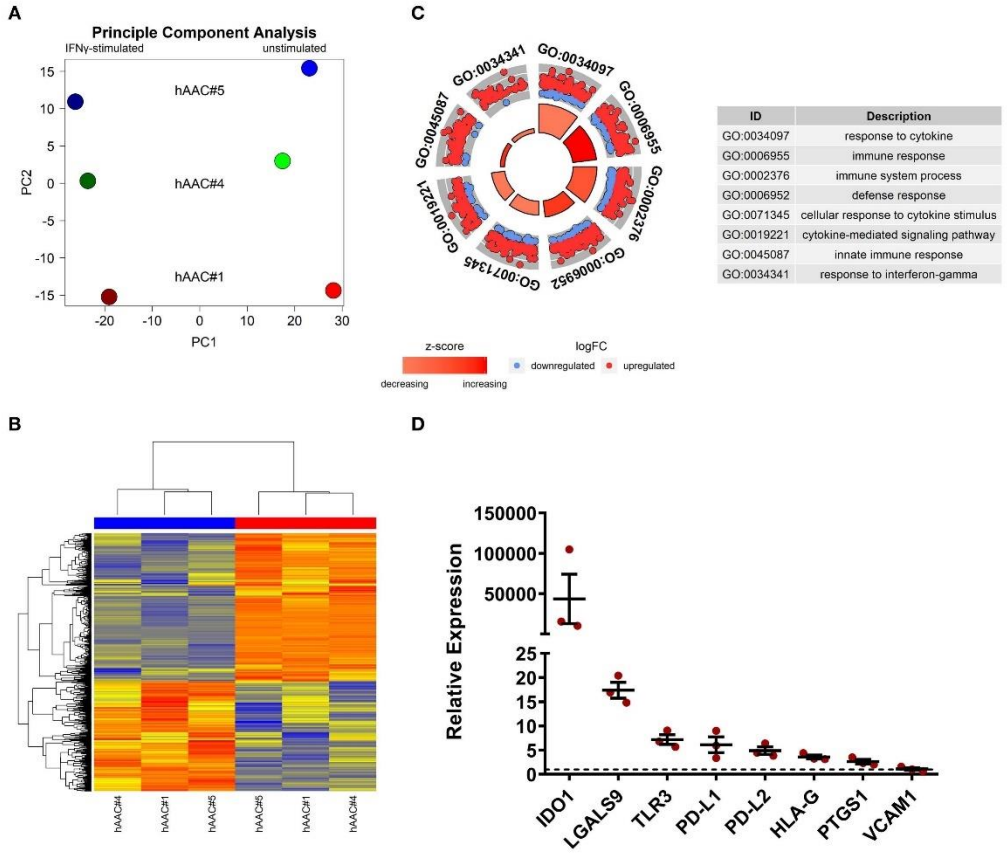

FIGURE 5 | Whole genome expression analysis and quantitative verification of immunomodulatory gene expression of unstimulated and IFNγ pre-stimulated hAACs. **(A)** Microarray expression data of unstimulated and IFNγ-stimulated hAACs were normalized and log2-transformed. Thousand probe sets with the highest variances across all samples were selected and used in a principle component analysis, showing PC1 vs. PC2 for $n = 3$ hAAC donors (#1, #4, #5). **(B)** Differentially expressed probe sets were determined by fitting linear models to the data and apply Bayesian statistics. *P*-values were adjusted for multiple testing using false discovery rate. Probe sets with an adjusted *p*-value below.05 and a minimal absolute log2-foldchange of 1 are shown in the heatmap. The blue column bar indicates the unstimulated and the red bar the IFNγ pre-stimulated hAACs of donors #1, #4, #5. **(C)** Differentially expressed probe sets were used in an overrepresentation analysis utilizing the gene ontology system. The eight top-ranking results of the category biological process are shown. **(D)** The differentially expressed immunomodulatory genes *IDO1, LGALS9, TLR3, PD-L1, PD-L2, HLA-G, PTGS1* and *VCAM1*, identified in the global microarray analysis, were validated by qPCR. Values of IFNγ pre-stimulated hAACs were normalized to the unstimulated samples (set to 1; black dotted line) by means of a ΔΔCt analysis and upregulation is shown as mean of relative expression ± SEM for $n = 3$ hAAC donors (#1, #4, #5).

suitable and effective cell type. In this context, cells isolated from close origin to the target tissue seem to be the most promising cell therapeutic strategy (48, 49). Therefore, cardiac-derived cell types excelled as a potentially powerful cell source due to their known cardio-protective and pro-angiogenic effects. Due to the lack of scientific evidence and understanding regarding these positive effects of cell-based therapies, a return to the bench-side would not only help to understand the mode of action, but also may lead to a more reliable and effective therapy for the patient (12). Moreover, large batches of healthy and instantly available cells are needed for the realization of a broad and less expensive clinical application, which clearly favors allogeneic cell sources. To exclude any unwanted immunogenicity, especially under an inflammatory and disease-related condition, it is indispensable to analyze the interaction with immune cells *in vitro*. In the present study, we addressed these issues by analyzing first the main immunological characteristics of the allogeneic hAAC cell product to estimate its immunogenicity and secondly by investigating the immunomodulation capacity focusing on T cell responses.

We could convincingly show that human allogeneic cells from the right atrial appendage (hAACs) exhibit, even in an inflammatory environment, an inherently low immunogenicity, as demonstrated by the absence of adversely induced T cell responses in immune cell co-cultures. Moreover, we could clearly present that hAACs are effective modulators of already induced

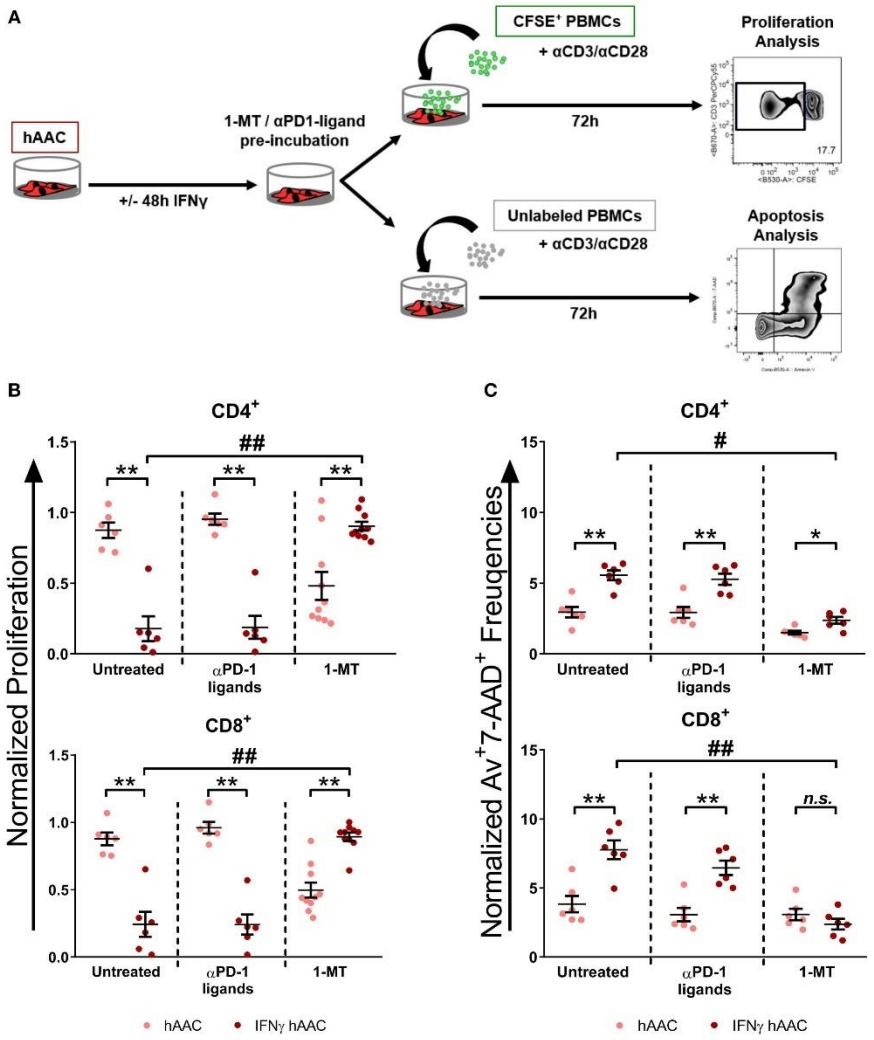

FIGURE 6 | Inhibition of T cell proliferation by hAACs is indoleamine-2,3-dioxygenase (IDO)-dependent and involves apoptosis. **(A)** The experimental setup to evaluate the potential involvement of IDO and programmed death-1 (PD-1) ligands in hAAC effects on T cells is shown schematically: hAACs were seeded and stimulated with IFNγ or left unstimulated for 48 h. Before co-cultivation with immune cells, 1-mehtyl-L-tryptophan (1-MT) as specific inhibitor of IDO or blocking antibodies against PD-L1 and PD-L2 (αPD1 ligands) were applied. Subsequently, either CFSE-labeled or unlabeled PBMCs were activated by adding a cocktail of anti-CD3/anti-CD28 (+αCD3/αCD28) antibodies and left alone as controls or cultured with hAACs for 72 h. $CD4^+$ or $CD8^+$ T cell proliferation levels as well as the percentage of Annexin-V^+ (Av+) 7-AAD^+ late apoptotic cells were determined by flow cytometry. **(B)** The normalized proliferation values for $CD4^+$ or $CD8^+$ T cell subsets were calculated based on the respective PBMC controls and are presented as mean ± SEM ($n = 6$–10; four independent experiments with seven different hAAC donors). **(C)** The normalized percentages of late-apoptotic Annexin-V^+ (Av^+) 7-AAD^+ cells within the $CD4^+$ and $CD8^+$ T cell subsets were calculated based on the respective PBMC controls and are presented as mean ± SEM (n = 6; two independent experiments with six different hAAC donors). Unstimulated (hAAC) and IFNγ-stimulated hAACs (IFNγ hAAC) within the same treatment were considered significantly different when $*p \leq 0.05$; $**p \leq 0.01$ with the Mann-Whitney *t*-test. Differences between treatments were considered significant when $\#p \leq 0.05$; $\#\#p \leq 0.01$ with Kruskal Wallis ANOVA and Dunn's post-test.

immune cell responses by suppressing T cell proliferation and pro-inflammatory cytokine release, especially after triggering with IFNγ. We could additionally show that IDO is one of the key mediators responsible for the observed immunomodulating features of hAACs. Our data strongly support the use of these allogeneic cardiac-derived cells for the therapeutic application in cardiovascular diseases.

So far, application of allogeneic cells for therapeutic approaches was only taken into account for mesenchymal cell types, like mesenchymal stromal cells (MSC) and cardiac

progenitor cells (CPC) due to their known low immunogeneic phenotype (22, 25, 50, 51). Therefore, we checked our newly described hAAC cell product for the presence of characteristic mesenchymal cell markers and could confirm a similar expression pattern as seen in MSCs, with the only exception of a significantly reduced CD90 expression. A low CD90 expression might be an advantage for future therapeutic approaches by reducing fibrosis, as shown in a prospective analysis of a clinical trial using cardiosphere-derived cells (33). Inversely, another study using human tissue revealed that CD90 expressing fibroblasts are mainly responsible for the fibrotic thickening in peritoneal dialysis patients (52).

However, more important for the clinical application of an allogeneic cell product is to determine its potential immunogenicity (53, 54) by evaluating the expression of immunological markers under constitutive and inflammatory conditions. In the present study, we could clearly demonstrate that hAACs constitutively expressed HLA-ABC and partially HLA-E, but not HLA-DR as well as the main co-stimulatory molecules CD80 and CD86. After IFNγ stimulation, the expression profile shifted toward a further increased expression level of HLA-class I molecules and *de novo* induction of HLA-DR expression. Yet, the co-stimulation molecules remained absent. Additionally, hAACs showed expression of the immunomodulatory molecules PD-L1 and PD-L2 on a considerable proportion of cells that was further enhanced after inflammatory stimulation. Comparatively, this surface marker profile was already described for MSCs (45, 55, 56) and related cardiac cell types (30, 57).

Despite the upregulated expression of both classes of HLA-molecules after IFNγ stimulation, hAACs evaded an adaptive immune response and were thereby not able to trigger substantial $CD4^+$ and $CD8^+$ T cell proliferation, when co-cultured with human PBMCs. The in parallel tested human MSCs induced a similar proliferation response pattern in T cells. Although these results might suggest the conclusion that hAACs and MSCs share a common mode of action, they clearly differed in the spectrum of secreted cytokines within PBMC co-culture supernatants. Whereas, unstimulated and IFNγ stimulated MSCs and hAACs did not induce any TNFα release, only the cardiac mesenchymal-like hAACs showed significantly enhanced induction of the anti-inflammatory cytokine IL-10 in both conditions. However, it is striking, that exclusively IL-1ß and IL-33 levels were significantly higher in co-cultures with hAACs, which exceeded the constitutive secretion of both cytokines by hAACs alone. So far it is unclear, which effects both cytokines of the IL-1 family would have after transplantation of hAACs in a therapeutic setting. It is known that they are classical pro-inflammatory factors with an ambivalent function. On the one hand, IL-1β secretion of MSCs is involved in monocyte dependent regulation of $CD4^+$ and $CD8^+$ T cell activation by triggering the release of TGFβ (58). IL-33, on the other hand, could play an important role in cardiac tissue preservation and repair in response to myocardial injury (59–62).

Our results regarding the induction of immune cell responses with $CD90^{low}$ hACCs are comparable to data described for $CD90^+$ allogeneic human CPCs (30). Therefore, the expression or absence of CD90 on cardiac-derived cells apparently seems to be of inferior importance for the immunogenicity of the respective allogeneic cell product. However, in contrast to our study Lauden et al. demonstrated a rather low, but significant induction of $CD4^+$ T cell proliferation. Consequently, they were able to prove the induction of regulatory T cells in co-cultures of purified $CD4^+$ T cells with human CPCs.

For the potential clinical application of the hAAC cell product, not only a low immunogenicity, but also the capacity to suppress ongoing inflammatory immune responses is important, since it is widely believed to be responsible for the adverse remodeling after cardiac injury (63, 64). In co-cultures with human allogeneic PBMCs, we were able to demonstrate the capacity of hAACs as well as MSC controls to suppress $CD4^+$ and $CD8^+$ T cell proliferation nearly to the same extent. Both cell types inhibited T cell proliferation by trend if cells were cultured under unstimulated conditions and strongly enhanced their suppressive capacity after IFNγ pre-stimulation. The "licensing" effect of IFNγ was already well-described by several groups for MSCs from different sources (65–69). In contrast, no clear similarities between human CPCs and MSCs were detectable regarding the inhibitory capacity of T cell proliferation in PHA stimulated immune cell cultures as well as in mixed lymphocyte reaction settings (30). However, the experimental design of our study relied on different cell sources and a diverging setup of immune cell co-cultures, which might explain varying results of the immunomodulation. The comparable immunomodulatory efficacy of $CD90^{low}$ hAACs and the $CD90^+$ control umbilical cord MSCs argues, that CD90 expression does not play a fundamental role in our experimental setup. Although, a potential correlation was described by others for human MSCs derived from bone marrow, amnion and chorion (70), other factors seem to determine the immunosuppressive features of this specific hAAC product.

The high potency of hAACs to efficiently down-regulate already ongoing immune responses was additionally confirmed by a strong suppression of the pro-inflammatory mediators IFNγ, TNFα, and IL-17A as well as IL-2 to a minor extent. Again, these effects were further enhanced in co-cultures with IFNγ-licensed cells. The typical induction of a shift from an inflammatory toward a more anti-inflammatory secretion profile was described for human MSCs (71–74) and for CPCs (25, 75). However, presence of hAACs in triggered immune cell co-cultures rather lowered anti-inflammatory cytokines like TGFß and IL-10 instead of inducing those as described for MSCs (58, 73, 76).

Next, we wanted to get a deeper understanding of the molecular changes in hAACs after pre-stimulation with IFNγ that are likely to be responsible for the immunosuppressive or modulatory efficacy. For this, we compared unstimulated and IFNγ stimulated hAACs in a whole genome analysis by Affymetrix® microarray technology and could determine similar characteristics for all three donors between each treatment group, despite visible biological heterogeneities in their individual RNA profiles. More interestingly, the global analysis revealed, that pathways of general immune system responses (innate and adaptive), as well as cytokine signaling and IFNγ responses were

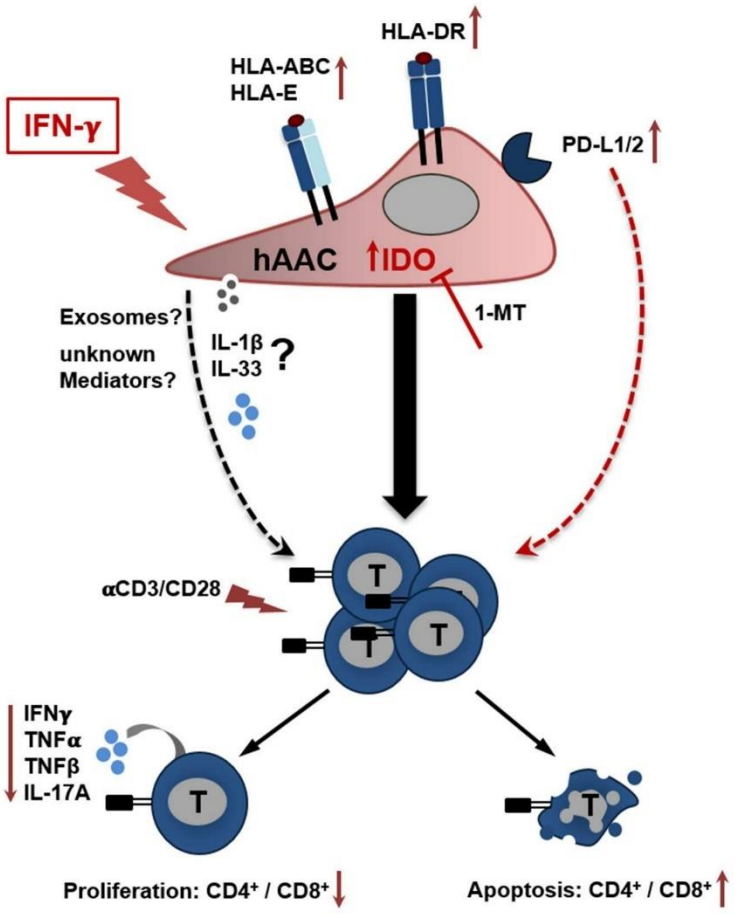

FIGURE 7 | Potential crosstalk between hAACs and T cells in an inflammatory milieu. The scheme illustrates the impact of IFNγ stimulation on CD90^{low} hAACs and its implication on the interplay with αCD3/αCD28 activated human T cells. Stimulation of hAACs alone induces upregulation of HLA-class I (HLA-ABC, HLA-E) and *de novo* expression of HLA-class II molecules (HLA-DR). Even though expression of the inhibitory co-stimulatory molecules PD-L1 and PD-L2 is enhanced on the cell surface, no specific effects in the interaction with activated T cells were detectable. Similarly, the role of the specific secretion of IL-1 family cytokines (IL-1β, IL-33) by hAACs and additional unknown mediators like exosomes remain unclear. However, a global genome-wide expression profile analysis revealed IDO as one of the strongest expressed genes in IFNγ stimulated hAACs. Specific blocking by 1-MT proved the essential involvement of IDO in the interaction with T cells. It mediates the suppression of CD4$^+$ and CD8$^+$ T cell proliferation, reduces the secretion of pro-inflammatory cytokines (IFNγ, TNFα, TNFβ, IL-17A) and induces apoptosis of both T cell subsets. We hypothesize, that this mode of hAAC interaction might contribute to the resolution of immune responses and limit thereby the effects of adverse remodeling after cardiac injury.

preferentially involved. A closer look into specific, immune-relevant molecules, that were significantly up-regulated under IFNγ stimulation, exposed *IDO1* as one of the strongest expressed genes among other interesting candidates, such as *LGALS9* (Galectin-9), *TLR3, HLA-G, PTGS1* (COX-1). The particularly high degree of *IDO1*-upregulation in IFNγ pre-stimulated hAACs was also confirmed by qPCR. IDO is often discussed to be involved in immunosuppressive effects exerted by MSCs on T cells by depletion of tryptophan and accumulation of metabolites like kynurenin (77–81). In correlation with the strong up-regulation of IDO, we could prove the involvement of this particular molecule in the suppression of T cell proliferation and the induction of their apoptosis by application of the specific inhibitor 1-MT. These observations are in accordance with a recent study, which correlated the suppressive capacity of IFNγ licensed MSCs on third party T cell proliferation to enhanced IDO and PD-L1 expression (82).

Interestingly, PD-L1 and PD-L2 were found to be up-regulated on RNA and protein level in hAACs after inflammatory stimulation. The interaction of these two molecules with PD-1 on T cells might also contribute to the observed immunosuppressive effects. For bone marrow MSCs it was recently demonstrated

that the expression and secretion of both PD-1 ligands mediated suppression of $CD4^+$ T cell activation, down-regulated IL-2 secretion and induced hypo-responsiveness and cell death in T cells (45). However, in our experimental settings the application of blocking antibodies against both PD-1 ligands could neither reverse the suppression of T cell proliferation nor prevent the induction of apoptosis. We also found, that IFNγ pre-stimulated hAACs showed nearly the same suppression of αCD3/αCD28-induced T cell proliferation in direct contact as well as transwell settings. That implies that hAACs mainly mediate their immunomodulatory effects in an inflammatory milieu by soluble factors or vesicles that are able to cross the transwell membrane. A paracrine mode of action has often been suggested by others for MSCs and related mesenchymal cell types (83–86). The missing blocking effect of PD-1 ligands, which are secreted and also expressed on the cell surface, clearly discriminates hAACs from the before mentioned $CD90^+$ CPCs, that exert a more contact-dependent mode of suppression by PD-L1 involvement on ongoing immune responses (30). Conclusively, the observed increase of PD-L1 and PD-L2 expression on the cell surface seems to play only an inferior role in the immune regulation mediated by hAACs. Even though their general cellular characteristics are clearly distinguishable from fibroblasts and conventional MSCs (32), hAACs behave more like MSCs in this immunological context. The importance of the observed up-regulation of other potential immunoregulatory genes such as Galcetin-9 for the immunomodulatory capacity of hAACs has to be analyzed in more detail in future studies.

There are also still open questions remaining regarding the nature of how hAACs avoid unwanted immune responses in clinically relevant settings of cardiac injury. Apart from the proved involvement of IDO in the efficient T cell immunosuppression under IFNγ treatment, the interaction of antigen-presenting cells, like monocytes, has also to be taken into account. In this regard, it became evident that MSCs could skew monocytes toward anti-inflammatory macrophages (87–89) and induce the generation of regulatory T cells (58, 76). Additionally, it was found that MSCs could be taken up by monocytic cells and induce changes toward a non-classical monocyte phenotype with enhanced expression of PD-L1 and secretion of IL-10 that subsequently modulates adaptive immune responses (90). Furthermore, it was recently published that human CPCs attracted monocytes by a set of released cytokines and mediators and consequently changed the polarization of differentiating macrophages toward an M2-type cell (25, 91). Future studies will therefore focus on this hAAC/antigen-presenting cell interplay to gain a better understanding of the underlying mechanism of action and ensure the safe and effective translation of this hAAC cell product.

In the present study we could show, that $CD90^{low}$ hAACs isolated from human heart tissue represent a new allogeneic off-the-shelf mesenchymal-like cell product with therapeutically interesting features. Most importantly, hAACs do not trigger immunogeneic effects based on the low expression of HLA-DR and absence of co-stimulatory molecules after pro-inflammatory IFNγ stimulation. Moreover, hAACs clearly demonstrated a strong potential to inhibit ongoing immune responses even in inflammatory environments. Ultimately, we could illustrate that IDO-upregulation under IFNγ pre-treatment seems to be one of the most important players mediating the observed suppressive effects (**Figure 7**). However, the involvement of other so far not identified soluble factors cannot be excluded. This paracrine mode of action would also suggest the opportunity to isolate and use extracellular vesicles derived from hAACs for a clinical application. Our data in general would argue for a safe application of the hAAC cell product in an allogeneic setting, which also facilitates high potential to suppress already ongoing immune responses and thereby limit the progression of adverse remodeling after cardiac injury.

DATA AVAILABILITY

The genome-wide Affymetrix® gene expression profile datasets generated for this study can be found in the Gene Expression Omnibus repository: https://www.ncbi.nlm.nih.gov/geo/query/acc.cgi?acc=GSE126461. The remaining raw data supporting the conclusions of this manuscript will be made available by the authors, without undue reservation, to any qualified researcher.

ETHICS STATEMENT

Human atrial appendage-derived cells (hAACs) were isolated from atrial appendages of eight donors according to the local guidelines of the Charité-Universitätsmedizin Berlin as well as the Declaration of Helsinki and the study was approved by the ethics committee of the Charité-Universitätsmedizin Berlin (No. 4/028/12). Human peripheral blood mononuclear cells (PBMCs) were isolated from buffy coats (German Red Cross, Berlin, Germany; approved by the local Ethical Committee, EA1/226/14). Umbilical cord mesenchymal stromal cells were obtained for human cell and tissue sample collection from the Institutional Review Board of the Medical University of Graz (protocol 19-252 ex 07/08). Umbilical cord samples were collected from mothers that gave written informed consent after full-term pregnancies in accordance with the Declaration of Helsinki.

AUTHOR CONTRIBUTIONS

FD led the project and was responsible for study design, execution of experiments, collection and assembly of data, data analysis, and interpretation, as well as manuscript writing. MSt established methods, performed experiments, and interpreted data. KJ designed experimental approaches, performed and interpreted the microarray analyses and revised the manuscript. MH and MSi supplied the study materials, provided administrative support, and revised the manuscript. MSe was responsible for the project conception and design, administrative support, data analysis and interpretation, manuscript writing, and final approval of the manuscript.

FUNDING

This study was supported by the BCRT [Bundesministerium für Bildung und Forschung (BMBF) grant (13GW0099)]. In part, the work was supported by the Berlin Institute of Health (BIH) with a medical doctoral research stipend and by DFG funding through the Berlin-Brandenburg School for Regenerative Therapies GSC 203 to FD.

ACKNOWLEDGMENTS

We would like to acknowledge the assistance of the BIH Core Facility Flow & Mass Cytometry—BIH FlowMassCore headed by D. Kunkel; H. Stachelscheid, and P. Mergenthaler of the Charité High Content Imaging Facility; I. Savidis and A. Levent from the Core Unit Biomarker—Immunological Study Lab (both BCRT, Charité-Universitätsmedizin Berlin) for their excellent technical assistance with the Luminex® analyses; B. Kurtze and K. Hariharan for the technical help with the qPCR measurement (both BCRT, Charité-Universitätsmedizin Berlin); A. Fleischmann and J. Ringe (both BCRT—Charité-Universitätsmedizin Berlin) for their skillful support with sample preparation and measurement of RNA microarray experiments and Laymik from the Noun Project for provision of graphical icons. We specially thank K. Schütze and H. Kremling (CellTool GmbH, Tutzing, Germany) for the extraordinary help with Raman analysis. We thank C. Stamm (Deutsches Herzzentrum Berlin) for the procurement of atrial appendages, S. Detert (BCRT—Charité-Universitätsmedizin Berlin) for the isolation of the hAAC cell product and C. Beez, M. Schneider, and N. Souidi for helpful discussions. We express our gratitude to D. Strunk (Paracelsus Medical University, Salzburg) for the supply of umbilical cord MSCs. We acknowledge support from the German Research Foundation (DFG) and the Open Access Publication Fund of the Charité-Universitätsmedizin Berlin.

SUPPLEMENTARY MATERIAL

The Supplementary Material for this article can be found online at: https://www.frontiersin.org/articles/10.3389/fimmu.2019.01716/full#supplementary-material

REFERENCES

1. Cahill TJ, Choudhury RP, Riley PR. Heart regeneration and repair after myocardial infarction: translational opportunities for novel therapeutics. *Nat Rev Drug Discov.* (2017) 16:699–717. doi: 10.1038/nrd.2017.106
2. Owens AT, Brozena SC, Jessup M. New management strategies in heart failure. *Circul Res.* (2016) 118:480–95. doi: 10.1161/CIRCRESAHA.115.306567
3. Fernández-Avilés F, Sanz-Ruiz R, Climent AM, Badimon L, Bolli R, Charron D, et al. Global position paper on cardiovascular regenerative medicine. *Eur Heart J.* (2017) 38:2532–46. doi: 10.1093/eurheartj/ehx248
4. Schächinger V, Erbs S, Elsässer A, Haberbosch W, Hambrecht R, Hölschermann H, et al. Intracoronary bone marrow–derived progenitor cells in acute myocardial infarction. *N Engl J Med.* (2006) 355:1210–21. doi: 10.1056/NEJMoa060186
5. Houtgraaf JH, Den Dekker WK, Van Dalen BM, Springeling T, De Jong R, Van Geuns RJ, et al. First experience in humans using adipose tissue–derived regenerative cells in the treatment of patients with ST-segment elevation myocardial infarction. *J Am Coll Cardiol.* (2012) 59:539–40. doi: 10.1016/j.jacc.2011.09.065
6. Lilyanna S, Martinez EC, Vu TD, Ling LH, Gan SU, Tan AL, et al. Cord lining-mesenchymal stem cells graft supplemented with an omental flap induces myocardial revascularization and ameliorates cardiac dysfunction in a rat model of chronic ischemic heart failure. *Tissue Eng Part A.* (2013) 19:1303–15. doi: 10.1089/ten.tea.2012.0407
7. Zhao JJ, Liu XC, Kong F, Qi TG, Cheng GH, Wang J, et al. Bone marrow mesenchymal stem cells improve myocardial function in a swine model of acute myocardial infarction. *Mol Med Rep.* (2014) 10:1448–54. doi: 10.3892/mmr.2014.2378
8. Beltrami AP, Barlucchi L, Torella D, Baker M, Limana F, Chimenti S, et al. Adult cardiac stem cells are multipotent and support myocardial regeneration. *Cell.* (2003) 114:763–76. doi: 10.1016/S0092-8674(03)00687-1
9. Messina E, De Angelis L, Frati G, Morrone S, Chimenti S, Fiordaliso F, et al. Isolation and expansion of adult cardiac stem cells from human and murine heart. *Circul Res.* (2004) 95:911–21. doi: 10.1161/01.RES.0000147315.71699.51
10. Oh H, Bradfute SB, Gallardo TD, Nakamura T, Gaussin V, Mishina Y, et al. Cardiac progenitor cells from adult myocardium: Homing, differentiation, and fusion after infarction. *Proc Nat Acad Sci USA.* (2003) 100:12313–8. doi: 10.1073/pnas.2132126100
11. Smith RR, Barile L, Cho HC, Leppo MK, Hare JM, Messina E, et al. Regenerative potential of cardiosphere-derived cells expanded from percutaneous endomyocardial biopsy specimens. *Circulation.* (2007) 115:896–908. doi: 10.1161/CIRCULATIONAHA.106.655209
12. Crisostomo V, Casado JG, Baez-Diaz C, Blazquez R, Sanchez-Margallo FM. Allogeneic cardiac stem cell administration for acute myocardial infarction. *Expert Rev Cardiovasc Therapy.* (2015) 13:285–99. doi: 10.1586/14779072.2015.1011621
13. Bolli R, Chugh AR, D'Amario D, Loughran JH, Stoddard MF, Ikram S, et al. Cardiac stem cells in patients with ischaemic cardiomyopathy (SCIPIO): initial results of a randomised phase 1 trial. *Lancet.* (2011) 378:1847–57. doi: 10.1016/S0140-6736(11)61590-0
14. Chugh AR, Beache GM, Loughran JH, Mewton N, Elmore JB, Kajstura J, et al. Administration of cardiac stem cells in patients with ischemic cardiomyopathy: The SCIPIO trial: surgical aspects and interim analysis of myocardial function and viability by magnetic resonance. *Circulation.* (2012) 126(11 SUPPL.1):54–64. doi: 10.1161/CIRCULATIONAHA.112.092627
15. Makkar RR, Smith RR, Cheng K, Malliaras K, Thomson LEJ, Berman D, et al. Intracoronary cardiosphere-derived cells for heart regeneration after myocardial infarction (CADUCEUS): a prospective, randomised phase 1 trial. *Lancet.* (2012) 379:895–904. doi: 10.1016/S0140-6736(12)60195-0
16. Malliaras K, Makkar RR, Smith RR, Cheng K, Wu E, Bonow RO, et al. Intracoronary cardiosphere-derived cells after myocardial infarction: evidence of therapeutic regeneration in the final 1-year results of the CADUCEUS trial (CArdiosphere-derived aUtologous stem CElls to reverse ventricular dysfunction). *J Am Coll Cardiol.* (2014) 63:110–22. doi: 10.1016/j.jacc.2013.08.724
17. Haag M, Van Linthout S, Schröder SEA, Freymann U, Ringe J, Tschöpe C, et al. Endomyocardial biopsy derived adherent proliferating cells - a potential cell source for cardiac tissue engineering. *J Cell Biochem.* (2010) 109:564–75. doi: 10.1002/jcb.22433
18. Miteva K, Haag M, Peng J, Savvatis K, Becher PM, Seifert M, et al. Human cardiac-derived adherent proliferating cells reduce murine acute coxsackievirus B3-induced myocarditis. *PLoS ONE.* (2011) 6:e28513. doi: 10.1371/journal.pone.0028513
19. Dehne T, Adam X, Materne E-M, Reimann MC, Krüger JP, Van Linthout S, et al. A P19 and P19CL6 cell-based complementary approach to determine paracrine effects in cardiac tissue engineering. *Cells Tissues Org.* (2014) 199:24–36. doi: 10.1159/000362540
20. Miteva K, Van Linthout S, Pappritz K, Müller I, Spillmann F, Haag M, et al. Human endomyocardial biopsy specimen-derived stromal cells modulate

angiotensin II-induced cardiac remodeling. *Stem Cells Transl Med.* (2016) 5:1707–18. doi: 10.5966/sctm.2016-0031

21. Haag M, Stolk M, Ringe J, Linthout S, Van Tschöpe C, Sittinger M, et al. Immune attributes of cardiac-derived adherent proliferating (CAP) cells in cardiac therapy. *J Tissue Eng Regener Med.* (2013) 7:362–70. doi: 10.1002/term.531
22. Young PP, Schäfer R. Cell-based therapies for cardiac disease: a cellular therapist's perspective. *Transfusion.* (2015) 55:441–51. doi: 10.1111/trf.12826
23. Malliaras K, Marbán E. Cardiac cell therapy: where we've been, where we are, and where we should be headed. *Br Med Bull.* (2011) 98:161–85. doi: 10.1093/bmb/ldr018
24. Najar M, Bouhtit F, Melki R, Afif H, Hamal A, Fahmi H, et al. Mesenchymal stromal cell-based therapy: new perspectives and challenges. *J Clin Med.* (2019) 8:626. doi: 10.3390/jcm8050626
25. Al-Daccak R, Charron D. Allogenic benefit in stem cell therapy: cardiac repair and regeneration. *Tissue Antigens.* (2015) 86:155–62. doi: 10.1111/tan.12614
26. Hogen R, DiNorcia J, Dhanireddy K. Antibody-mediated rejection: what is the clinical relevance? *Curr Opin Organ Transpl.* (2017) 22:97–104. doi: 10.1097/MOT.0000000000000391
27. Terasaki PI, Cai J. Humoral theory of transplantation: further evidence. *Curr Opin Immunol.* (2005) 17:541–5. doi: 10.1016/j.coi.2005.07.018
28. Clarkson MR, Sayegh MH. T-cell costimulatory pathways in allograft rejection and tolerance. *Transplantation.* (2005) 80:555–63. doi: 10.1097/01.tp.0000168432.60022.99
29. Wood KJ, Zaitsu M, Goto R. Cell mediated rejection. *Methods Mol Biol.* (2013) 1034:71–83. doi: 10.1007/978-1-62703-493-7_3
30. Lauden L, Boukouaci W, Borlado LR, López IP, Sepúlveda P, Tamouza R, et al. Allogenicity of human cardiac stem/progenitor cells orchestrated by programmed death ligand 1. *Circul Res.* (2013) 112:451–64. doi: 10.1161/CIRCRESAHA.112.276501
31. Fernández-Avilés F, Sanz-Ruiz R, Bogaert J, Casado Plasencia A, Gilaberte I, Belmans A, et al. Safety and efficacy of intracoronary infusion of allogeneic human cardiac stem cells in patients with ST-segment elevation myocardial infarction and left ventricular dysfunction. *Circul Res.* (2018) 123:579–89. doi: 10.1161/CIRCRESAHA.118.312823
32. Detert S, Stamm C, Beez C, Diedrichs F, Ringe J, Van Linthout S, et al. The atrial appendage as a suitable source to generate cardiac-derived adherent proliferating cells for regenerative cell-based therapies. *J Tissue Eng Regener Med.* (2018) 12:e1404–17. doi: 10.1002/term.2528
33. Cheng K, Ibrahim A, Hensley MT, Shen D, Sun B, Middleton R, et al. Relative roles of CD90 and c-kit to the regenerative efficacy of cardiosphere-derived cells in humans and in a mouse model of myocardial infarction. *J Am Heart Assoc.* (2014) 3:e001260. doi: 10.1161/JAHA.114.001260
34. El-Shaffeey M, Pappritz K, Diedrichs F, Seifert M, Stamm C, Haag M, et al. Cardioprotective and immunomodulatory effects of endomyocardial biopsy- and atrial appendage-derived stromal cells in an acute model of Coxsackievirus B3-induced myocarditis. *Eur J Heart Fail.* (2018) 20: P1982.
35. Souidi N, Stolk M, Rudeck J, Strunk D, Schallmoser K, Volk H-D, et al. Stromal cells act as guardians for endothelial progenitors by reducing their immunogenicity after Co-transplantation. *Stem Cells.* (2017) 35:1233–45. doi: 10.1002/stem.2573
36. Reinisch A, Hofmann NA, Obenauf AC, Kashofer K, Rohde E, Schallmoser K, et al. Humanized large-scale expanded endothelial colony–forming cells function *in vitro* and *in vivo*. *Blood.* (2009) 113:6716–25. doi: 10.1182/BLOOD-2008-09-181362
37. Stolk M, Klatte-Schulz F, Schmock A, Minkwitz S, Wildemann B, Seifert M. New insights into tenocyte-immune cell interplay in an in vitro model of inflammation. *Sci Rep.* (2017) 7:9801. doi: 10.1038/s41598-017-09875-x
38. Gautier L, Cope L, Bolstad BM, Irizarry RA. affy–analysis of Affymetrix GeneChip data at the probe level. *Bioinformatics.* (2004) 20:307–15. doi: 10.1093/bioinformatics/btg405
39. Ritchie ME, Phipson B, Wu D, Hu Y, Law CW, Shi W, et al. limma powers differential expression analyses for RNA-sequencing and microarray studies. *Nucleic Acids Res.* (2015) 43:e47. doi: 10.1093/nar/gkv007
40. Huang DW, Sherman BT, Lempicki RA. Systematic and integrative analysis of large gene lists using DAVID bioinformatics resources. *Nat Protocols.* (2009) 4:44–57. doi: 10.1038/nprot.2008.211
41. Huang DW, Sherman BT, Lempicki RA. Bioinformatics enrichment tools: paths toward the comprehensive functional analysis of large gene lists. *Nucleic Acids Res.* (2009) 37:1–13. doi: 10.1093/nar/gkn923
42. Yu G, Wang LG, Han Y, He QY. clusterProfiler: an R package for comparing biological themes among gene clusters. *Omics J Integr Biol.* (2012) 16:284–7. doi: 10.1089/omi.2011.0118
43. Walter W, Sánchez-Cabo F, Ricote M. GOplot: an R package for visually combining expression data with functional analysis. *Bioinformatics.* (2015) 31:2912–4. doi: 10.1093/bioinformatics/btv300
44. Pedregosa F, Weiss R, Brucher M. Scikitlearn: machine learning in python. *J Mach Learn Res.* (2011) 12:2825–30. doi: 10.1007/s13398-014-0173-7.2
45. Davies LC, Heldring N, Kadri N, Le Blanc K. Mesenchymal stromal cell secretion of programmed death-1 ligands regulates T cell mediated immunosuppression. *Stem Cells.* (2017) 35:766–76. doi: 10.1002/stem.2509
46. Hausenloy DJ, Garcia-Dorado D, Bøtker HE, Davidson SM, Downey J, Engel FB, et al. Novel targets and future strategies for acute cardioprotection: position paper of the European Society of Cardiology Working Group on Cellular Biology of the Heart. *Cardiovasc Res.* (2017) 113:564–85. doi: 10.1093/cvr/cvx049
47. Nigro P, Bassetti B, Cavallotti L, Catto V, Carbucicchio C, Pompilio G. Cell therapy for heart disease after 15 years: Unmet expectations. *Pharmacol Res.* (2018) 127:77–91. doi: 10.1016/j.phrs.2017.02.015
48. Li TS, Cheng K, Malliaras K, Smith RR, Zhang Y, Sun B, et al. Direct comparison of different stem cell types and subpopulations reveals superior paracrine potency and myocardial repair efficacy with cardiosphere-derived cells. *J Am Coll Cardiol.* (2012) 59:942–53. doi: 10.1016/j.jacc.2011.11.029
49. Rossini A, Frati C, Lagrasta C, Graiani G, Scopece A, Cavalli S, et al. Human cardiac and bone marrow stromal cells exhibit distinctive properties related to their origin. *Cardiovasc Res.* (2011) 89:650–60. doi: 10.1093/cvr/cvq290
50. Karantalis V, Hare JM. Use of mesenchymal stem cells for therapy of cardiac disease. *Circul Res.* (2015) 116:1413–30. doi: 10.1161/CIRCRESAHA.116.303614
51. Ward MR, Abadeh A, Connelly KA. Concise review: rational use of mesenchymal stem cells in the treatment of ischemic heart disease. *Stem Cells Transl Med.* (2018) 7:543–50. doi: 10.1002/sctm.17-0210
52. Kawka E, Witowski J, Bartosova M, Catar R, Rudolf A, Philippe A, et al. Thy-1+/- fibroblast subsets in the human peritoneum. *Am J Physiol Renal Physiol.* (2017) 313:F1116–123. doi: 10.1152/ajprenal.00274.2017
53. Berglund AK, Fortier LA, Antczak DF, Schnabel LV. Immunoprivileged no more: measuring the immunogenicity of allogeneic adult mesenchymal stem cells. *Stem Cell Res Therap.* (2017) 8:288. doi: 10.1186/s13287-017-0742-8
54. Lohan P, Treacy O, Griffin MD, Ritter T, Ryan AE. Anti-donor immune responses elicited by allogeneic mesenchymal stem cells and their extracellular vesicles: are we still learning? *Front Immunol.* (2017) 8:1626. doi: 10.3389/fimmu.2017.01626
55. Wang WB, Yen ML, Liu KJ, Hsu PJ, Lin MH, Chen PM, et al. Interleukin-25 mediates transcriptional control of PD-L1 via STAT3 in multipotent human mesenchymal stromal cells (hMSCs) to suppress Th17 responses. *Stem Cell Rep.* (2015) 5:392–404. doi: 10.1016/j.stemcr.2015.07.013
56. Kim JY, Park M, Kim YH, Ryu KH, Lee KH, Cho KA, et al. Tonsil-derived mesenchymal stem cells (T-MSCs) prevent Th17-mediated autoimmune response via regulation of the programmed death-1/programmed death ligand-1 (PD-1/PD-L1) pathway. *J Tissue Eng Regener Med.* (2018) 12:e1022–33. doi: 10.1002/term.2423
57. Di Trapani M, Bassi G, Ricciardi M, Fontana E, Bifari F, Pacelli L, et al. Comparative study of immune regulatory properties of stem cells derived from different tissues. *Stem Cells Dev.* (2013) 22:2990–3002. doi: 10.1089/scd.2013.0204
58. Groh ME, Maitra B, Szekely E, Koç ON. Human mesenchymal stem cells require monocyte-mediated activation to suppress alloreactive T cells. *Exp Hematol.* (2005) 33:928–34. doi: 10.1016/j.exphem.2005.05.002
59. Altara R, Ghali R, Mallat Z, Cataliotti A, Booz GW, Zouein FA. Conflicting vascular and metabolic impact of the IL-33/sST2 axis. *Cardiovasc Res.* (2018) 114:1578–94. doi: 10.1093/cvr/cvy166
60. Ghali R, Altara R, Louch WE, Cataliotti A, Mallat Z, Kaplan A, et al. IL-33 (Interleukin 33)/sST2 (Soluble Suppression of Tumorigenicity 2) Axis in *Hypertension* and heart failure. *Hypertension.* (2018) 72:818–28. doi: 10.1161/HYPERTENSIONAHA.118.11157

61. Griesenauer B, Paczesny S. The ST2/IL-33 axis in immune cells during inflammatory diseases. *Front Immunol.* (2017) 8:475. doi: 10.3389/fimmu.2017.00475
62. Martin NT, Martin MU. Interleukin 33 is a guardian of barriers and a local alarmin. *Nat Immunol.* (2016) 17:122–31. doi: 10.1038/ni.3370
63. Sattler S, Fairchild P, Watt FM, Rosenthal N, Harding SE. The adaptive immune response to cardiac injury—the true roadblock to effective regenerative therapies? *NPJ Regener. Med.* (2017) 2:19. doi: 10.1038/s41536-017-0022-3
64. Prabhu SD, Frangogiannis NG. The biological basis for cardiac repair after myocardial infarction. *Circul Res.* (2016) 119:91–112. doi: 10.1161/CIRCRESAHA.116.303577
65. Crop MJ, Baan CC, Korevaar SS, IJzermans JNM, Pescatori M, Stubbs AP, et al. Inflammatory conditions affect gene expression and function of human adipose tissue-derived mesenchymal stem cells. *Clin Exp Immunol.* (2010) 162:474–86. doi: 10.1111/j.1365-2249.2010.04256.x
66. Kronsteiner B, Wolbank S, Peterbauer A, Hackl C, Redl H, van Griensven M, et al. Human mesenchymal stem cells from adipose tissue and amnion influence T-cells depending on stimulation method and presence of other immune cells. *Stem Cells Dev.* (2011) 20:2115–26. doi: 10.1089/scd.2011.0031
67. Sivanathan KN, Gronthos S, Rojas-Canales D, Thierry B, Coates PT. Interferon-gamma modification of mesenchymal stem cells: implications of autologous and allogeneic mesenchymal stem cell therapy in allotransplantation. *Stem Cell Rev Rep.* (2014) 10:351–75. doi: 10.1007/s12015-014-9495-2
68. Li X, Xu Z, Bai J, Yang S, Zhao S, Zhang Y, et al. Umbilical cord tissue-derived mesenchymal stem cells induce T lymphocyte apoptosis and cell cycle arrest by expression of indoleamine 2, 3-dioxygenase. *Stem Cells Int.* (2016) 2016:1–11. doi: 10.1155/2016/7495135
69. de Witte SFH, Merino AM, Franquesa M, Strini T, van Zoggel JAA, Korevaar SS, et al. Cytokine treatment optimises the immunotherapeutic effects of umbilical cord-derived MSC for treatment of inflammatory liver disease. *Stem Cell Res Therapy.* (2017) 8:140. doi: 10.1186/s13287-017-0590-6
70. Campioni D, Rizzo R, Stignani M, Melchiorri L, Ferrari L, Moretti S, et al. A decreased positivity for CD90 on human mesenchymal stromal cells (MSCs) is associated with a loss of immunosuppressive activity by MSCs. *Cytometry Part B Clin Cytometry.* (2009) 76:225–30. doi: 10.1002/cyto.b.20461
71. Gebler A, Zabel O, Seliger B. The immunomodulatory capacity of mesenchymal stem cells. *Trends Mol Med.* (2012) 18:128–34. doi: 10.1016/j.molmed.2011.10.004
72. Wang Y, Chen X, Cao W, Shi Y. Plasticity of mesenchymal stem cells in immunomodulation: pathological and therapeutic implications. *Nat Immunol.* (2014) 15:1009–16. doi: 10.1038/ni.3002
73. Kyurkchiev D, Bochev I, Ivanova-Todorova E, Mourdjeva M, Oreshkova T, Belemezova K, et al. Secretion of immunoregulatory cytokines by mesenchymal stem cells. *World J Stem Cells.* (2014) 6:552. doi: 10.4252/wjsc.v6.i5.552
74. Uccelli A, Moretta L, Pistoia V. Mesenchymal stem cells in health and disease. *Nat Rev Immunol.* (2008) 8:726–36. doi: 10.1038/nri2395
75. van den Akker F, Deddens JC, Doevendans PA, Sluijter JPG. Cardiac stem cell therapy to modulate inflammation upon myocardial infarction. *Biochim et Biophy Acta.* (2013) 1830:2449–58. doi: 10.1016/j.bbagen.2012.08.026
76. Melief SM, Schrama E, Brugman MH, Tiemessen MM, Hoogduijn MJ, Fibbe WE, et al. Multipotent stromal cells induce human regulatory T cells through a novel pathway involving skewing of monocytes toward anti-inflammatory macrophages. *Stem Cells.* (2013) 31:1980–91. doi: 10.1002/stem.1432
77. Tipnis S, Viswanathan C, Majumdar AS. Immunosuppressive properties of human umbilical cord-derived mesenchymal stem cells: role of B7-H1 and IDO. *Immunol Cell Biol.* (2010) 88:795–806. doi: 10.1038/icb.2010.47
78. Croitoru-Lamoury J, Lamoury FMJ, Caristo M, Suzuki K, Walker D, Takikawa O, et al. Interferon-γ regulates the proliferation and differentiation of mesenchymal stem cells via activation of indoleamine 2,3 dioxygenase (IDO). *PLoS ONE.* (2011) 6:e14698. doi: 10.1371/journal.pone.0014698
79. François M, Romieu-Mourez R, Li M, Galipeau J. Human MSC suppression correlates with cytokine induction of indoleamine 2,3-dioxygenase and bystander M2 macrophage differentiation. *Mol Therapy.* (2012) 20:187–95. doi: 10.1038/mt.2011.189
80. Hong J, Hueckelhoven A, Wang L, Schmitt A, Wuchter P, Tabarkiewicz J, et al. Indoleamine 2,3-dioxygenase mediates inhibition of virus-specific CD8(+) T cell proliferation by human mesenchymal stromal cells. *Cytotherapy.* (2016) 18:621–9. doi: 10.1016/j.jcyt.2016.01.009
81. van den Akker F, de Jager SCA, Sluijter JPG. Mesenchymal stem cell therapy for cardiac inflammation: immunomodulatory properties and the influence of toll-like receptors. *Medi Inflamm.* (2013) 2013:181020. doi: 10.1155/2013/181020
82. Guan Q, Li Y, Shpiruk T, Bhagwat S, Wall DA. Inducible indoleamine 2,3-dioxygenase 1 and programmed death ligand 1 expression as the potency marker for mesenchymal stromal cells. *Cytotherapy.* (2018) 20:639–49. doi: 10.1016/j.jcyt.2018.02.003
83. Liang X, Ding Y, Zhang Y, Tse HF, Lian Q. Paracrine mechanisms of mesenchymal stem cell-based therapy: current status and perspectives. *Cell Transpl.* (2014) 23:1045–59. doi: 10.3727/096368913X667709
84. Bruno S, Deregibus MC, Camussi G. The secretome of mesenchymal stromal cells: role of extracellular vesicles in immunomodulation. *Immunol Lett.* (2015) 168:154–8. doi: 10.1016/j.imlet.2015.06.007
85. Vizoso F, Eiro N, Cid S, Schneider J, Perez-Fernandez R. Mesenchymal stem cell secretome: toward cell-free therapeutic strategies in regenerative medicine. *Int J Mol Sci.* (2017) 18:1852. doi: 10.3390/ijms18091852
86. Zheng G, Huang R, Qiu G, Ge M, Wang J, Shu Q, et al. Mesenchymal stromal cell-derived extracellular vesicles: regenerative and immunomodulatory effects and potential applications in sepsis. *Cell Tissue Res.* (2018) 374:1–15. doi: 10.1007/s00441-018-2871-5
87. Kim J, Hematti P. Mesenchymal stem cell-educated macrophages: a novel type of alternatively activated macrophages. *Exp Hematol.* (2009) 37:1445–53. doi: 10.1016/j.exphem.2009.09.004
88. Selleri S, Bifsha P, Civini S, Pacelli C, Dieng MM, Lemieux W, et al. Human mesenchymal stromal cell-secreted lactate induces M2-macrophage differentiation by metabolic reprogramming. *Oncotarget.* (2016) 7:30193–210. doi: 10.18632/oncotarget.8623
89. Chiossone L, Conte R, Spaggiari GM, Serra M, Romei C, Bellora F, et al. Mesenchymal stromal cells induce peculiar alternatively activated macrophages capable of dampening both innate and adaptive immune responses. *Stem Cells.* (2016) 34:1909–21. doi: 10.1002/stem.2369
90. de Witte SFH, Luk F, Sierra Parraga JM, Gargesha M, Merino A, Korevaar SS, et al. Immunomodulation by therapeutic mesenchymal stromal cells (MSC) is triggered through phagocytosis of MSC by monocytic cells. *Stem Cells.* (2018) 36:602–15. doi: 10.1002/stem.2779
91. Dam N, Hocine HR, Palacios I, DelaRosa O, Menta R, Charron D, et al. Human cardiac-derived stem/progenitor cells fine-tune monocyte-derived descendants activities toward cardiac repair. *Front Immunol.* (2017) 8:1413. doi: 10.3389/fimmu.2017.01413

Conflict of Interest Statement: MSi and MH are inventors of patent family of EP2129774B1 (Cells for heart treatment). MSi is shareholder of CellServe GmbH (Berlin, Germany) and BioRetis GmbH (Berlin, Germany). CellServe GmbH holds a license of the above patent family.

The remaining authors declare that the research was conducted in the absence of any commercial or financial relationships that could be construed as a potential conflict of interest.

Curriculum Vitae

The curriculum vitae is not included in the electronic version of my thesis due to legal data protection considerations.

Complete List of Publications

1) Publications with Peer Review Process

a) Detert S, Stamm C, Beez C, **Diedrichs F**, Ringe J, Van Linthout S, Seifert M, Tschöpe C, Sittinger M, & Haag M. The atrial appendage as a suitable source to generate cardiac-derived adherent proliferating cells for regenerative cell-based therapies. J Tissue Eng Regen Med 2018;12:e1404–17. https://doi.org/10.1002/term.2528.
Impact Factor: 3.319

b) **Diedrichs F**, Stolk M, Jürchott K, Haag M, Sittinger M, & Seifert M. Enhanced Immunomodulation in Inflammatory Environments Favors Human Cardiac Mesenchymal Stromal-Like Cells for Allogeneic Cell Therapies. Front Immunol 2019;10:1716. https://doi.org/10.3389/fimmu.2019.01716.
Impact Factor: 4.716

2) Abstracts and Posters

a) El-Shafeey M, Pappritz K, **Diedrichs F**, Seifert M, Stamm C, Haag M, Sittinger M, Tschöpe C & Van Linthout S. Cardioprotective and immunomodulatory effects of endomyocardial biopsy and atiral appendage-derived stromal cells in an acute model of Coxsackievirus B3-induced myocarditis. Eur J Heart Fail 2018;20(Suppl. S1):517; P1982.

Acknowledgements

First, I would like to express my gratitude for the possibility to learn about science beyond practiced medicine, which is, without a doubt, one of the most important pillars of evidence-based therapies. I am especially thankful to **Prof. Dr. Martina Seifert**, who not only entrusted me with this exciting topic, but also introduced me to the overwhelmingly complex and fascinating world of immunology and basic science. I am truly grateful for her unparalleled supervision and care as well as all our scientific and personal conversations together over the many years.

Furthermore, I would like to thank **Prof. Dr. Michael Sittinger**, **Dr. Naima Souidi** and **Prof. Dr. Carsten Tschöpe** for their important supervision within the scope of the Mentoring Committee of the “Berlin-Brandenburg School for Regenerative Therapies” (BSRT). Moreover, I am very thankful to broaden my scientific horizon through the many workshops and events organized by the BSRT under the guidance of **Dr. Sabine Bartosch**.

Over the last years I got to know many inspiring people in science and I specifically value all members of our group, namely **Dr. Naima Souidi**, **Dr. Maria Schneider**, **Christien Beez**, **Constanze Wild, Meaghan Stolk**, **Niklas Fellmer** and **Viktoriia Vorobeva**. I always enjoyed our interesting discussions and the many hours in the laboratory together. I specially thank **Thu Thao Nguyen** for the exceptional collaboration, that filled my work and all our shared breaks with lightheartedness and humor.

Additionally, I express my gratitude to our collaboration partners in AG Sittinger. Particularly, I would like to thank **Dr. Marion Haag**, **Dr. Stephan Detert** and **Anja Fleischmann** for their technical assistance, the preparation of hAACs and all the scientific input from our shared meetings.

Lastly, I thank my **parents**, my **whole family** and all my **friends**, who accompanied me all these years on my scientific journey and never failed to build me up and support me when I needed it most. After all, I thank **Antonia** for her long-standing love and unwearyingly patience.